Jean Guex · Federico Galster
Øyvind Hammer

Discrete Biochronological Time Scales

Springer

Discrete Biochronological Time Scales

Jean Guex · Federico Galster
Øyvind Hammer

Discrete Biochronological Time Scales

Springer

Jean Guex
Department of Geology
University of Lausanne—SWISS NSF
Lausanne
Switzerland

Federico Galster
University of Lausanne—SWISS NSF
Lausanne
Switzerland

Øyvind Hammer
Natural History Museum
University of Oslo
Oslo
Norway

ISBN 978-3-319-21325-5 ISBN 978-3-319-21326-2 (eBook)
DOI 10.1007/978-3-319-21326-2

Library of Congress Control Number: 2015950029

Springer Cham Heidelberg New York Dordrecht London

Printed on acid-free paper

Springer International Publishing AG Switzerland is part of Springer Science+Business Media (www.springer.com)

Some enthusiastic structural geologists will claim they are able to unravel the structure and the structural history of mountain chains without a single fossil. This is quite true…provided that there are no fossils.

R. Truempy (1971)

In Memoriam
Milos Rakus
Jean Marcoux
Jean Gabilly
Rudolf Truempy

Foreword

Several quantitative methods designed to elaborate relative timescales based on fossils have been published during the last decades. The most popular techniques at the moment are those based on a statistical-probabilistic approach, on particular optimization methods (simulated annealing) and on graph theory.

The major difficulties related to the construction of such timescales are related to the conflicting intertaxa relationships and the intersamples contradictions. This book describes in detail a method to construct discrete biochronological timescales based on graph theory, called the Unitary Association Method (UAM). This method, first introduced in 1977 by Guex, is a graph theoretical model designed for the construction of concurrent range zones using a fully deterministic approach. Its basic idea is to construct a discrete sequence of coexistence intervals of species. Each interval, corresponding to one UA, is of minimal duration while consisting of a maximal set of intersecting ranges. Each UA is characterized by a set of species allowing its identification in the stratigraphical sections. The chronological significance of the units generated by the UA software (UAgraph by Hammer Guex Savary, http://folk.uio.no/ohammer/uagraph) depends on two important parameters: (1) their lateral traceability (what is called 'reproducibility'); and (2) their superpositional control between two adjacent units. The major difficulties related to the construction of such units discussed in detail in the book are related to the conflicting intertaxa stratigraphic relationships (=cycles in the biostratigraphical graph) and the intermaximal cliques contradictions (strongly connected components in the maximal clique graph). Such contradictions are generally eliminated by adding virtual coexistences. The goal of the method was not to reduce the number of virtual coexistences at all cost, but to produce a robust solution that reflects the quality of the data, i.e., a solution optimizing the reproducibility and interunits superpositional control. UAs should be considered as intervals of uncertainty on which we have established an order relation: The UA sequences represent units which are ordered as older, sub-contemporaneous, or younger. The order of the event within a single particular unit is not known and cannot be solved by means of statistical techniques;

they can only be solved by constructing composite stratigraphical sections, whenever possible. Several examples of applications of the UAM are given in Chaps. 5–9 and the results produced by the statistical-probabilistic methods are discussed in the concluding chapters of this book.

Arthur Escher

Preface

This book is a complementary of a former version published by Springer Verlag (Guex's 1991 "Biochronological Correlations"). Most of its material is new or presented in a more didactic and simpler way, especially the problems of reworking and diachronism of datums.

The readers who are acquainted with the basic graph theory and formal approaches have a detailed explanation of the new program UAgraph in Chaps. 2 and 3 of the book.

The new edition contains recent examples of applications of the Unitary Association Method (UAM) related to the analysis of post-extinction recovery around the Triassic Jurassic Boundary, evolutionary rates of the Lower Jurassic radiolarians and presents a new discussion of the Deboo's classical problem of correlation of the Paleogene in Mississippi and Alabama. The recent Constrained Optimization Method (Conop program) is discussed in detail and its results are compared with the RASC and UAM outputs.

As Fåhreus used to say: "In recent years many biostratigraphic zonations proposed in the literature either imply or directly state such a fine biostratigraphic resolution that in many cases has to be considered beyond the point of practical reproducibility, i.e. correlations attempted back onto such zonations carry with them little or no precision." It should be clear since the beginning of our book that the power of resolution of the UA method is contained in the data under the study and not in the method itself. Our theoretical model is unique in providing a full analysis of the internal complexity of biochronological problems, and in this manner, it differs from all other quantitative methods available today.

Jean Guex

Acknowledgments

Several colleagues and friends with whom we had useful discussions are warmly thanked:

Špela Gorican, Luis O'Dogerthy, Arthur Escher, Dave Taylor, François Reuse, John H. Hubbard, Elizabeth Carter, Peter Baumgartner, Lucy Edwards, Junfeng Bai, Aymon Baud.

Contents

Chapter 1
Biochronological Scales

1.1 Introduction

The goal of the present book is to address once again the most classical problem of stratigraphy: how to use fossils to construct reliable relative time scales based on paleontological data. Such scales are what we call order relations and the durations of their units are not known.

There are three main types of scales

1. The discrete biochronological time scales where the units (Oppel Zones or Assemblage Zones) are based on the global fossil content of the sedimentary rocks. The Unitary Associations method explained below is designed to construct this kind of time scales.
2. The continuous relative time scales where the units (Interval Zones) are defined by the first or last occurrences of the taxa.
3. The continuous relative time scales where the units are defined by the relative abundance of the taxa (Abundance Zones or Acme Zones).

1.2 Discrete Biochronological Time Scales

The discrete biochronological scales are represented by a sequence of mutually exclusive associations of fossil taxa. Each unit of that scale is characterized by a diagnostic taxon or by the diagnostic co-occurrence of several taxa allowing to assign a relative chronologic position to a given fossiliferous bed.

The difficulties inherent to the construction of that scale are mainly caused by the discontinuities of the fossil record (discontinuous sedimentation, reworking, contaminations or condensations etc.), by the ecological control over the distribution of the faunas (resp. floras) and by biogeographical exclusions of taxa.

J. Guex et al., *Discrete Biochronological Time Scales*,
DOI 10.1007/978-3-319-21326-2_1

As a result, the data the biostratigrapher must use to construct biochronologic scales are sporadic because only a small fraction of the total duration and geographic distribution of each species is generally recorded in the sediments.

The problem of constructing our scale can be addressed by means of the following simple reasoning, assuming that all the taxa are correctly identified and that there is no reworking.

If a given taxon x_1 is present in sedimentary bed B, we conclude that B was deposited during the existence interval of x_1, noted $J(x_1)$. If B contains x_1 and x_2 we conclude that B was deposited during the interval of coexistence of x and y (or $J(x_1, x_2)$). Similarly if B contains n taxa, it was deposited during the interval of coexistence of the n taxa: $J(x_1, x_2, \ldots, x_n)$.

Suppose now that all the coexistence intervals we have found are strictly distinct from each other. That means that none of them is contained in another one. From a mathematical point of view, we say that all the intervals represent maximal sets of coexisting taxa. Each set is then characterized by the presence, in one of them, of a taxon x which is not present in the other set, and by the presence in the other of a taxon y which is not present in the first. In other words the maximality of the taxonomic sets guarantees the uniqueness of each association and is at the base of what we call the Unitary Associations (UAs) method.

That method is a deterministic mathematical model designed to construct concurrent range zones, like the ones illustrated in Fig. 1.1. The basic idea of the method is to construct a discrete sequence of coexistence intervals of species where each interval consists of a maximal set of intersecting ranges (=intervals of minimal duration or UAs). As noted above, each of these units is characterized by a set of species or species pairs allowing us to identify it in the stratigraphic sections.

We should note in passing that the fundamental rule which must be followed to construct a relative time scale based on inter-taxa coexistences is that all coexistences must be taken into consideration during the logical treatment of the data, at the exclusion of misidentifications and reworking (i.e. as noted above, those must be ignored). Rare coexistences are often of outstanding paleontological interest because they can reflect the true first evolutionary of a new phylum and it is a non-sense to eliminate them automatically during a computer analysis of the original data. We will see later (Chaps. 6 and 10) that several quantitative methods tend to systematically ignore rare coexistences.

The basic steps of the UA method are summarized in Fig. 1.1. In this figure we represent 4 stratigraphic sections with the local distribution of 10 species (1–10) which may be present or absent in the sections. The observed inter-species coexistences are compiled in the species-species matrix, also called the neighborhood matrix (or compatibility matrix). This matrix can be organized by a permutation of its rows and columns to allow the appearance of sets of mutually coexisting species. Note that such a permutation is based on a theorem given in Chap. 3 and explaining the properties of a lower triangular matrix. From this reorganized matrix we can extract maximal sets of intersecting species' ranges and represent them in a table called a UA range chart (referential). This chart is used to go back to the data and assign relative ages to the fossiliferous beds of the different sections, given in the

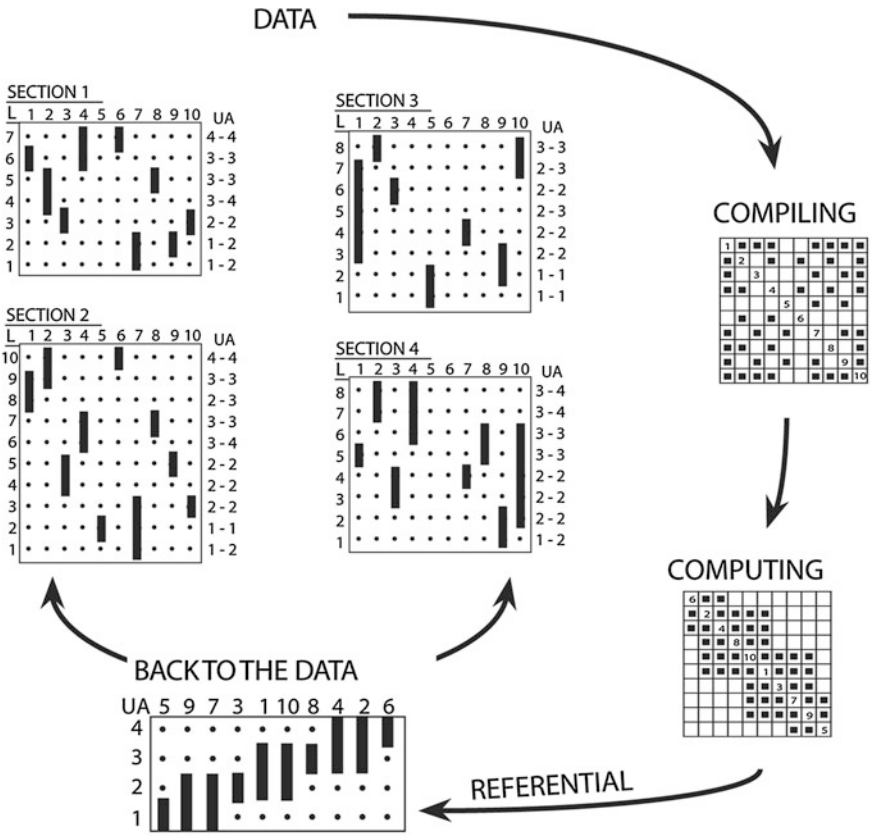

Fig. 1.1 Diagram explaining the basic steps of the Unitary Association method (see text)

column at the right of the stratigraphic sections (column UA). The code of each unit is duplicated for a simple reason: in many cases, one fossiliferous bed cannot be assigned to a single UA but to a union (or coalescence) of UAs. For example, beds 1 and 2 of section 1 are assigned to units 1 or 2 (noted as 1–2) because they contain only taxa existing during intervals 1 and 2. Bed 3 of the same section contains species 3 and therefore can be assigned strictly to unit 2 (hence the notation 2–2). Such standard age assignments give a clear view of the uncertainty of the age of the bed under consideration.

Biostratigraphic data are usually complicated by the fact that species' ranges are highly conflicting from place to place. In such cases it is not possible to operate the simple permutation given in Fig. 1.1. As an example, consider two pairs of coexisting species (*ad*) and (*bc*). We say that their ranges are conflicting if species "*a*" occurs below species "*c*" and if species "*b*" occurs below species "*d*" in some localities. Such stratigraphic relationships mean that either the range of "*a*" virtually overlaps that of "*c*" or that the range of "*b*" virtually overlaps that of "*d*" (see

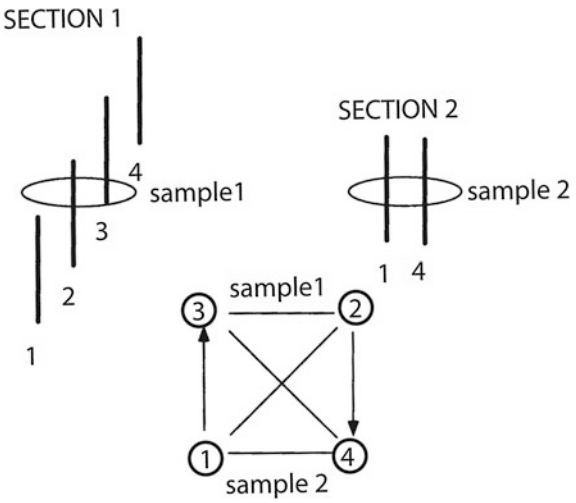

Fig. 1.2 Stratigraphic distribution of *4* species in two sections *1* and *2*: sample *1* contains species *2* and *3* and sample *2* contains species *1* and *4*: the two samples are simultaneously *above* and *below* each other. This is what we call a contradiction, i.e. the relation between samples *1* and *2* is cyclic

Fig. 1.2). Note that the most usual case of virtual coexistence, which we call the trivial case, is when a taxon "a" is found below a taxon "b" in one locality and in the reverse superposition in another locality. Such trivial virtual coexistences do not affect the data processing by permutation of the above matrix.

The computer program UAgraph discussed later in the present book optimizes the constructions of such virtual coexistences and produces discrete range charts where the conflicting stratigraphic relationships are expressed as virtual co-occurrences.

1.3 Diachronism of Datums and Interval Zones

The most usual case of inter-datum diachronism is illustrated in Fig. 1.3, showing that the relative stratigraphic positions observed locally among fossil species commonly are not constant from one place to the other: most species occupy apparently contradictory positions in the four different locations of our diagram. That diagram is based on the local stratigraphic distributions of the 10 taxa represented in Fig. 1.1 and shows that the lines of correlations linking the first occurrences of the taxa in the 4 different localities are affected by a multitude of crossovers, making it difficult to distinguish a chronologically significant event allowing a reliable correlation of the different stratigraphic sections.

That diagram also illustrates the fact that the stratigraphic position of a given taxon x can be recorded anywhere within its total existence interval, leading to contradictive chronological positions in the different fossil localities where the taxon is found.

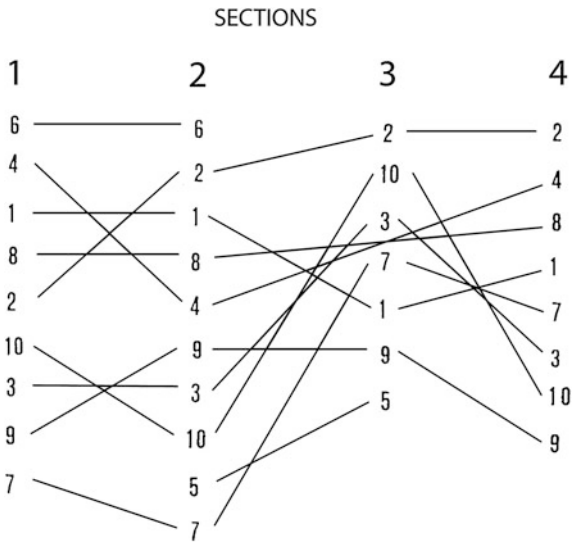

Fig. 1.3 Local stratigraphic distribution of the *10* species (*1–10*) represented in Fig. 1.1. The relative positions of the first local appearances of the 10 species in these sections are diachronous from one section to the other

Suppose that we have only paleontological data to demonstrate which of two contradictive datums is older than the other one, in the absence of any physical proxy (paleomagnetism, geochronology, lithological marker bed etc.). The only way to solve such a problem is to consider the stratigraphic position of the contradictive datums in relation to the taxa which are characteristic of the units of a discrete time scale. This allows to demonstrate that one datum is older in one given section than in the other. For example, the first local occurrence of taxon 10 in Fig. 1.3 is located below unit 2 in section 4 and above it in section 3.

The following theorem justifies the present reasoning.

1.4 Helly's Theorem

A very simple but fundamental theorem is hidden behind the above statement.

It is indeed important to keep in mind that the uniqueness of a coexistence interval of n species (a clique) can be established based on fragmentary biostratigraphic data coming from a great many localities (at most $(n^2 - n)/2$ localities in which only a pair of species is found each time).

This fundamental property of cliques whose vertices (i.e. the points of the graph) represent intervals is called Helly's property and it can be stated as follows: "If a family of intervals does not contain two disjoint intervals, then a point exists that is common to all of them."

We can prove this proposition as follows (Guex 1987).

Let:

$J = \{J_1, J_2, \ldots, J_n\}$ be a family of intervals;
x be the set of points of the interval J_i;
m_i and M_i be the minimum and maximum of J_i so that:

$$J_i = [m_i, M_i] = \{x | m_i \leq x \leq M_i \quad \text{for all } i\};$$

J_k be the interval with the smallest M_k;
J_j be the interval with the largest m_j.

By hypothesis, $J_j \cap J_k \neq \varnothing \Rightarrow m_i \leq M_k$ for all i. In other words we have: $m_i \leq M_k$ and consequently: $[m_j, M_k] = \cap [m_i, M_j] \neq \varnothing$.

It follows from this assertion that, in an interval graph (i.e. a graph representing a sequence of intervals), a maximal clique characterizes a unique interval. This interval of minimal duration is the intersection of all the intervals making up the maximal clique.

Further in this book we will demonstrate that the construction of interval zones based on datums is a problem which can be partly solved only when a robust relative chronological framework (order relation) based on co-occurrences has been established, allowing to know which datums can be used for correlations and which are diachronous and useless for direct correlations. We will also establish that several recent interval zonations pretend to a precision which is not realistic. The resolution of a relative time scale is usually inversely proportional to the lateral traceability of its units.

1.5 Relative Abundance Zones

Relative abundance zones are continuous biochronologic scales based on the abundances of taxa whose preservation is not selective (e.g. not diagenetically biased) vis-a-vis the different species of the group used. The subdivisions (Abundance Zones and Acme Zones) that make up such scales are contiguous. The Calpionellid zonation introduced by Remane in 1963 belongs to this category.

In cases where preservational bias is not prevalent, it can sometimes be useful to study the variations in frequencies and the apparent acme of species (i.e., the stratigraphic intervals in which a taxon is particularly abundant).

In using this kind of information in the unitary association method, we must consider the local apparent acme of a species x as a taxon x′, distinct from x.

1.6 Reproducibility, Superpositional Control and UA Zones

As already noted, the distribution of fossil taxa is controlled by two main factors: time and ecology, the latter being the most important when we consider short intervals of time.

To get an accurate idea of the respective influence of the two factors, we use a double-entry table whose rows correspond to the subdivisions of the referential ("range chart") and whose columns correspond to the stratigraphic sections under study. The sequences of subdivisions identified in the different sections are transcribed on this table, which we call a reproducibility matrix or reproducibility table.

In other words that table shows simultaneously the geographic location of the characteristic taxa of each unit and the superpositional control constraining their vertical distribution.

It is easy to realize that highly significant units (like ammonite zones) will show a strong superpositional control between widely distributed locations where the zones are identified. On the contrary, long ranging and ecologically sensitive fossil groups like the Radiolaria will show a scattered overall distribution and it will not be obvious how to establish a chronologically significant sequence of zones from such data (see Baumgartner et al. 1995 for a full discussion of that problem).

It should be obvious that unions (or coalescences) of adjacent and non-reproducible subdivisions of a referential acquire a lateral traceability which makes them useful for correlation, provided that their mutual superpositional control is robust.

In summary we can say that the only units (or unions of individually non-reproducible units) which can be identified over vast geographic areas by means of their characteristic species have a chance of being chronologically meaningful. Such subdivisions are said to be reproducible and we call them Unitary Association zones (=UAZ).

References

Baumgartner, P.O., Bartolini, A., Carter, E. S., Conti, M., Cortese, G., Danelian, T., De Wever, P., et al. (1995). Middle Jurassic to Early Cretaceous radiolarian biochronology of Tethys based on Unitary Associations. In P. O. Baumgartner, L. O'Dogherty, Š Gorican, E Urquhart, A Pillevuit & P. De Wever (Eds.), *Middle Jurassic to Lower Cretaceous radiolaria of Tethys: Occurrences, systematics, biochronology* (Vol. 23, pp. 1013–1038). Lausanne: Mémoires de Géologie.

Remane, J. (1963). Les Calpionelles dans les couches de passage Jurassique-Crétacé de la Fosse Vocontienne. *Travaux du Laboratoire de Géologie de Grenoble, 39*, 25–82.

Guex, J. (1987). Corrélations biochronologiques et Associations Unitaires (p. 244). Lausanne: Presses Polytechniques Romandes.

Chapter 2
Graph Theoretical Approach

Notations

A–B	Difference between sets A and B
$A \cup B$	Union of sets A and B
$A \cap B$	Intersection of sets A and B
$A \subset B$	A is a subset of B
$X \in A$	x is an element of A
$X \notin A$	x is not an element of A
$\|A\|$	Cardinality of A (=number of elements of A)
Ø	Empty set
$G = (X, E)$	Non-oriented graph (coexistences)
$Gs = (X, U)$	Oriented graph (superpositions)
$G^* = (X, E + U)$	Biostratigraphic graph
U	Set of arcs of *G*s and *G**
E	Set of edges of *G* and *G**
X	Set of vertices of *G*, *G*s and *G**
{x, y}	Edges of *G* and *G**
(x, y)	Arcs of *G*s and *G**
G^c	Complement of *G*
$\Gamma(x)$	Set of neighbors of x in *G* (neighborhood)
$\Gamma^+(x)$	Set of successors of x in *G*s and *G**
$\Gamma^-(x)$	Set of predecessors of x in *G*s and *G**
Z_n	Circuit of length n without chord in *G* and *G**
C_n	Cycle of length n in *G*s and *G**
S_n	Semi-oriented circuit of length n in *G**
$\Rightarrow$	Implies that
$\Longleftrightarrow$	If and only if
|	Such that
$\exists$	There exists
$\neq$	Different from

J. Guex et al., *Discrete Biochronological Time Scales*,
DOI 10.1007/978-3-319-21326-2_2

2.1 Representing Stratigraphic Relationships

The ideas summarized in Figs. 1.1–1.3 can be expressed with the help of certain aspects of graph theory. This field of applied mathematics provides several useful theorems for overcoming the concrete difficulties so often met in biochronology. In addition, its notation is convenient to describe the algorithms which are used in the UAgraph program both to explain the structure of difficult biostratigraphic data, and to construct unitary associations and identify them in fossil-bearing beds.

The basic concepts of graph theory have been made comprehensible to non-specialists in several classical works: Golumbic (2004) and especially Roberts (1976, 1978). Stratigraphers interested in the mathematical aspects of the problems discussed in the following chapters can refer to these books.

2.2 Definitions

2.2.1 Graph

In introducing the technical definitions that follow, we will first appeal to the paleontologist's intuition. Imagine that the fossil species whose relationships are being analyzed are represented by a set of points (or vertices) and by oriented or non oriented lines (arcs and edges): the resulting diagram is called a graph.

1. the stratigraphic superpositions observed among these species can be represented by arcs (arrows) joining the points. These arcs are, by convention, oriented in the sense x → y when species x has been observed below species y;
2. coexistences (observed or virtual) among the species are represented by edges (lines) joining the points y and z and indicating that y and z occur together.

The absence of known stratigraphic relation between two species (vertices of the graph) means that their relation is not defined.

Three kind of graphs should be distinguished in our discussion.

2.2.2 The Non Oriented Graph G

A non-oriented graph $G = (X, E)$ is composed of a finite set of points $X = \{x_1, x_2, \ldots, x_n\}$ and a family $E = \{e_1, e_2, \ldots, e_m\}$ of unordered pairs of distinct points of X.

Each pair $e = \{x, y\}$ of E is called an edge of the graph, and the points of X are called the vertices of the graph.

The order of the graph is the number of points of X. It is denoted |X|.

The edges of G (i.e. the elements of E) represent neighbour (or compatible) species. Edges that represent truly associated pairs of species (i.e. observed

coexistences) are called real edges; those that represent virtually associated pairs of species are called virtual edges.

Two vertices connected by an edge are neighbors in G. The set of neighbors of a vertex x is denoted $\Gamma(x)$: this set corresponds to the neighbourhood of the species x. It contains x.

The graph G in Fig. 2.1 represents the coexistences of species 1–8. Such a graph is called a coexistence graph.

The neighbourhood of species 4 (i.e. the set of neighbours of vertex 4 in G) is denoted $\Gamma(4) = \{2, 3, 5\}$.

2.2.3 The Adjacency Matrix of G

Let $G = (X, E)$ be a non-oriented graph. The adjacency matrix $A = (a_{ij})$ of G is defined by

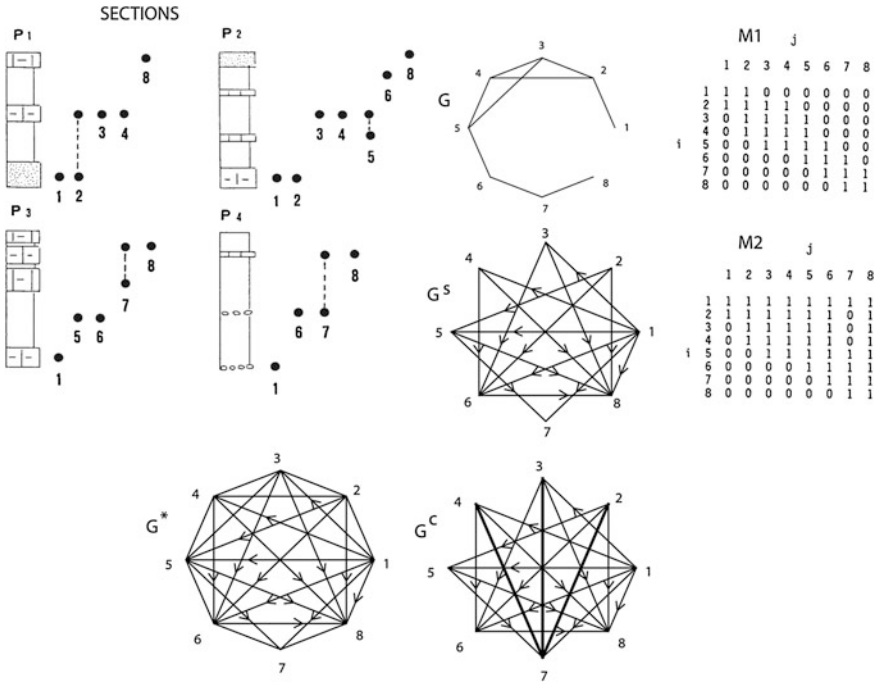

Fig. 2.1 Stratigraphic distribution of 8 species (*1–8*) in four imaginary sections (P_1–P_4). G Coexistence graph of the 8 species. M1 Species-species matrix associated with G. G^s Superposition graph of species *1–8*. G^* Biostratigraphic graph of species *1–8*. M2 Species-species matrix associated with G^*. G^c Semi-oriented complementary graph of G

$$a_{ij} = \begin{matrix} 1 & \text{if } x_i \text{ and } x_j \text{ are neighbors} \\ 0 & \text{otherwise.} \end{matrix}$$

The matrix M1 given in Fig. 2.1 is the adjacency matrix of the graph *G* in Fig. 2.1.

2.2.4 The Oriented Graph Gs

An oriented graph $Gs = (X, U)$ is a finite set $X = \{x_1, x_2, \ldots, x_n\}$ of vertices and a family $U = \{u_1, u_2, \ldots, u_m\}$ of ordered pairs of distinct vertices of *X*. Each such pair $u = (x, y)$ is called an arc of the graph.

Two incompatible species whose superposition is known form an arc of *Gs*; by convention the arc (x, y) means that species x lies beneath species y.

The species that have been observed above species x in stratigraphic sections form the set of successors of x: this set is denoted $\Gamma^{+}(x)$. Similarly, the species that have been observed beneath x form the set of predecessors of x; this set is denoted $\Gamma^{-}(x)$.

Such a graph is called a superposition graph *Gs*.

We will use the words pair and couple interchangeably, unlike some specialists in graph theory for whom pairs are unordered and couples are ordered.

2.2.5 The Biostratigraphic Graph G*

The semi-oriented graph $G^* = (X, E + U)$, which combines the edges (or arcs) of *G* and *Gs*, is called a biostratigraphic graph. It contains all available information about the stratigraphic relationships of species: neighborhoods (i.e. coexistences) and exclusions with known or unknown stratigraphic relationships (Fig. 2.1).

In the following pages, $X = \{x_1, \ldots, x_n\}$ denotes a set of fossil species. The stratigraphic relationships observed among the species of *X* can be expressed using a matrix $A = (a_{ij})$ as follows:

$$a_{ij} = \begin{matrix} 1 & \text{if} x_i \text{ is in the same level or in a lower level than } x_j \\ 0 & \text{otherwise.} \end{matrix}$$

This matrix *A* is the *adjacency matrix* of the biostratigraphic graph G^*. The edges of G^* represent pairs of chronologically coexisting species. Edges that represent truly associated pairs of species (i.e. observed coexistences) are called *real* edges; those that represent virtually associated pairs of species are called *virtual* edges (Fig. 2.1).

2.2.6 The Complementary Graph G^c

If G is a non-oriented graph, then the complementary graph G^c of G is the graph whose vertices are the same as the vertices of G, but where an edge (or an arc) connects two vertices precisely if no edge connects the vertices in G (Fig. 2.1).

In our biochronologic problem, the edges of G^c represent any exclusions of species (i.e. superpositions and undetermined stratigraphic relationships). In practice then, we must admit that some of those edges are already oriented: these orientations represent pairs of stratigraphically superposed species. This is why, in our problem, G^c is semi-oriented (Fig. 2.1).

2.2.7 Maximal Horizons and Residual Maximal Horizons

A fossil-bearing bed in an isolated stratigraphic section is a maximal horizon if the set of species that coexist in the bed is maximal (NB: in the framework of a study limited to the section).

The maximal horizons of a given section are separated from each other by separation intervals corresponding to the minimal intersections of existence intervals. In other words, all the beds located between two minimal intersections (= separation intervals) are equivalent to the maximal horizon framed by them.

Maximal horizons that are strictly distinct from each other in all sections(with regard to the inclusion relationship) are called residual maximal horizons.

2.3 Basic Technical Terms

2.3.1 Chain, Circuit and Chord

In a non-oriented graph G, a chain is an alternating sequence of distinct vertices and edges beginning and ending in a vertex. The length of the chain is the number of its vertices.

A circuit is a closed chain. A chord is an edge connecting two non-consecutive vertices of a circuit. A circuit of length n admitting no chords is denoted Zn. See Fig. 2.2.

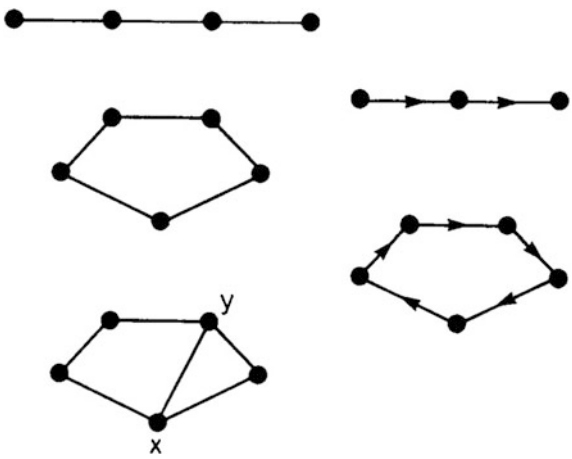

Fig. 2.2 Chain of length 4. Z_5 circuit. Chord: the edge {x, y} is a chord of the Z_5 circuit. Path of length 3. C_5 cycle

2.3.2 *Path, Maximal Path, Cycle and Strongly Connected Graph*

A path in an oriented graph *Gs* = (X, U) is a sequence of arcs (u1, u2,…, un), such that the end vertex of each arc coincides with the beginning vertex of the next arc in the sequence (Fig. 2.2). A path is maximal if it is not a subpath of any longer path.

A Cn cycle is a closed path (Fig. 2.2), i.e. the end-point of its last arc coincides with the origin of its first arc.

An oriented graph *Gs* = (X, U) is strongly connected if, for every pair of vertices x and y, there is a path from x to y and a path from y to x.

2.3.3 *Subgraphs, Generated Subgraphs and Strong Components*

Let H = (X, F) be a graph. A graph H′ = (X′, F′) is a subgraph of H = (X, F) if X′ is a subset of X and F′ is a subset of F.

If H′ contains all the edges (resp. arcs) connecting vertices of X′, then H′ is a generated subgraph of H.

The graph H′ in Fig. 2.3 is a subgraph of H, and H″ is a generated subgraph of H.

A strongly connected subgraph of an oriented graph *Gs* is called a strong component of *Gs*.

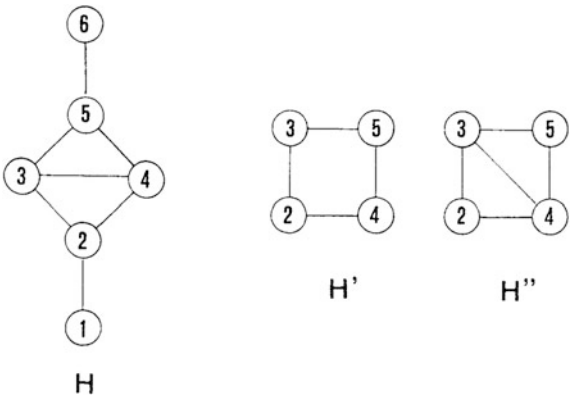

Fig. 2.3 H′ is a subgraph of H and H″ is a generated subgraph of H

2.3.4 Semi-oriented Circuit

Our biostratigraphic graph *G** is semi-oriented; similarly we will say that a sequence of edges and arcs is a semi-oriented circuit if all the edges in that sequence can be oriented to make a cycle. Such structures will be denoted Sn, where n is the number of vertices.

The graphs S3 and S4 in Fig. 2.4 are semi-oriented circuits: they represent conflicting stratigraphic relationships of species 1, 2 and 3 (for S3) and species 4, 5, 6 and 7 (for S4). These structures will be studied in detail in the following chapters.

2.3.5 Orientation of a Graph

2.3.5.1 Transitive Orientation

An oriented graph $Gs = (X, U)$ is transitive if whenever $(x, y) \in U$ and $(y, z) \in U$, then $(x, z) \in U$.

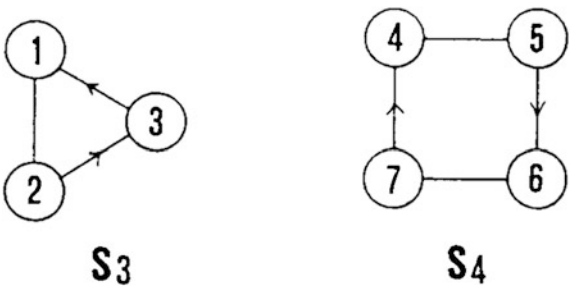

Fig. 2.4 Semioriented graphs of length 3 and 4 denoted S_3 and S_4

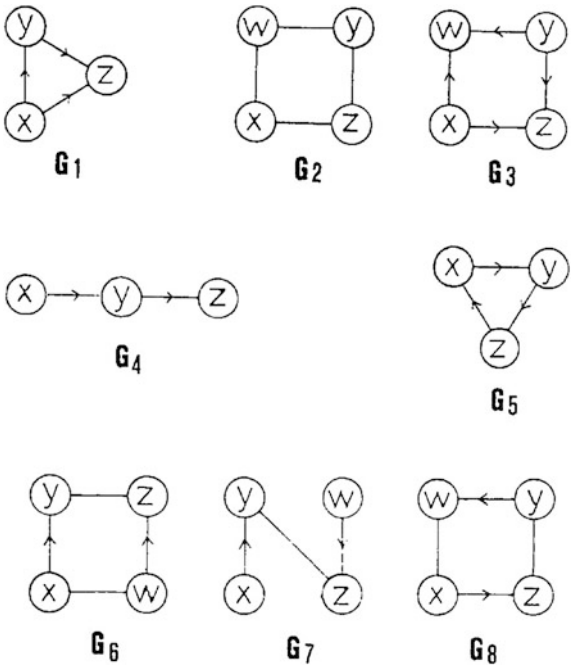

Fig. 2.5 Examples of transitive graphs (G_1 and G_3), non-transitive graphs (G_4 and G_5), transitively orientable graphs (G_2 and G_8) and non-transitively orientable graphs (G_6 and G_7)

Graphs G_1 and G_3 of Fig. 2.5 are transitive, but graphs G_4 and G_5 are not: the arc (x, z) is missing.

2.3.5.2 Transitively Orientable Graph

A non-oriented graph is transitively orientable if and only if an orientation can be chosen for all the edges so that the resulting oriented graph is transitively oriented.

Graph G_2 of Fig. 2.5 is transitively orientable: G_3 is a transitive orientation of G_2.

The properties of transitively orientable graphs are described in detail in Roberts (1976) and Golumbic (2004).

2.3.5.3 Orientability of a Semi-oriented Graph

A semi-oriented graph is transitively orientable if its partial orientation can be extended to an orientation making the resulting oriented graph transitively oriented.

2.3.5.4 Examples

Four examples of transitively orientable and non-transitively orientable graphs are given in Fig. 2.5.

1. The edge {x, z} of graph G_6 is lacking; if the edge {y, z} of G_6 is oriented in the direction y → z, the graph is not transitive. Since the edge {y, w} is also lacking, the opposite orientation of {y, z} also fails to make G_6 transitive.
2. As above, the edges {x, z} and {y, w} of graph G_7 are both lacking; neither orientation of {y, z} makes G_7 transitive.
3. Graph G_8 of Fig. 2.5 is transitively orientable: G_3 is a transitive orientation of G_8.
4. If the edges {2, 7}, {3, 7} and {4, 7} are given the orientations (2, 7), (3, 7) and (4, 7), the graph of Fig. 2.1 H becomes transitively oriented.

2.3.6 *Clique, Maximal Clique and Unitary Association*

A clique of G is a collection of vertices, each of which is a neighbor of every other. A clique is maximal if it is contained in no larger clique. Maximal cliques will be denoted *k*.

Strictly speaking, a maximal clique has only real edges. A *unitary association*, however, is a maximal clique of which some edges may be virtual. We will use the same notation for maximal cliques and for unitary associations.

2.3.7 *Incidence Matrix and Maximal Clique Matrix*

Let $X = \{x_1, x_2, \ldots, x_n\}$ be a set of n vertices and $S = \{s_1, \ldots, s_m\}$ be a family of m subsets of X. The subset-vertex incidence matrix is the m by n matrix (m rows and n columns) whose (i, j)th entry (ith row, jth column) is 1 if vertex x_i belongs to subset s_j and 0 otherwise.

The subset-vertex incidence matrix in which S represents the maximal cliques of a graph G and X represents the vertices of G is called the maximal clique matrix of G.

Figure 1.1d is a subset-vertex incidence matrix where the subsets $UA_1, \ldots, UA_4$ are precisely the maximal cliques of the graph G in Fig. 2.1. This matrix is the maximal clique matrix of *G* in Fig. 2.1.

2.3.8 Consecutive 1's Property

A matrix composed of 1's and 0's has the consecutive 1's property if its rows can be permuted so that the 1's in each column have no 0's between them (Fig. 2.1 M1).

2.3.9 Triangular Matrix

A matrix is upper (resp. lower) triangular if all the entries beneath (resp. above) its main diagonal are 0.

2.3.10 Triangulated Graph

A non-oriented graph is triangulated if all its circuits of length greater than 3 have a chord.

2.3.11 Forbidden Generated Subgraph

If a class of graphs is defined by requiring that no elements of some explicit list of subgraphs appear as generated subgraphs, this class will be said to be defined by forbidden subgraphs.

For instance, triangulated graphs are defined by forbidding the list of graphs Zn, $n > 3$.

2.3.12 Asteroidal Triple

Vertices x, y, z of a non-oriented graph G form an asteroidal triple if there exists a chain C_1 between x and y, a chain C_2 between x and z, and a chain C_3 between y and z, such that there is no edge between z and C_1, y and C_2 or x and C_3.

Figure 2.6 shows one example of asteroidal triple.

2.3.13 Interval

Technically, an interval is a line segment, which we will take to be closed, i.e. containing its own extremities.

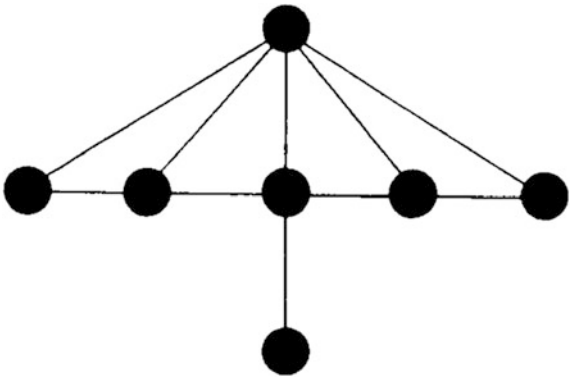

Fig. 2.6 Example of asteroidal triple

In our problem, we will be concerned with the time intervals corresponding to the life span of species, already called existence intervals. We should not expect an existence interval to be entirely recorded in a single section, or the record of an existence interval in different sections to be synchronous.

By convention we consider that if a fossil species has a discontinuous vertical distribution in a given stratigraphic section, it is considered as virtually present in all the beds that are flanked by its first local appearance and disappearance.

2.3.14 Intersection Graph

Let S be a set, and $A = \{A_1, \ldots, A_n\}$ be a family of subsets of S. The intersection graph of (A, S) has one vertex x_i for each subset A_i, and an edge joining x_i to x_j if and only if $A_i \cap A_j \neq \emptyset$.

For instance, to Fig. 2.1 we can associate a set S consisting of four distinct time axes T_1, T_2, T_3, T_4, one for each section, and subsets $A_1, \ldots, A_8$ of S, $A_i \cap T_k$ being the observed (and partially recorded) existence interval of the ith species in the *k*th section. Figure 2.1 (M1) is the intersection graph of this family.

More generally, the same procedure allows us to interpret any coexistence graph as an intersection graph.

2.3.15 Interval Graph

The intersection graph of a family of intervals on a line is called an interval graph.

This means that if $J = \{J_1, \ldots, J_n\}$ is a family of intervals, then the corresponding intersection graph has a set $X = \{x_1, \ldots, x_n\}$ of vertices, with an edge connecting x_i and x_j if and only if J_i and J_j intersect.

For instance, the graph in Fig. 2.1 is an interval graph. This is not obvious from the definition, and will not generally be true of coexistence graphs. However, it is easy to verify that this one is the interval graph associated to the intervals of Fig. 2.1.

References

Golumbic, M. (2004) Algorithmic graph theory and perfect graphs. *Annals of Discrete Mathematics 57*, 340.

Roberts, F. (1976). *Discrete mathematical models*. New Jersey: Prentice Hall. 559 p.

Roberts, F. (1978). *Graph theory and its application to problems of society* (Vol 29, 122 p.). Philadelphia: NFS-CBMS Monograph.

Chapter 3
Interval Graphs and Stratigraphic Contradictions

3.1 Main Characterizations

We have already seen above that a discrete biochronological range chart strictly corresponds to the maximal clique matrix associated to an interval graph. The literature contains several characterizations of such graphs. Three basic theorems are particularly adapted to linking graph theory with our biochronologic problems; they are due to Fulkerson and Gross (1965), Gilmore and Hoffman (1964) and Lekkerkerker and Boland (1962). The interpretation of these theorems will allow us to establish clearly what kind of contradictive stratigraphic relationships should be particularly studied to transform any biostratigraphic graph G^* into an interval graph.

3.2 Fulkerson and Gross (1965)

A graph G is an interval graph if and only if its maximal clique matrix has the consecutive 1's property.

3.2.1 Discussion

This statement concerns the relationship between a discrete biochronologic referential and the maximal clique matrix of an interval graph. For example, the referential given in Fig. 1.1d has the consecutive 1's property, and its associated graph is an interval graph.

J. Guex et al., *Discrete Biochronological Time Scales*,
DOI 10.1007/978-3-319-21326-2_3

This indicates that constructing a referential is the same problem as transforming a coexistence graph (representing the local intersections of partially recorded existence intervals) of species into an interval graph.

3.3 Gilmore and Hoffman (1964)

A graph G is an interval graph if and only if (1) G has no Z_4 as generated subgraph; (2) the complementary graph G^c admits a transitive orientation.

3.3.1 Discussion

We first observe that the theorem characterizes interval graphs by forbidden generated subgraphs.

Clearly, a Z_4 circuit does not represent a sequence of intervals on a line (Fig. 1.2). More generally the reader will easily realize that any graph containing chordless Z_n circuits ($n > 4$) as generated subgraphs does not represent such a sequence.

Figure 3.1 shows three different kinds of circuits of length 4 that appear frequently as generated subgraphs in a biostratigraphic graph.

Property (2) of the theorem can be understood as follows: if two intervals of an oriented line do not intersect, then one lies above the other; this induces an orientation on the complementary graph that is clearly transitive. One can verify easily that the edges of a graph can be transitively oriented if and only if this graph has no non-transitively orientable generated subgraphs. In other words, the generated subgraphs of G^c that are not transitively orientable are (by definition) forbidden configurations in the complement of an interval graph.

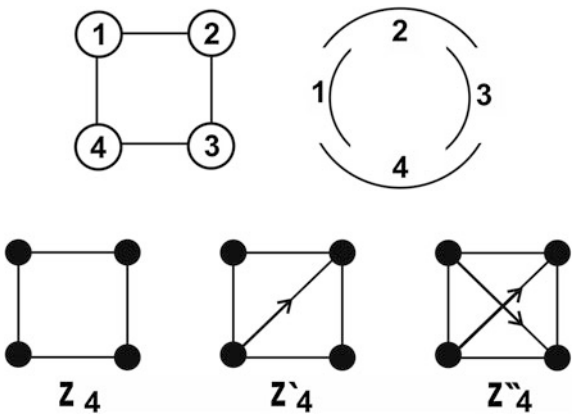

Fig. 3.1 Most common circuits of length 4

The practical consequences of the second condition of this theorem are not evident and should be discussed in some detail.

We begin by recalling that in the problem studied here, the edges of G^c represent mutual exclusions of species. These exclusions have two possible origins:

1. The stratigraphic relationship between two species (x and y) is undetermined, for the species have never been found together in the same section.
2. x and y are only observed in stratigraphic sequence (they are never found in the same bed).

In the case of our particular problem, this means that some orientations of edges of G^c are imposed by the stratigraphic observations that must be interpreted during the process of constructing our discrete scale. These orientations are those of the arcs of G^* that represent observed superpositions of the species. It is this constraint that led us to define G^c as a semi-oriented graph whose edges represent undetermined stratigraphic relationships and whose arcs represent superpositions.

It means that our problem of transforming G into an interval graph is a double problem: not only must we determine whether G^c is transitively orientable but also (and most important) we must determine whether the orientations of its arcs can be completed to make a transitive orientation.

Taking into account the above discussion, this means that we must also detect the generated subgraphs of G^c that are not transitively orientable (and of course those that are not transitive). These subgraphs are the forbidden configurations of the complement of our biostratigraphic graph G^*: they correspond precisely to the graphs representing conflicting (i.e. cyclic) stratigraphic relationships of fossil species. The most common are the C3 cycles and the semi-oriented S3 and S4 circuits of the biostratigraphic graph G^* (Fig. 2.4).

3.4 Lekkerkerker and Boland (1962)

A graph G is an interval graph if and only if it is triangulated and does not admit asteroidal triples as generated subgraphs.

3.4.1 Discussion

This theorem is very useful since it enables us to limit drastically the number of forbidden configurations that must be detected in a biostratigraphic graph G^*. However, as far as our problem is concerned, the presence of asteroidal triples (Fig. 2.6) in G (i.e. the non-oriented part of G^*) has no consequence for the transformation of this graph into an interval graph: these structures are generated by species whose distribution is limited to restricted biogeographic domains and they are automatically destroyed by the algorithm described in Sect. 4.12.

3.4.2 *Technical Remark: Difference Between a Maximal Clique and a Unitary Association*

In our problem, a maximal clique that has virtual edges may contain disjoint intervals. For this reason we must distinguish between the terms maximal clique and unitary association. It is clear that in general, a unitary association is a union of maximal cliques.

In practice, unitary associations and maximal cliques have identical properties. Thus we will use the same notation for these two objects in all the set-theoretical calculations (complements, unions and intersections) we will perform later.

3.5 Guex (1987)

If a vertex-vertex incidence matrix is triangular and has, vertically, the consecutive 1's property, then its rows are cliques.

Proof Let $A = (a_{ij})$ be a triangular matrix with:

$$a_{ij} = \begin{matrix} 1 & \text{if } x_i \text{ is a neighbor of } x_j \text{ and if } i \leq j \\ 0 & \text{otherwise.} \end{matrix}$$

Let $\Gamma_h(x_i) = \{x_j | a_{ij} = 1\}$
Let $\Gamma_v(x_i) = \{x_j | a_{ji} = 1\}$
The property of consecutive 1's means that for all x and y such that

$$\Gamma_h(x) \cap \Gamma_v(y) \neq \emptyset$$
$$\text{either } x \in \Gamma_v(y)$$
$$\text{or } y \in \Gamma_v(x).$$

We wish to prove that $\Gamma_h(x_i)$ is a clique.
To do this we must prove that all x and $y \in \Gamma_h(x_i)$ are neighbors.
If x and $y \in \Gamma_h(x_i)$, then $\Gamma_v(x)$ and $\Gamma_v(y)$ contain x_i.
Thus $\Gamma_v(x) \cap \Gamma_v(y) \neq \emptyset$ implies that, because of the consecutive 1's property

$$\text{either } x \in \Gamma_v(y)$$
$$\text{or } y \in \Gamma_v(x).$$

In both cases x and y are neighbors.

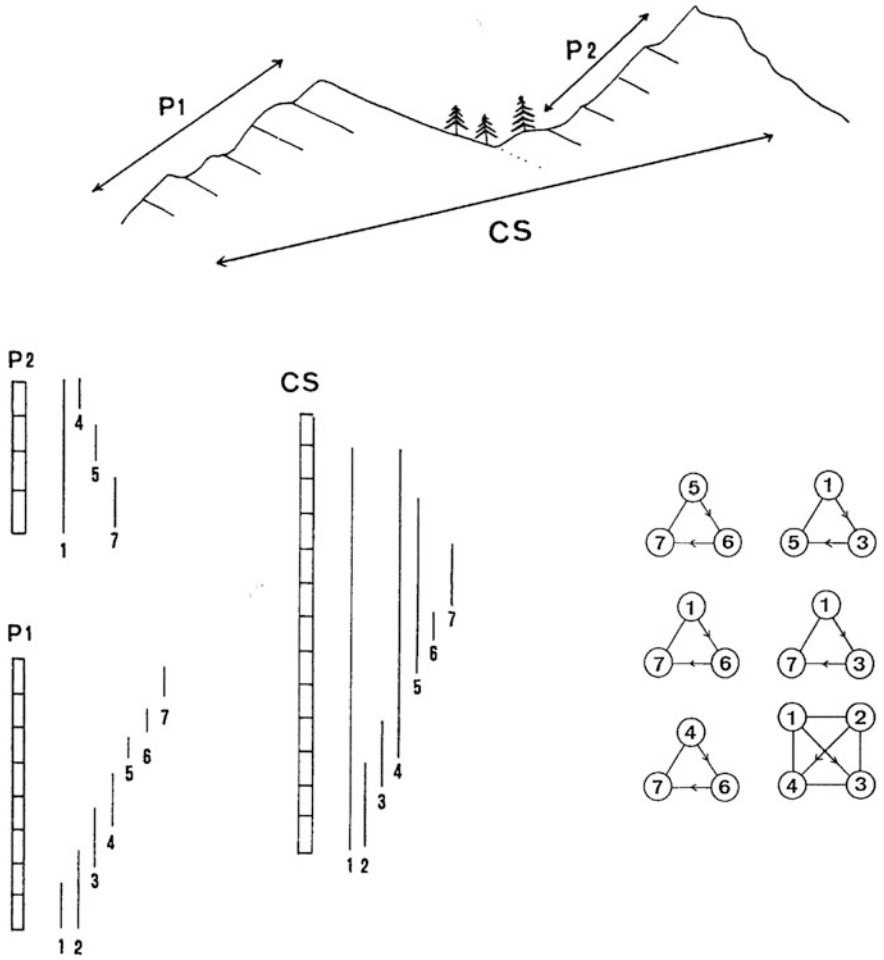

Fig. 3.2 Two imaginary sections (P_1 and P_2) whose superposition gives a composite section (CS). Stratigraphic distribution of 7 species in P_1 and P_2. Synthesis of these ranges in the composite section CS. Cyclic generated subgraphs associated to the conflicting stratigraphic relationships between species 1 and 7 when P_1 and P_2 are considered separately

Remark It is obvious that the maximal clique-vertices incidence matrix that corresponds to the triangular matrix considered here also has the consecutive 1's property. Therefore the graph associated to it is an interval graph. The manual method of searching for unitary associations that we described in Fig. 1.1 is based on the above theorem.

3.6 Technical Remark About Composite Sections

Before going further we can note that the existence of these conflicting structures is partially due to the obvious fact that the local stratigraphic sections record only a very small portion of the existence domains of the species. Figure 3.2 shows in a simple way that the prior construction of composite sections enables us to immediately eliminate some of these configurations. The relationships of the species whose ranges are sketched in Fig. 3.2 generate six subgraphs that represent conflicting stratigraphic relationships. These forbidden configurations do not appear if we use geological arguments, such as marker lithologic levels or marker biostratigraphic horizons. Such arguments allow the superposition of sections P1 and P2 in order to work on a unique composite section CS.

Composite sections should also be made when treating data collected from several and dispersed biogeographical realms (see Chap. 7). In such cases it is worthwhile to treat each realm separately and then calculate the final UAs with the restricted number of synthetic numerical range charts of each region established by UAgraph.

The user can also make his choice of separate treatment by using the option "similarities between sections" of the program to start comparing the sections which have the most species in common and then the ones with more endemic faunas. This was done in the book on Jurassic—Cretaceous radiolarian UAZ 95 (Baumgartner et al. 1995).

References

Baumgartner, P. O., Bartolini, A., Carter, E. S., Conti, M., Cortese, G., Danelian, T., De Wever, P., Dumitrica, P., et al. (1995). Middle Jurassic to Early Cretaceous radiolarian biochronology of Tethys based on Unitary Associations. In P. O Baumgartner, L. O'Dogherty, Š. Gorican, E. Urquhart, A. Pillevuit & P. De Wever (Eds.), *Middle Jurassic to Lower Cretaceous radiolaria of tethys: Occurrences, systematics, biochronology* (Vol. 23, pp. 1013–1038). Lausanne: Mémoires de Géologie.

Fulkerson, D. R., & Gross, O. A. (1965). Incidence matrices and interval graphs. *Pacific Journal of Mathematics 15*(3), p835–p855.

Gilmore, P. C., & Hoffman, A. J. (1964). A characterization of comparatibility graphs and of interval graphs. *Canadian Journal of Mathematics, 16*, 539–548.

Lekkerkerker, C. B., & Boland, J. C. (1962). Representation of finite graphs by a set of intervals on the real line. *Fundamenta Mathematicae 51*, 45–64.

Chapter 4
The UA Method and the UAgraph Program

4.1 Introduction

The logical steps of the UA method described below are strictly followed by the UAgraph program of Hammer and Guex. For that reason each step of the method will be illustrated by an example of application of that program.

4.2 The Ilerdian Alveolinids from Yougoslavia

In the following pages we will analyze once more a concrete problem that is significantly difficult. It concerns data published by Drobne (1977) on the stratigraphic distribution of the Ilerdian alveolinids from Yugoslavia. In that problem, the number of conflicting stratigraphic relations between the species is more than twice the size of the database (36 forbidden subgraphs vs. 15 species: see Figs. 4.1 and 4.2).

The discussion is limited to analyzing the relationships of the 15 species of alveolinid with the largest geographical distribution in the territory studied by Drobne.

The identifications considered uncertain (cf. or aff. in Drobne 1977) have been omitted from our list (see below).

The local stratigraphic distribution of the 15 species is given in appendix 1-C. This table shows only associations and superpositions observed locally among the species: only the maximal horizons generated by relationships among the species are considered.

Horizon 4 of section 1 (Drobne's sample Fatji-hrib-5) contains a reworked fauna. Note that this fact makes the problem particularly interesting as it gives us an opportunity to discuss some problems related to the biochronologic discontinuities in the distribution of some taxa. The graph G^* representing the stratigraphic

J. Guex et al., *Discrete Biochronological Time Scales*,
DOI 10.1007/978-3-319-21326-2_4

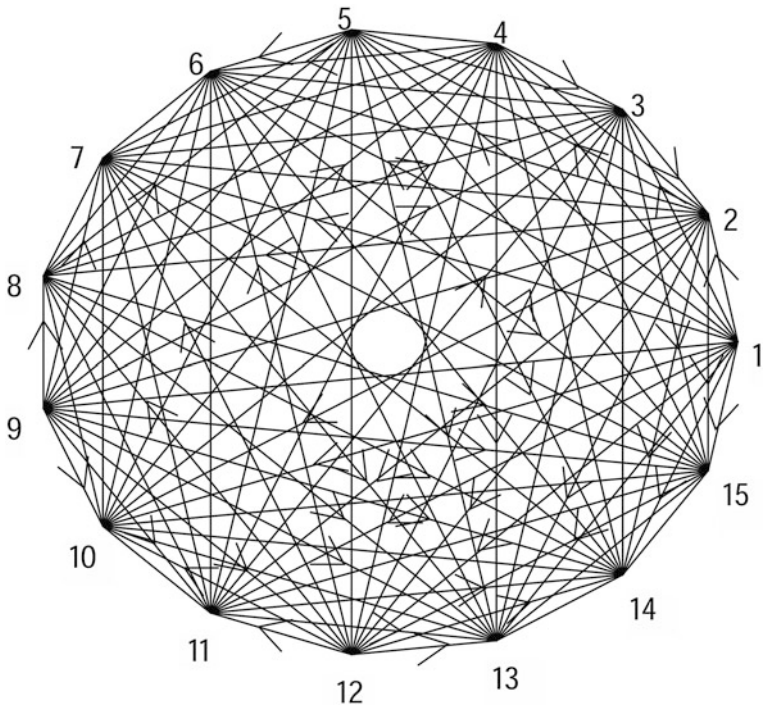

Fig. 4.1 Biostratigraphic graph of the alveolinids given in Appendix 1-C

relationships among these alveolinids is illustrated in Fig. 4.1 and the stratigraphic contradictions hidden in this graph are illustrated in Fig. 4.2.

4.3 Graphical User Interface and Tools Provided by the UAgraph Program

4.3.1 Description

Figure 4.3 illustrates the different options offered by the graphical user interface of UAgraph. Most of the keys are self-explanatory but we will of course apply them to illustrate the kind of outputs produced by the program. This will lead the reader to realize that the U.A.M. is basically a powerful tool designed to analyze the complexity of biochronological problems and secondarily, in the cases where the data are sufficiently reliable, a tool to make robust correlations.

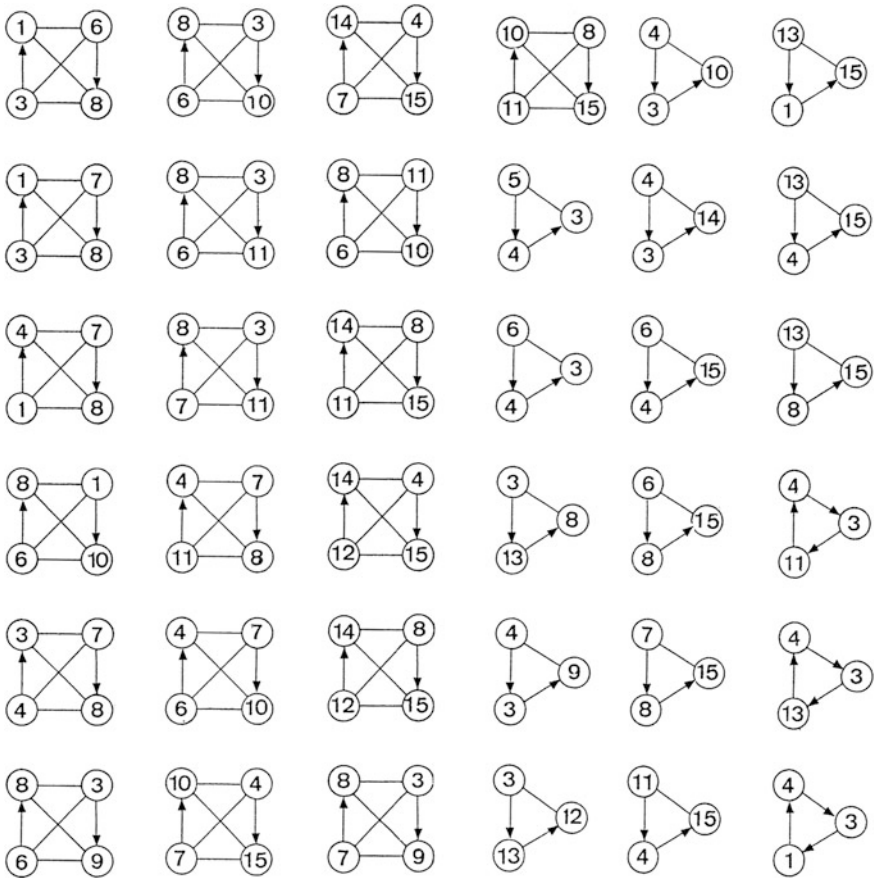

Fig. 4.2 Graphs showing the stratigraphic contradictions hidden in the alveolinids biostratigraphic graph

4.3.2 Input of the Data

The data can be uploaded into the program in two different ways.

1. By using the local vertical ranges of the species which is called the DATUM input. In that case we recall that if a species has a discontinuous vertical distribution in a stratigraphic section, it is considered as virtually present in all the horizons that are flanked by its first local appearance and disappearance ("range through").
   For a given stratigraphic section, the standard UAGraph data input is a triplet of numbers:
   Species number code, FAD (first appearance "datum") level number code, LAD (last appearance "datum") level number code.

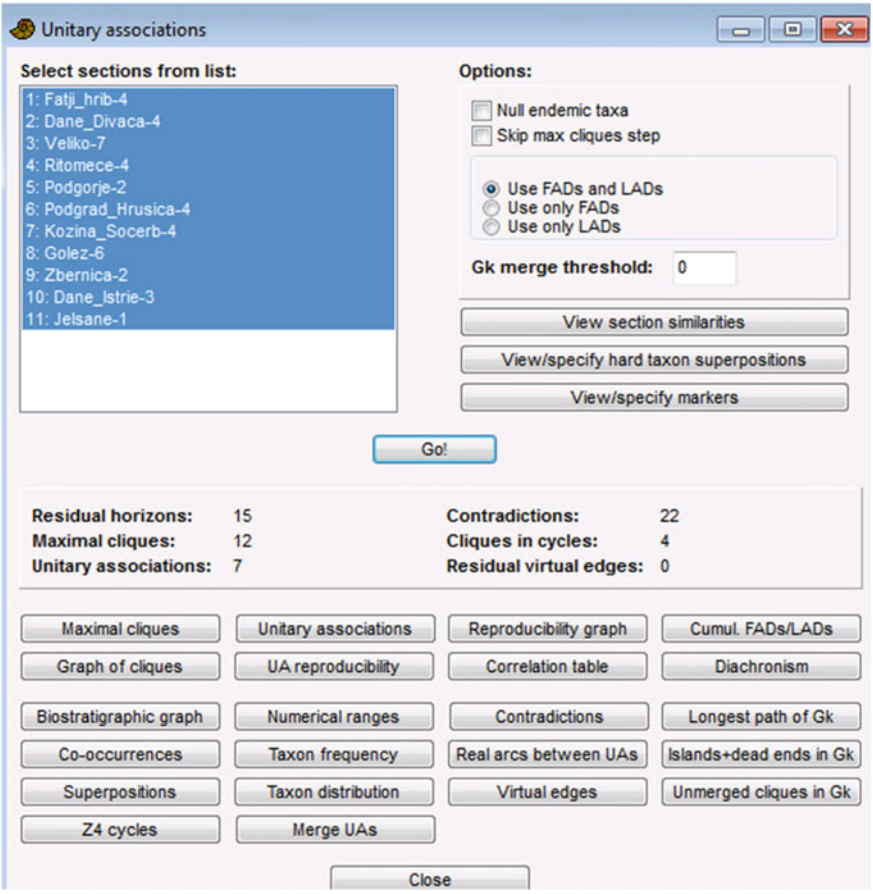

Fig. 4.3 Menu of the UAgraph program

For example, the alveolinid ranges in Drobne's section 1 are: 2 1 1, 3 4 4, 4 3 3, 6 2 2, 7 3 3, 8 4 4, 12 3 3 (see Appendix 1-C).

2. The second kind of input is by giving the lists of taxa (codes) present in each stratigraphic level. This is called the SAMPLES input. It is more time consuming to compile that kind of input but has the enormous advantage to facilitate the detection of taxa which are affected by discontinuities in their global range (see below), because those discontinuities are already recorded in the input file.

   The stratigraphic input file must be saved as txt format (*.txt). It can be accompanied by a file called dictionary (extension *.dct) containing the list of the taxa names. The filename must be the same as the stratigraphic file, except for the extension (i.e. dct). When such a file is made available, the range chart computed by UAgraph will provide the full taxonomic names (genera and

species) in the columns giving the ranges of the taxa. Examples are given in the taxonomic appendices.

4.3.3 Special Choices

4.3.3.1 Null Endemic Taxa

This choice will force the program to ignore taxa present in only one section.

4.3.3.2 Skip Maximal Cliques Step

Allows the user to get an exact output of the inter-samples contradictions (i.e. before computing the maximal cliques). This is important during the phase where the user analyses the internal structure and the complexity of his problem.

4.3.3.3 Fads Only or Lads Only

Produces the oriented graph of the inter-fads (resp inter-lads) relationships. Allows to find some of the datums which are not diachronous or weakly diachronous. The program treats the datums as if they were intervals and not punctual events.

4.3.3.4 View Similarities

View the statistical similarities between the sections.

4.3.3.5 Hard Superposition

Allows the user to declare that one superposition cannot be transformed into a virtual coexistence, due to the internal contradictions of the data.

4.3.3.6 Outputs Which Are Self-explanatory

In this category we include the following outputs. The way of establishing them is explained in the following theoretical part (Sect. 4.4).

Maximal cliques
Unitary associations
Reproducibility graph
Graph of cliques

UA reproducibility
Correlation table
Diachronism
Longest path of G_k
Co-occurrences
Taxon frequency
Real arcs between UAs
Superpositions
Virtual edges
Z4 cycles (list)

The special outputs which need more explanation are discussed in Sect. 4.3.3.7 etc.

4.3.3.7 Cumulated Fads-Lads

This output gives a bivariate relation between the number of Fads in a given UA and the number of Lads in the same UA. The plot gives a clear picture of the evolutionary rates of the taxa which are considered in the database. Of course it does not make sense to introduce non biochronologic events such as paleomagnetic zones into the database used for an evolutionary purpose. One application is discussed in detail in Sect. 7.3 (Fig. 7.2).

4.3.3.8 Biostratigraphic Graph

That output contains an analytical tool to compare the biostratigraphic graph of a given problem with the biostratigraphic graph of a solution produced by another program. An example of application is given in Sect. 6.9 where the concept of "average range" in Conop and Rasc, leading to enormous range reductions, is discussed.

4.3.3.9 Numerical Range

This output gives the ranges of the taxa in terms of UAs. For example if taxon n starts in UA i and ends in UA j, it will be noted n i j in the numerical range table.

That file can be introduced into other data files to make easy correlations with new data etc.

4.3.3.10 Contradictions

This output gives the total number of arcs going from one sample i to another sample j together with the list of arcs going from j to i. In other words it provides the list of contradictive superpositions linking the two samples.

4.3.3.11 Merge UAs

This option is designed to give the possibility to merge UAs to establish chronologically significant zones (in general zones are coalescences of UAs), with large lateral traceability and strong superpositional control.

4.4 The UA-Method

*4.4.1 Constructing Maximal Cliques of G**

The enumeration of maximal cliques of a graph is well known to be an NP-complete problem. In other words, the number of maximal cliques can grow exponentially as the number of vertices of the graph increases (see Golumbic 2004 for a discussion and Moon and Moser 1963 for the first theorem concerning extremal graphs generated by the maximal clique problem).

To impose a limit to the number of operations to be done by the computer program UAgraph we have developed a technique where the clique construction is based on the maximal residual horizons. In that procedure, each maximal horizon of the stratigraphic database which is analyzed by the program is augmented by one taxon if the neighborhood of this taxon contains the maximal horizon which is considered (see below for details). The consequence of this is that the total number of maximal cliques constructed by the program cannot exceed the number of samples studied in the stratigraphic database. Another consequence is that all the maximal cliques of the graph under consideration are not necessarily constructed at the end of this operation. Such omitted cliques are recovered when the clique graph G_k is transformed into an interval graph, at the end of the computations.

To construct the maximal cliques of the biostratigraphic graph G^* using residual maximal horizons, we proceed as follows.

Let k_m be the residual horizon with the greatest cardinality, and let $\Gamma(x_i)$ be the set of neighboring vertices of x_i in G^*.

- If $k_m - \Gamma(x_i) = \varnothing$, we add x_i to k_m ((x_i) is compatible (neighbor) with all the elements of k_m). The result is then denoted $k_m{}^* = \{k_m \cup x_i\}$.
- To $k_m{}^*$ we then add the next element x_j, for which $k_m{}^* - \Gamma(x_j) = \varnothing$ ($k_m{}^*$ thus becomes equal to $\{k_m \cup x_i \cup x_j\}$). We thus compare the enlarged $k_m{}^*$ successively to all the vertices of G^*.

- At the end of this operation, we eliminate all the residual horizons that are contained in $k_m{}^*$, then we follow the same procedure for the next k_m, etc. The resulting $k_m{}^*$ are now distinct cliques of G^*.

4.4.2 Example

The first step of the calculation consists of constructing the residual maximal horizons in our alveolinid problem. This first output is given in Table 4.1. The residual horizons are denoted by the code of their origin locality name.

Using the original database (Appendix 1-C), we establish the biostratigraphic graph G^* showing the relationships between the taxa (Fig. 4.1).

The second calculation consists of constructing the maximal cliques from the residual horizons, and eliminating horizons that are not maximal at the end of this operation.

Residual horizons whose initial content has been augmented are denoted $k_{i,j}{}^*$ in the following discussion.

In the example studied here, we note that the horizon Kozina 4 (={7, 13, 15}) is included in $\Gamma(6)$ (see Table 4.1b). This set thus becomes Kozina 4* = {6, 7, 13, 15}. Similarly, we see that Veliko 3 (={6, 7, 13}) is included in $\Gamma(15)$. This set thus becomes Veliko 3* = {6, 7, 13, 15}. Since Veliko 3* = Kozina 4* we eliminate Veliko 3* from the list of maximal cliques (Table 4.1). We also see that Ritomece 3 (= {4, 9, 10, 14}) is included in $\Gamma(8)$, so it becomes Ritomece 3* = {4, 8, 9, 10, 14} etc…

The list of initial maximal cliques constructed by UAgraph is given in the following Table 4.2.

4.5 Stratigraphic Relationships Among the Maximal Cliques

4.5.1 The Three Main Kinds

The stratigraphic relationship between two maximal cliques, k_i and k_j, can be deduced from the relationships observed among the species belonging respectively to k_i and to k_j. Three kinds of relationships exist.

- The clique k_i is above (or below) k_j if there exists at least one species of k_i that is above (or below) a species of k_j (unambiguous superposition).
- The relationship between k_i and k_j is undetermined if the species of k_i are not compatible with those of k_j and if their superpositional relationships are undetermined.
- The relationship between k_i and k_j is conflicting if some species of k_i are above some species of k_j, while other species of k_i are below some species of k_j.

Table 4.1 *A* Residual maximal horizons of the Alveolinids sections. *B* $\Gamma(x_i)$ (=edges of G^*) (Appendix 1-C)

A	Species															
	1	2	3	4	5	6	7	8	9	10	11	12	13	14	15	
Zbernica-2	0	0	0	0	0	1	0	0	0	1	0	1	0	0	0	(6, 10, 12)
Golez-1	0	1	0	0	1	0	0	0	0	0	0	0	0	0	0	(2, 5)
Golez-5	0	0	0	0	0	0	0	1	0	0	0	0	0	1	0	(8, 14)
Kozina_4	0	0	0	0	0	0	1	0	0	0	0	0	1	0	1	(7,13,15)
Ritomece-2	1	0	0	0	0	0	0	1	1	0	1	1	0	0	0	(1, 8, 9, 11, 12)
Ritomece-3	0	0	0	1	0	0	0	0	1	1	0	0	0	1	0	(4, 9, 10, 14)
Ritomece-4	0	0	0	0	0	0	0	0	1	1	0	0	0	1	1	(9, 10, 14, 15)
Veliko-2	0	0	1	0	0	1	1	0	0	0	0	0	0	0	0	(3, 6, 7)
Veliko-3	0	0	0	0	0	1	1	0	0	0	0	0	1	0	0	(6,7,13)
Veliko-4	0	0	0	0	0	0	0	0	0	0	0	1	0	0	1	(12,15)
Veliko-5	0	0	0	0	0	0	0	0	0	0	1	0	0	0	1	(11,15)
Dane_Div-1	0	0	1	0	1	0	1	0	0	0	0	0	0	0	0	(3, 5, 7)
Dane_Div-3	1	0	0	0	0	1	1	0	1	0	1	1	0	0	0	(1, 6, 7, 9, 11, 12)
Fatji_hrib-3	0	0	0	1	0	0	1	0	0	0	0	1	0	0	0	(4, 7, 12)
Fatji_hrib-4	0	0	1	0	0	0	0	1	0	0	0	0	0	0	0	(3, 8)

B	$\Gamma(x_i)$ (=edges of G*)
1	6, 7, 8, 9, 11, 12
2	5
3	5, 6, 7, 8, 12
4	7, 8, 9, 10, 12, 14
5	7
6	7, 9, 10,1 1, 12, 13, 15
7	9, 11, 12, 13, 15
8	10, 11, 12, 14, 15
9	11, 12, 14, 15
10	12, 14, 15
11	12, 15
12	15
13	15
14	15

4.5.2 Example

The relationship between $k1{,}4^*$ and $k12{,}4$ is conflicting: 6 arcs are going from $k1.4$ to $k12.4$ and 5 arcs are going in the opposite direction (see Fig. 4.4). Note that the numbers next to arcs show reproducibility (number of times the superposition is observed)

Table 4.2 List of initial maximal cliques constructed by UAgraph

12 Golez-1	2, 5
11 Golez-5*	4, 8, 9, 10, 14
10 Veliko-4*	6, 7, 9, 11, 12, 15
9 Fatji-hrib-4*	3, 8, 12
8 Zbernica-2*	6, 9, 10, 12, 15
7 Kozina-Socerb-4*	6, 7, 13, 15
6 Veliko-2*	3, 6, 7, 12
5 Dane Divaka-1	3, 5, 7
4 Fatji-hrib-3*	4, 7, 9, 12
3 Ritomece-4	9, 10, 14, 15
2 Ritomece-2	1, 8, 9, 11, 12
1 Dane Divaka-3	1, 6, 7, 9, 11, 12

Once the stratigraphic relationships of the cliques have been established, they are entered in a "maximal clique-maximal clique" matrix M from which we contruct the oriented graph G_k associated to it (Fig. 4.5)

4.5.3 Searching for and Eliminating Contradictions

To transform a biostratigraphic graph into an interval graph by ordering its maximal cliques according to raw biostratigraphic observations, it is clearly essential to eliminate any contradictory superpositions of species generating conflicting relationships between the cliques.

This can be done in two ways. The first consists of detecting all the forbidden configurations of G^* and replacing certain superpositions by deduced virtual coexistences. This was done in our first program Guex and Davaud (1984). The second consists of ignoring certain contradictory and poorly reproducible superpositions between two maximal cliques.

The UAgraph program uses the latter approach. It is based on the following principle: faced with two conflicting superpositions, we are forced to admit (in the absence of non-biochronologic arguments) that a superposition that is reproducible (i.e. observed over a vast geographic area) has more chronologic "value" than one that is not. In other words, if two distinct cliques of G^* contain species that situate them both above and below each other, we will in each case consider as "true" the superposition that is more reproducible and as "false" (i.e.: generated by insufficient documentation, by reworking or bad taxonomy) the superposition that is less reproducible.

To do this, we proceed as follows. For each pair k_i, k_j of maximal cliques of G^* showing a contradictory stratigraphic relationship, we define two sets of arcs, A and B, where A is the set of arcs that links the elements of k_i to those of k_j (in the direction $k_i \rightarrow k_j$) and where B is the set of arcs (of the opposite orientation) that

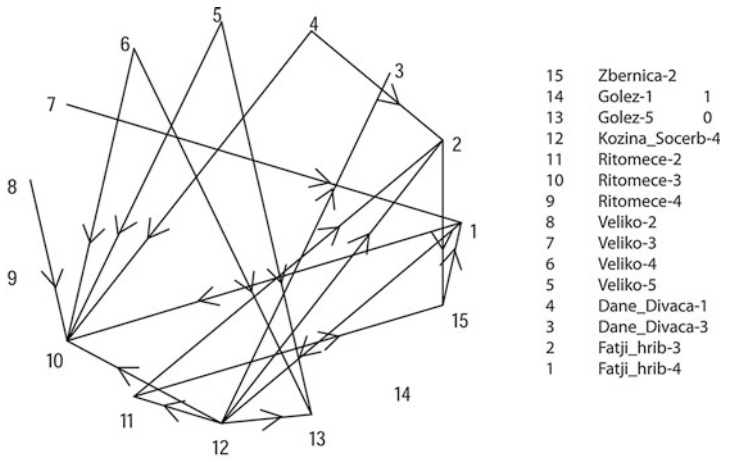

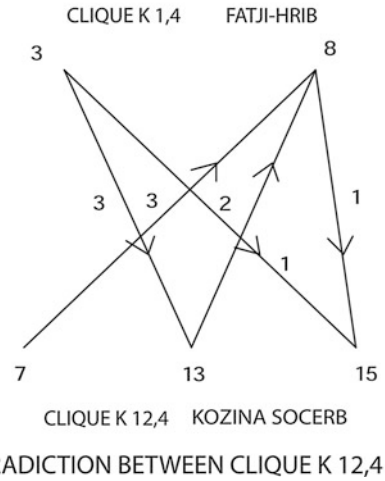

Fig. 4.4 Graph showing the contradictions between the 15 residual maximal horizons and detail of the contradictions between cliques $k12{,}4$ and $k1{,}4$. The values associated to the arcs linking the taxa represent their reproducibility

links the elements of k_j to those of k_i. To each set A and B we attribute a value $V(A)$ (resp. $V(B)$) equal to the sum of the individual reproducibilities of the arcs belonging to A (resp.B) added to the number of arcs of A (resp.B).

If $V(A) > V(B)$ we say that the clique k_j is "located above" k_i (keeping in mind that this is an abuse of language and that the superposition is conflicting).

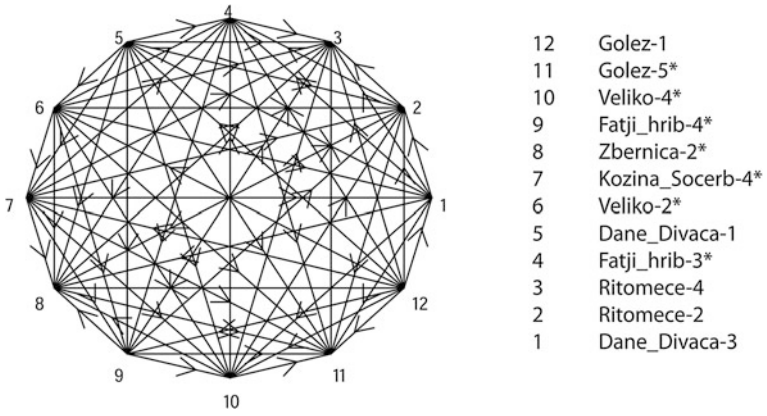

Fig. 4.5 Alveolinid graph G_k

If $V(A) = V(B)$ we say that the stratigraphic relationship between k_i and k_j is undetermined.

This procedure is equivalent to making a global search for the forbidden configurations of G^* (Fig. 4.2).

4.5.4 *Technical Remark About the Optimal Preservation of the Initial Arcs of G**

In an earlier version of the program designed to construct the Unitary Associations (Guex and Davaud 1984) we used an optimization procedure based on the following reasoning. To begin, all the generated C_3, S_3, S_4 and Z''_4 subgraphs (e.g. see Fig. 4.2) are detected, and the pairs of arcs jointly implicated in these structures are recorded in an arc-arc matrix $T = (t_{ij})$ where:

$$t_{ij} = \begin{matrix} 1 & \text{if the arc i is jointly implicated with the arc j in a forbidden generated subgraph} \\ 0 & \text{if not.} \end{matrix}$$

Figure 4.6 shows an example of graph consisting in six imbricated Z''_4. The arc-arc matrix T highlights the fact that arc $1 \rightarrow 2$ is jointly implicated with the six other arcs (i.e. $3 \rightarrow 4$, $3 \rightarrow 5$, $3 \rightarrow 6$, $4 \rightarrow 5$, $4 \rightarrow 6$, $5 \rightarrow 6$).

Replacing arc $1 \rightarrow 2$ by a virtual edge is sufficient to destroy all the forbidden subgraphs of length 4. Doing so we preserve a maximum of information on the species' superpositional relationships, while eliminating as many forbidden configurations as possible.

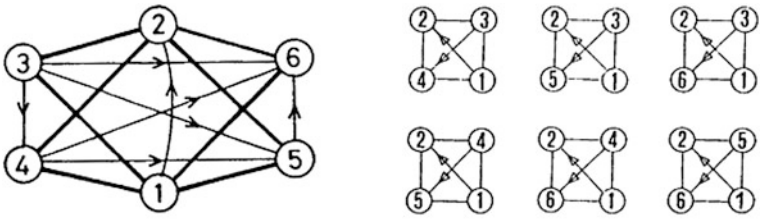

ARC-ARC MATRIX T

	1,2	3,4	3,5	3,6	4,5	4,6	5,6
1,2	1	1	1	1	1	1	1
3,4	1	1	0	0	0	0	0
3,5	1	0	1	0	0	0	0
3,6	1	0	0	1	0	0	0
4,5	1	0	0	0	1	0	0
4,6	1	0	0	0	0	1	0
5,6	1	0	0	0	0	0	1

Fig. 4.6 Graph consisting in six imbricated Z''_4. The arc-arc matrix T shows that arc $1 \rightarrow 2$ is jointly implicated with the six other arcs in the circuits of length 4

We note however that arc $1 \rightarrow 2$ is the only one which represents a reproducible superposition (it must be observed in at least 6 distinct localities).

From that point of view this is a weakness of the algorithm because what we want is to find the strongest chronological constraints which are given by the lateral traceability and by the inter-units superpositional control of the relative time scale and not by its apparent number of units. There is no correlation between the number of units and the quality of a biochronological scale, contrary to a popular belief. This is the reason why we have modified our optimization method. In the new program UAgraph, that procedure has been abandoned in favor of a routine which destroys the conflicting superpositions by taking simultaneously, for each conflicting stratigraphic inter-horizon contradiction, the number of arcs plus the sum of their individual reproducibility.

Note that in one of it's options, Sadler's (2006) Conop program uses a method of optimization which is almost identical to the one of our T-matrix, in order to preserve a bigger number of superpositions, at the expense of the lateral reproducibility.

4.5.5 *Strongly Connected Components of G_k*

4.5.5.1 Detection and Destruction

Poorly documented biostratigraphic data (polluted by undetected reworking, by false taxonomic identifications or by highly discontinuous record of the species) often are responsible for the presence of strongly connected components (cycles) in G_k. These components must of course be eliminated.

The algorithm used to detect them is similar to the one described by Carre (1979, p. 47): we will not discuss the latter further here.

In our program, the connected components are destroyed according to the following rule:

Consider, in a given component of G_k, the set of pairs (k_i, k_j) of cliques whose deduced stratigraphic relationship is conflicting (i.e. $\rightarrow$ or $\leftarrow$ in the matrix M). We denote A the set of arcs that link k_i to k_j and B the set of arcs of opposite orientation. To each set A and B we attribute a value $V(A)$ (resp. $V(B)$) equal to the sum of the individual reproducibilities of the arcs belonging to A (resp.B) added to the number of arcs of A (resp.B) (see above). To each arc $k_i \rightarrow k_j$ we now attribute a value

$$C_{ij} = \min(V(A);\ V(B))/\max(V(A);\ V(B))$$

The arc $k_i \rightarrow k_j$ for which the value C_{ij} is the greatest is destroyed (the relationship k_i,k_j is considered to be undetermined). If this undetermination is not sufficient to destroy the connected component, we proceed in the same way for the next couple (k_i, k_j), etc.

4.5.5.2 Example

In our example, the oriented graph G_k associated to the matrix M contains a strongly connected component (Fig. 4.7): ${k_{3,4}}^*, k_{4,2}, {k_{1,3}}^*, {k_{1,4}}^*$. The destruction of the arcs ${k_{1,4}}^* \rightarrow {k_{3,4}}^*$ and $k_{4,2} \rightarrow {k_{1,3}}^*$ results in the destruction of the component.

4.5.5.3 Technical Remark

It is essential to stress the fact that in the case of particularly poor data, the destruction of the connected components takes place in a quasi-arbitrary fashion, and depends on the order in which G_k is examined. Such situations can be detected by permuting the order of the stratigraphic sections in the input (which has the effect of modifying the indexing of the maximal horizons and consequently that of the vertices of G_k). If the solutions thus obtained differ from one output to the next, it is then necessary to generate virtual coexistences artificially by grouping the

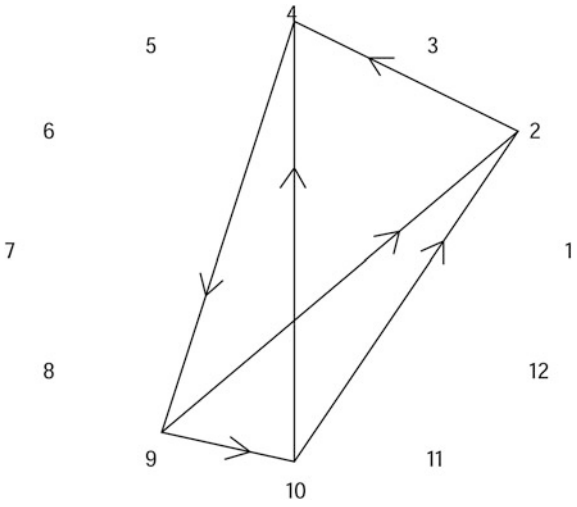

Fig. 4.7 Strongly connected component of the Alveolinid G_k graph (Fig. 4.5)

unitary associations whose characteristic elements were permuted: the different positions that were assigned to them in the different solutions tested result from the fact that their real chronologic relationships are impossible to determine.

4.6 Maximal Paths of G_k

After destroying all cyclic configurations present in G_k, we can finally start the process of extracting the Unitary Associations by analyzing the maximal path of this graph.

A path of G_k can be characterized by the list of its vertices. We call such a list a vector. The length of this vector equals the number of elements it contains.

Let K = {{k}} be the set of unitary associations whose superpositional relationships are represented by G_k.

Let V = {{v}} be a (variable) set of vectors of elements of K, all the vectors the same length, and each representing a partial path of G_k.

Initialization: V = the set of vectors of length 1 that consist of the elements $k_1 \cap$ K such that $\Gamma^+(k_1) = \emptyset$.

Algorithm: at each step we associate to each element v = (k_1, k_2, …, k_n) of V the set of vectors (k_1, k_2, …, k_n, k_{n+1}) such that k_{n+1} is an immediate predecessor of kn (in other words: $\Gamma^+(k_{n+1}) \cap \Gamma^-(k_n) = \emptyset$).

If k_n has no immediate predecessor, we write (k_1, k_2, …, k_n) which is then a maximal path of G_k, and we eliminate it from V.

The maximal path calculated by UAgraph in our current problem is given in Table 4.3. (numbering 1–12: see Table 4.5)

Table 4.3 Maximal path of G_k

3	(12)	Ritomece-4
11	(11)	Golez-5*
8	(10)	Zbernica-2*
2	(9)	Ritomece-2
9	(8)	Fatji_hrib-4*
4	(7)	Fatji_hrib-3*
10	(6)	Veliko-4*
1	(5)	Dane_Divaca-3
7	(4)	Kozina_Socerb-4*
6	(3)	Veliko-2*
5	(2)	Dane_Divaca-1
12	(1)	Golez-1

4.7 Reduction of G_k to a Unique Path

The graph G_k of superpositions between maximal cliques will generally not consist of a simple sequence of cliques, but contain parallel paths and sometimes even several disconnected parts. It is therefore necessary to find the longest possible linear path L through the graph, forming a "backbone" of the graph which will be used as the basis for the zonation. The algorithm for finding the longest path L through the graph of cliques G_k given above (Sect. 4.6 from Guex 1991) is conceptually simple, but somewhat cumbersome to implement in the computer. We therefore decided to use another algorithm for finding L.

First, a topological ordering of G_k (=a linear ordering of its vertices) is found using a standard algorithm (Cormen et al. 1990), such that whenever we have an arc from x to y, the ordering visits x before y. The algorithm for the construction of a topological ordering T from a graph G proceeds as follows.

list T = empty
while (G is not empty)
  find a vertex v with no incoming arc
  delete v from G
  add v to T

Given a topological ordering, we can trivially calculate the distance d(s,y) from a given vertex s to all other vertices y:

for each vertex y in a topological ordering of G (starting with vertex s)
choose arc (x, y) maximising $d(s, x)$ in the set of vertices already visited

$$d(s, y) = d(s, x) + 1$$

In other words, the algorithm traverses the graph in topological order starting from *s*, always calculating distance at the present vertex as one plus the maximal distance from *s* to any of its immediate predecessors. Using this algorithm, the head (bottom, or first vertex) and tail (top, or last vertex) of the longest path are selected.

The distances from the head to all vertices are then calculated again, and the longest path is finally constructed starting at the tail, following arcs in the reverse direction back towards the head such that the precomputed distance from head to the present vertex always decreases by exactly one unit.

4.8 "Dead Ends" and "Islands" of G_k

The graph of cliques G_k may contain "dead ends" (vertices without predecessors or successors in the longest path) and "islands" (disconnected components). Since their stratigraphic position with respect to the longest path will normally be uncertain, the user is provided with a list of cliques in dead ends and islands of G_k. They are found by investigating each clique *k* using the set of predecessors $\Gamma^-(k)$ and the set of successors $\Gamma^+(k)$:

(a) If the intersection of *L* and $\Gamma^-(k)$ is empty, and the intersection of *L* and $\Gamma^+(k)$ is empty, then *k* is in an island (a component disjunct from *L*).
(b) If one and only one of the intersections of *L* with $\Gamma^-(k)$ and *L* with $\Gamma^+(k)$ is empty, then *k* is in a "dead end".

4.9 Threshold Value for Merging the Cliques

Cliques not contained in the longest path *L* of G_k may be merged with cliques in the longest path based on a "best fit" criterion (Guex 1991), such that a clique outside *L* is merged with its most similar clique within *L*. Cliques not merged with any clique in *L* will be called *lost cliques*. A number of new procedures have been developed for the handling and presentation of such cliques and the taxa they contain.

In UAgraph, the user can set a value for the percentage of taxa shared between the two cliques (relative to the total number of taxa in the two cliques only) necessary before a merge is allowed. By setting this threshold to 0, a merge is always allowed, as long as there is at least one shared taxon. A value of 100 will ensure that the best fit procedure is never used, and all cliques not in *L* will be lost except in the case of "sandwiched" cliques (see below). This is useful for providing

the maximally conservative result, at the cost of reducing the reproducibility of the unitary associations. Values between 0 and 100 allow any trade-off between robustness and reproducibility to be selected.

4.10 Rescue of Lost Cliques Sandwiched Between Two Cliques in *L*

There is one special case where a lost clique, not allowed to merge with any clique in L by the best fit procedure, can still be confidently placed in L and a merge be allowed. This is when the lost clique x is placed above a vertex a and below a vertex b in L such that there is only one clique y between a and b in L. x is then allowed to merge with y, and is removed from the set of lost cliques.

Search for a vertex y in L such that both:

The immediate predecessor y_p of y in L is an element of the set of predecessors of x in G_k
The immediate successor y_s of y in L is an element of the set of successors of x in G_k.

4.11 Calculation of Possible Range of a Lost Clique

Even when a clique x can not be merged with any specific clique in L, a total possible range within L can still be calculated simply from the topology of G_k, using the following rules (Fig. 4.2):

1. If x is in an island, then the total possible range is L (no information is available)
2. If the intersection of L with $\Gamma^{-}(x)$ is zero, then x is in a dead end pointing downwards (towards the head of L). The clique must then be below the lowest element of the intersection of L with $\Gamma^{+}(x)$.
3. If the intersection of L with $\Gamma^{+}(x)$ is zero, then x is in a dead end pointing upwards (towards the tail of L). The clique must then be above the highest element of the intersection of L with $\Gamma^{-}(x)$.
4. If x is neither in an island or a dead end, then x must be above the highest element of the intersection of L with $\Gamma^{-}(x)$ and below the lowest element of the intersection of L with $\Gamma^{+}(x)$.

As we are primarily interested in these ranges with respect to UA indices rather than clique indices, the indices must be updated through the later additions to and removals from the set of cliques in L in the process of producing the final UAs.

As mentioned above, the fact that UAgraph may leave some cliques unmerged with L can cause the "loss" of taxa only found in those cliques. In the UA range chart, these taxa are shown in gray, with a total range which is equal to the union of the ranges of the cliques in which the taxon is found.

4.12 Longest Maximal Path and Unitary Associations

The last step of the method consists of transcribing the species content of the cliques of that reduced graph L into the maximal cliques—species incidence matrix associated to it.

This matrix records the discontinuities in the stratigraphic distribution of the species. To give it the consecutive 1's property, it is sufficient to replace with 1's the 0's that are flanked by 1's in the columns (sometimes called "range through" method).

In the end only the rows of the resulting matrix that correspond to maximal cliques are conserved (the others are eliminated): each row of this final compacted matrix corresponds to a unitary association and the graph associated with it is an interval graph (see Table 4.4).

Table 4.4 Successive steps (*A*–*C*) starting from the reduced unique maximal path of G_k (column K) and the range-through operation leading to the compacted Unitary Associations 1–7

A															
Species															
K	1	2	3	4	5	6	7	8	9	10	11	12	13	14	15
12	0	0	0	0	0	0	0	0	1	1	0	0	0	1	1
11	0	0	0	1	0	0	0	1	1	1	0	0	0	1	0
10	0	0	0	0	0	1	0	0	1	1	0	1	0	0	1
9	1	0	0	0	0	0	0	1	1	0	1	1	0	0	0
8	0	0	1	0	0	0	0	1	0	0	0	1	0	0	0
7	0	0	0	1	0	0	1	0	1	0	0	1	0	0	0
6	0	0	0	0	0	1	1	0	1	0	1	1	0	0	1
5	1	0	0	0	0	1	1	0	1	0	1	1	0	0	0
4	0	0	0	0	0	1	1	0	0	0	0	0	1	0	1
3	0	0	1	0	0	1	1	0	0	0	0	1	0	0	0
2	0	0	1	0	1	0	1	0	0	0	0	0	0	0	0
1	0	1	0	0	1	0	0	0	0	0	0	0	0	0	0
B															
Species															
K	1	2	3	4	5	6	7	8	9	10	11	12	13	14	15
12	0	0	0	0	0	0	0	0	1	1	0	0	0	1	1

(continued)

Table 4.4 (continued)

B															
Species															
11	0	0	0	1	0	0	0	1	1	1	0	0	0	1	1
10	0	0	0	1	0	1	0	1	1	1	0	1	0	0	1
9	1	0	0	1	0	1	0	1	1	0	1	1	0	0	1
8	1	0	1	1	0	1	0	1	1	0	1	1	0	0	1
7	1	0	1	1	0	1	1	0	1	0	1	1	0	0	1
6	1	0	1	0	0	1	1	0	1	0	1	1	0	0	1
5	1	0	1	0	0	1	1	0	1	0	1	1	0	0	1
4	0	0	1	0	0	1	1	0	0	0	0	1	1	0	1
3	0	0	1	0	0	1	1	0	0	0	0	1	0	0	0
2	0	0	1	0	1	0	1	0	0	0	0	0	0	0	0
1	0	1	0	0	1	0	0	0	0	0	0	0	0	0	0
C															
Species															
K	1	2	3	4	5	6	7	8	9	10	11	12	13	14	15
7	0	0	0	1	0	0	0	1	1	1	0	0	0	1	1
6	0	0	0	1	0	1	0	1	1	1	0	1	0	0	1
5	1	0	1	1	0	1	0	1	1	0	1	1	0	0	1
4	1	0	1	1	0	1	1	0	1	0	1	1	0	0	1
3	0	0	1	0	0	1	1	0	0	0	0	1	1	0	1
2	0	0	1	0	1	1	1	0	0	0	0	0	0	0	0
1	0	1	0	0	1	0	0	0	0	0	0	0	0	0	0

4.13 Residual Virtual Edges

The procedure described above does not take into account the virtual edges in the initial step of the calculations. This is because (by definition) the pairs of species that correspond to these edges are not observed in any maximal horizon. In general these edges are generated artificially during the transformation of G^* into an interval graph. When this is not the case, we use a detecting procedure that enables us to recover them during the last step of the calculations (Table 4.5).

A residual virtual edge is detected if there is an original arc $x_j \rightarrow x_i$ when x_j belongs to an UA (k_{k+n}) located above the UA k_k containing x_i (Fig. 4.8).

To recover the virtual edge we must optimize the preservation of the arcs connecting x_i (resp. x_j) and its successors (resp. predecessors) present within the interval $k_k \ldots k_{k+n}$.

Let $A = (k_{k+1} \cup \ldots \cup k_{k+n}) - k_k$ and $B = (k_k \cup \ldots \cup k_{k+n+1}) - k_{k+n}$.

Table 4.5 Restoration of a residual arc

SPLIT	1	2	3	4	5	6	7	8	9	10	11	12	13	14	15
U.A.3 (j)	0	0	1	0	0	1	1	0	0	0	0	1	1	0	1
U.A.3 (i)	0	0	1	0	0	1	1	0	0	0	0	1	1	0	1
RESTORE	1	2	3	4	5	6	7	8	9	10	11	12	13	14	15
U.A.3 (j)	0	0	1	0	0	1	1	0	0	0	0	1	0	0	1
U.A.3 (i)	0	0	1	0	0	1	1	0	0	0	0	0	1	0	1
REDUCE	1	2	3	4	5	6	7	8	9	10	11	12	13	14	15
U.A.4 =	1	0	1	1	0	1	1	0	1	0	1	1	0	0	1
U.A.3 (j)	0	0	1	0	0	1	1	0	0	0	0	1	0	0	1
U.A.3	0	0	1	0	0	1	1	0	0	0	0	0	1	0	1

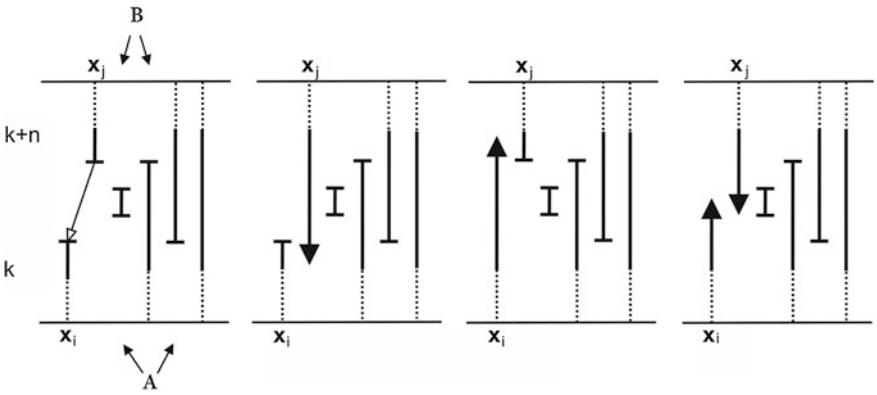

Fig. 4.8 Four successive steps in recovering residual virtual edges (see text)

The sum of the reproducibility of the arcs $x_i \rightarrow A$ and $B \rightarrow x_j$ provides 2 values, $V(A)$ and $V(B)$, that can be used to make a choice between three possible solutions for recovering the virtual edge (x_i, x_j) (Fig. 4.8):

If $V(A) > V(B)$, then x_j is added to the interval $k_{k+n-1} \ldots k_n$
If $V(A) < V(B)$, then x_i is added to the interval $k_{k+1} \ldots k_{k+n}$
If $V(A) = V(B)$, then x_i is added to $k_{k+1} \ldots k_{k+n/2}$ and x_j is added to $k_{k+n-1} \ldots k_{k+n/2}$.

4.14 Residual Arcs

Certain conflicting stratigraphic superpositions destroyed during the transformation of G^* can be restored during the last step of the procedure. This is done as follows.

In each unitary association k_i of the *first* "range chart" calculated by the program (i.e. constructed immediately after compacting the matrix associated with L), we define two sets of species, A and D, where A is the set of species that appear in k_i and where D is the set of species that disappear in k_i.

If there exists an arc $x \rightarrow y$ between an element x of D and an element y of A, we turn k_i into two associations, k_i and k_j (initially $k_i = k_j$). Next we remove species x from k_j and species y from k_i.

If there exist several distinct arcs of the type $x \rightarrow y$, we repeat the operation for each arc, verifying at each step that the removal of x from k_j (resp.y from k_i) does not lead to the destruction of a real edge (e.g. $\{x, z\}$ or $\{y, z\}$). If it does, the species is not removed.

When this operation has been completed for all the unitary associations, the test of maximality is applied once more and sets that are not maximal are eliminated.

A residual arc ($13 \rightarrow 12$) is restored in the U.A. 3 of the present solution. The details of this restoration are given in Table 4.5.

4.15 Identification of Unitary Associations and Correlations

The last operation performed by our program consists of constructing correlation tables based on the unitary associations. This is done as follows.

We denote X_{ij} the specific content of the ith level of the jth section.

We denote $K = \{k_m, m = 1 \text{ to } p\}$ the set of unitary associations obtained.

For each level of each section we calculate

$$X_{ij} - k_m = I$$

If $| I | = 0$, the level is assigned to the corresponding unitary association (or unitary associations).

The last stage of the procedure (identifying the U.A. and constructing the reproducibility matrix) is identical to that described in Chap. 1.

The correlations and reproducibility matrix produced by UAgraph for the problem under study are illustrated in Tables 4.6 and 4.7.

Table 4.6 Correlation table produced by UAgraph

Fatji_hrib			Dane_Divaca			Veliko			Ritomece		
1-4	5	5	2-4	7	7	3-7	7	7	4-4	7	7
1-3	4	4	2-3	4	4	3-6	7	7	4-3	7	7
1-2	3	6	2-2	3	3	3-5	4	5	4-2	5	5
1-1	1	1	2-1	2	2	3-4	4	6	4-1	4	4
						3-3	3	3	Podgorje		
						3-2	3	4	5-2	4	7
						3-1	1	1	5-1	1	2

Podgrad_Hrusi			Kozina_Socerb			Golez			Zbernica		
6-4	7	7	7-4	3	3	8-6	7	7	9-2	6	6
6-3	4	7	7-3	2	4	8-5	7	7	9-1	6	7
6-2	4	4	7-2	1	2	8-4	3	3	Dane Istrie		
6-1	3	3	7-1	1	1	8-3	3	6	10-3	5	7
						8-2	2	4	10-2	6	7
						8-1	1	1	10-1	4	5

Jelsane		
11-1	7	7

Table 4.7 Reproducibility of the 7 UAs in the alveolinids problem

UA	Sections										
	1	2	3	4	5	6	7	8	9	10	11
7	0	2	2	2	1	2	0	2	0	1	2
6	0	0	0	0	1	0	0	0	2	1	0
5	2	0	1	2	1	0	0	0	0	1	0
4	2	2	1	2	1	2	0	0	0	1	0
3	0	2	2	0	0	2	2	2	0	0	0
2	0	2	0	0	1	0	0	0	0	0	0
1	2	0	2	0	1	0	2	2	0	0	0

The localities are noted as 1–11. The "1" in the columns represent the coalescences of identified UAs and the "2" represent the UAs which are strictly identified in the sections (see Table 4.6)

References

Carre, B. (1979). Graphs and networks. Oxford applied mathematics and computing science series (277p.).

Cormen, T., Leiserson, C., & Rivest, R. (1990). *Introduction to algorithms*. Cambridge, MA: MIT Press. 1028.

Drobne, K. (1977). Alvéolines paléogènes de l'Istrie et de la Slovénie. *Mémoires Suisses de Paléontologie 99*, 1–175.

Golumbic, M. (2004). Algorithmic graph theory and perfect graphs. *Annals of Discrete Mathematics*, *57*, 340.

Guex, J. (1991). *Biochronological correlations* (250 p.). Berlin: Springer.

Guex, J., & Davaud, E. (1984). Unitary associations method: Use of graph theory and computer algorithm. *Computers and Geoscience, 10*(1), 69–96.

Moon, J. W. & Moser, L. (1965). On cliques in graphs. *Israel Journal of Mathematics*, *3*, 23–28.

Sadler, P. M. (2006). Constrained optimization approaches to the paleobiologic correlation and seriation problems—Part 1 (a users guide to the CONOP Program Family) and part 2 (a reference manual to the CONOP Program Family).

Chapter 5
Transgressive-Regressive Cycles and Benthic Foraminifera

Abstract The study of the Jacksonian and Vicksburgian of the Paleogene in western Alabama and eastern Mississippi was published in the early 1960s by Deboo (Alabama Geol Surv Bull 80:1–84, 1965). The goal of Deboo was two-fold: first, he intended to solve some problems posed by correlating the lithologic units classically used in this region (Fig. 5.1) and second, he wanted to use new biochronologic arguments to determine more precisely the boundary between the Jacksonian and Vicksburgian local stages.

5.1 Introduction

One of the most brilliant micropaleontological studies of the Jacksonian and Vicksburgian stages of the Paleogene in western Alabama and eastern Mississippi was published in the early 1960s by Deboo (1965). The goal of Deboo was two-fold: first, he intended to solve some problems posed by correlating the lithologic units classically used in this region (Fig. 5.1) and second, he wanted to use new biochronologic arguments to determine more precisely the boundary between the Jacksonian and Vicksburgian local stages.

His investigations concerned mainly the distribution of foraminifera and ostracods in five sections which he sampled in great detail (Fig. 5.1).

His remarkable results have been used by Hazel (1970, 1977), McCammon (1970), Millendorf et al. (1978) and Brower (1985) in different attempts to establish quantitative correlations with the help of a number of more or less sophisticated statistical methods (cluster analysis, RBV, lateral tracing, etc.). Unfortunately these statistical solutions failed to improve on Deboo's correlations, and none of these techniques allowed to detect major transgressive/regressive cycles (fall and rise of sea level) based on the data which were quantitatively analyzed. In the present chapter, we will show what the unitary association method can contribute to this problem.

J. Guex et al., *Discrete Biochronological Time Scales*,
DOI 10.1007/978-3-319-21326-2_5

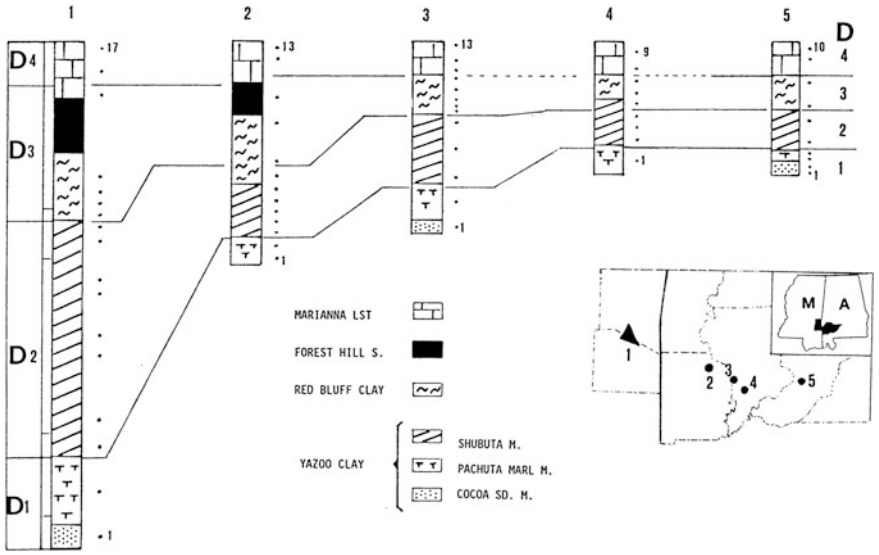

Fig. 5.1 Deboo's original sections and correlations. D_1–D_4 = Deboo's empirical zones

As an introduction, we will briefly examine the imaginary stratigraphic situation sketched in Fig. 5.2. These diagrams show the geometric arrangement of seven biochronologic zones that are identified in three stratigraphic sections aligned along a distal (P_1) → proximal (P_3) transect of a marine sedimentary basin.

The sequence of zones recorded in P_1 is complete, while that of P_3 has many gaps (zones 2, 3, 5 and 6 are absent).

This kind of situation is one of the simplest cases we can encounter when searching for transgressive/regressive cycles. We will show that Deboo's data on the benthic foraminifera enable us to construct a model similar to the one shown in Fig. 5.2.

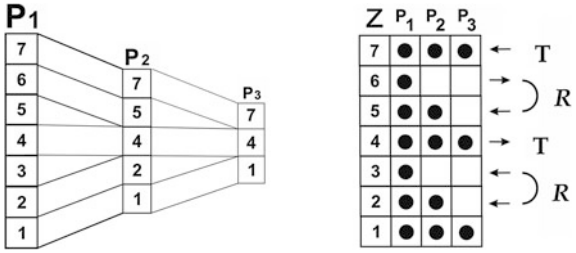

Fig. 5.2 Relationship between zonal correlation and geometry of a sequence of transgressive-regressive cycles (*T* and *R* in the reproducibility table)

5.2 Database

Benthic foraminifera are usually good bathymetric indicators, since they are notoriously sensitive to ecological fluctuations. For this reason, the present discussion will be limited to this group of organisms. Of the 147 species recognized by Deboo, we have chosen 100, according to their geographic distribution and the dissimilarity of their vertical ranges. The local vertical ranges of these species are given in Appendix 2-C.

5.3 Processing the Data

To correlate his sections with the help of benthic foraminifera, Deboo (1965, p. 27, Fig. 10) made a statistical analysis of the vertical variations in the similarity of adjacent fauna. This enabled him to recognize three major faunal discontinuities delimiting four distinct zones that we call D_1–D_4 in Fig. 5.1. The correlation of these zones with the sequence of unitary associations is well confirmed by our data processing by means of the UAgraph program (Fig. 5.3) which shows that the most proximal section (5) contains three well marked gaps, whereas the most distal section (1) has a more complete vertical record.

We should emphasize that our correlations coincide almost exactly with those of Deboo, with one exception: by means of the forams, samples 8 and 9 of section 4 are assigned to zone 3 (corresponding to Deboo's original beds 1 and 2), while Deboo assigns them to his zone 4. Note that the correlations done by means of the ostracods alone assign those two beds to zone 4 (Fig. 5.3 ostracods), but an integrated processing of the forams and ostracods together (155 taxa) also assign those beds to Deboo's zone D3 (Fig. 5.3 ostracods + forams).

5.4 Geometry of Lithologic Units

As can be seen in Fig. 5.3. Deboo's biostratigraphic observations yield slightly different correlations when we examine the distribution of benthic foraminifera alone than when we examine them together with ostracods. Nevertheless, whatever set of species we consider, the arrangement of the unitary biofacies generated by the forams and by the composite forams + ostracods corresponds to a sequence of two regressive phases located respectively at the base of the Shubuta Member and the base of the Red Bluff Clay Member. In the present example we are interested only in this aspect of the problem.

The relative arrangement of the lithologic units assigned to the zones discussed above and correlated in Fig. 5.3 is very similar to that shown in Fig. 5.2 and, as

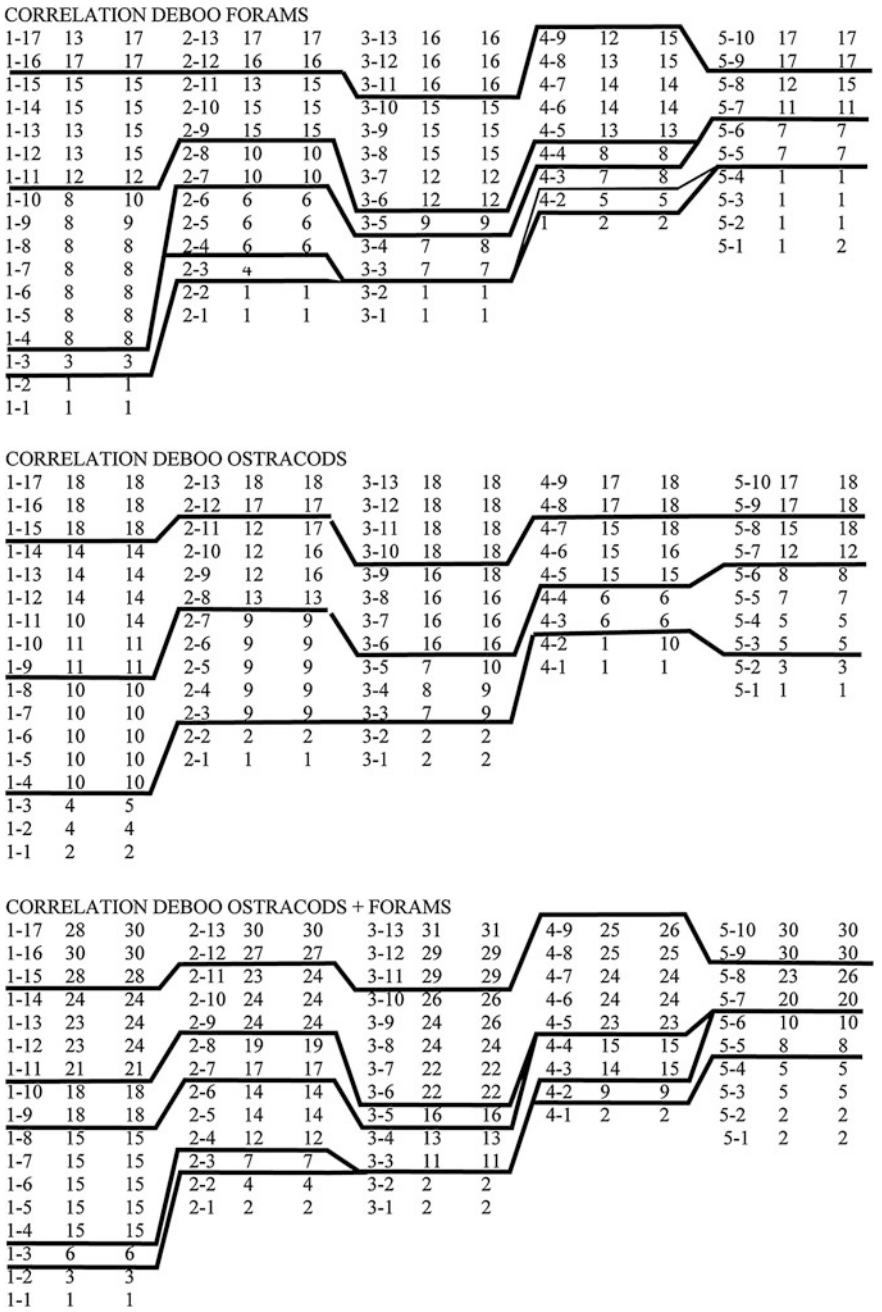

Fig. 5.3 Correlations based on foraminifera, ostracodes and forams + ostracods. Output of UAgraph program

noted above, it is clearly generated by a succession of transgressive/regressive cycles.

This conclusion is supported by the existence of erosional structures at the base of the Red Bluff Member (Cheetham and Deboo 1963) and by the complementary informations published by Siesser's (1984).

Note that Siesser (1984) gives a very interesting historical account of research on the stratigraphy of the Paleogene of the eastern coastal plains of the Gulf of Mexico. He notes in particular that the Red Bluff Clay was traditionally considered a shallow deposit and that it was Hazel (1970) who first proved that these deposits are actually deeper than those surrounding them. We demonstrate here that the same conclusion can be drawn directly from Deboo's original observations.

References

Brower, J. C. (1985). The index fossil concept and its application to quantitative biostratigraphy. In F. Gradstein, F. P. Agterberg, J. C. Brower, & W. S. Schwartzacher (Eds.), *Quantitative Stratigraphy* (pp. 43–64). Dordrecht: Reidel Publishing Company.

Cheetham, A. H., & Deboo, P. B. (1963). A numerical index for biostratigraphic zonation in the mid-Tertiary of the eastern Gulf. *Gulf Coast Association Geological Society Transactions, 13*, 139–147.

Deboo, P. B. (1965). Biostratigraphic correlation of the type Shubuta Member of the Yazoo Clay and Red Bluff Clay with their equivalents in southwestern Alabama. *Alabama Geological Survey Bulletin, 80*, 1–84.

Hazel, J. E. (1970). Binary coefficients and clustering in biostratigraphy. *Geological Society America Bulletin, 81*(11), 3237–3252.

Hazel, J. E. (1977). Use of certain multivariate techniques in assemblage zonal biostratigraphy. In E. G. Kauffman & J. E. Hazel (Eds.), *Concepts and Methods of Biostratigraphy* (pp. 187–212). Stroudsburg, PA: Dowden, Hutchinson and Ross Inc.

McCammon, R. B. (1970). On estimating the relative biostratigraphic values of fossils. *Bulletin Geological Institute University Uppsala (n.s.), 2*, 49–57.

Millendorf, S. A., Brower, J. C., & Dyman, T. S. (1978). A comparison of methods for the quantification of assemblage zones. *Computers and Geosciences, 4*(3), 229–242.

Siesser, W. G. (1984). Paleogene sea level and climates USA eastern Gulf coastal plain. *Paleogeogr Paleoclim Paleoecol, 47*, 261–275.

Chapter 6
Problems of Datums Diachronism and Comparison Between UAgraph and the Program Conop

6.1 Neogene Diatoms from the Antarctic Continental Margin

A very challenging quantitative biochronological problem integrating comprehensive diatom biostratigraphy, magnetostratigraphy, and tephrostratigraphy from 32 Neogene sections around the Southern Ocean and Antarctic continental margin has been recently studied by Cody et al. (2008). A new method, known as Constrained Optimization (Conop), which can be viewed as a multidimensional version of graphic correlation, is applied to that complex database. In this chapter we will review some discussions of a paper by Galster et al. (2010) concerning Conop and focus our analysis on the large scale correlations based on Cody's data and the implication of the diachronism of "datums" in the quantitative treatment of biostratigraphic data.

6.2 The Constrained Optimization Method

The Constrained Optimization method is designed to produce automated graphic correlation and sequences of events in a multidimensional space (Kemple et al. 1995) by means of the program named Conop (Sadler 2006; Sadler et al. 2009).

That program has adopted some basic rules of the UA method, like the fact that the output must satisfy the observed interspecies coexistences, but it also deals with some particular type of contradictory stratigraphic situations, such as the one illustrated in Fig. 6.1.

Instead of building a solution directly from the data (as in the UA method), Conop works through a series of iteratively improved guesses about the solution. Each guess is compared with the data; the misfit between the solution and data guides the next guess, a process called "inversion" by geophysicists. Cody et al.

J. Guex et al., *Discrete Biochronological Time Scales*,
DOI 10.1007/978-3-319-21326-2_6

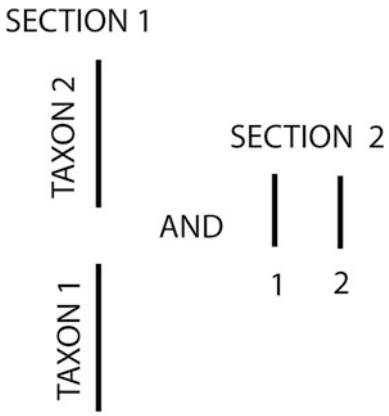

Fig. 6.1 Contradictory relationship between two taxa 1 and 2 according to Conop (Sadler and Cooper 2003, text-Fig. 3). Such a configuration is not contradictory in the UAM

(loc.cit. p. 107) use a penalty function to minimize the corrections of local ranges, i.e. the minimal value upon which the simulated annealing is calculated (details in Sadler 2006; Kirkpatrick et al. 1983).

Conop's treatment of the FO versus LO "contradictions" illustrated in Fig. 6.1 will be presented in a simplified manner. We will only mention the concepts useful for the following discussion and the reader is referred to the original publications of Cody et al. (2008) and Sadler (2006) for more details.

When a taxon i is below a taxon j in a given section S_1 and ij coexist in another section S_2, the last occurrence of i is moved upward in S1 and the database is examined to see if it minimizes the range extension in the range chart under construction. Then the same operation is done with the first occurrence of taxon j which is moved downward to overlap i. If the result is better than the one obtained during the first step, it is kept as a good solution. Applied to the complete database with multiple contradictions, such an algorithm is obviously NP-complete (i.e. the number of iterations will grow exponentially with the number of taxa).

From a more general point of view, Conop proposes a random order of the events respecting the observed inter-species coexistences. Then it compares this global random order with the local orders in each section and computes the number of levels that the local "FO" and "LO" must jump above or below to respect the global order (see Sect. 6.3). This provides an estimation of the misfit of the new order. The sole constraint is that the LO cannot jump below the FO of the same taxon and, similarly, the FO of this taxon cannot jump above its own LO. At this point the program has modified the global order of a given "energy". The comparison between the global order and the local orders is repeated and a new misfit is calculated. The two misfits are then compared and the only retained global solution is the one which implicates the smallest misfit. Then the program changes the global order again and if the first misfit resulting from the first trial was bigger than the second one, then the program diminishes the energy. On the contrary, if the first

misfit is followed by a bigger misfit, the program keeps the same energy level. After a certain number of unsuccessful trials (no smaller misfits found) the energy is increased to get out of the local minimum. That procedure is only applied as long as bigger misfits are found, allowing to keep the smallest misfit in the final solution.

The value of the misfit is used as a measurement of the global uncertainty. For each event, the program computes the local orders which are necessary to fit with the global solution. This gives an "event misfit" which could, in part, be used as an indicator of the diachronism of this event.

6.3 Conop's Option LEVEL

The following discussion will be limited to the option "LEVEL", the particular best choice made by Cody et al. (2008) to treat the diatoms data.

In summary, the main difference between UAs and Conop is that the goal of the first method is to construct discrete concurrent range zones whereas the second method constructs sequences of datums. Note that UA constructions are based on sample contents and their mutual stratigraphic relationships (i.e. the biostratigraphic graph G^*). Sequences of datums established by means of UAs consist of non-diachronous datums only which are constructed in a second run of the program, after a semi-empirical selection done during a first analytical phase by means of UAgraph. During the correlation process, such datums ("events") are treated as intervals of uncertainty, like the total ranges of the taxa calculated by the program, and some of them can be present in several UAs of the output.

Conop on its side is exclusively oriented towards a seriation of the events based on inter-stratigraphic sections comparisons (i.e. the bivariate graphic correlation philosophy of Shaw 1964 which was largely improved by Edwards 1978).

We can also notice that the UA method and Conop (and almost any other method) will reach similar conclusions when applied to very complete and not contradictive sets of empirical information relative to inter-taxa coexistences. For instance, Shaw (1964) used the trilobites from the Riley Formation as an example. His choice was limited to the study of the stratigraphic relationships between the 21 best distributed and most diagnostic taxons. It is well known that this trivial case is of limited theoretical interest because the inter-taxa graphic relationships are represented by an interval graph. In other words it is indeed a non problematic case which can be solved with a single matrix permutation (see Guex 1977). Using it as a case study has absolutely no significance concerning the intellectual quality of the theoretical model used to solve it because of its lack of internal contradictions. However Conop and the UAM differ significantly when the data are highly affected by internal stratigraphic contradictions, like it is the case in Cody's diatom problem.

6.4 UAgraph Correlations of Cody's Database

One major interest of the Cody et al. (2008) paper is that the complex problem which was originally addressed, the quantitative study of the biostratigraphy, magnetostratigraphy and tephrostratigraphy of 116 diatom species from 32 Neogene sections around the Southern Ocean and Antarctic continental margin has been analysed by the best specialists on the Conop program, producing a result which can be interpreted as the best possible results obtainable by means of Constrained Optimization. Another significant aspect of Cody's database is that the original taxonomy was carefully revised and homogenised before being applied to Conop and that the doubtful local range extremities (reworking and downworking, contaminations) were consciously eliminated.

All the data considered here are strictly taken from Cody's paper (see Appendix 2 in Cody et al. 2008 and Appendix 3-A in this book), which is considered, for theoretical reasons, as exact.

The goal of the present application is to produce an *integrated* solution given the complex input including the inter-species coexistences, selected moderately diachronous first and last occurrences of diatom taxa and paleomagnetic data. The database used for the computation is given in the Appendix 3-A.

The paleomagnetic data (base and top of the recognized reversals) have been included into the computed database to force an order on some contradictive (cyclic) relationships. As the truly oldest (respectively youngest) part of the considered reversals are not necessarily recorded in the local stratigraphic sequences, these events often display an apparent range which can span several distinct UAs.

We should also recall that a given datum, or first (respectively last) occurrence, is diachronous whenever its chronological position varies from one stratigraphic section to the other. Knowing how many zones a datum jumps from one place to the other allows us to quantify its diachronism, i.e. if a FO jumps one zone we say that its diachronism is equal to 1, if it jumps two zones, its diachronism is equal to 2 etc. Generally speaking, FOs and LOs sequences can be used only when these events are proven to be approximately synchronous or with very low apparent diachronism. In our treatment of Cody's data, we have introduced about 30 such datums (FOs) (list in Appendix 3-B).

Applying UAgraph to that database produces a sequence of 92 UAs (Fig. 6.2a, b). Most of those UAs do not show a good lateral traceability, as shown in the reproducibility table of Fig. 6.2c and we have merged some of them to increase that lateral reproducibility and the superpositional control between the units. That operation produces a referential of 20 UA-Zones which are highly significant from a chronological point of view.

The mergings applied to the 92 initial UA range chart (IUA) are listed in Appendix 3-C and the reproducibility and superpositional control between the 20 UA Zones is given in Fig. 6.3.

The details of the UA zonal correlation of sections 23–28 is given in Fig. 6.4a which is compared with the Conop correlation established by Cody et al. (2008)

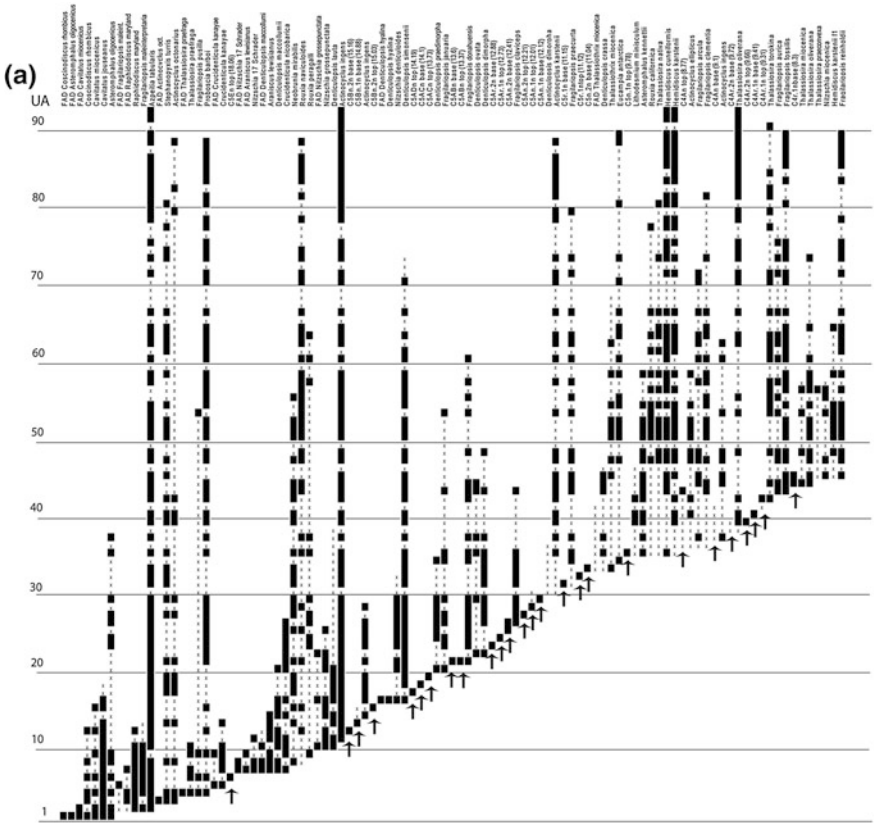

Fig. 6.2 **a**, **b** Range chart produced by UAgraph by processing approximately non diachronous diatoms datums, paleomagnetic events (*vertical arrows*) and total ranges of the 116 species chosen by Cody et al. (2008) to apply the Conop's program. *Dashed lines* = discontinuous distributions. **c** Lateral traceability of the UAs across the stratigraphic sections in (**a**, **b**). *Solid squares* are the identified UAs and *grey rectangles* are coalescences of identified UAs

(Fig. 6.4b). In the Conop correlation, we note that most of the lines of correlations generated by the "events" relationships are converging towards very short stratigraphic intervals. This is clearly generated by the differences in sedimentary rates between the sections and is perfectly correct, as the condensation at the top of section 23 is absolutely real. However some convergences are going from the stratigraphically reduced sections towards the thicker sections. Such "reverse" reductions are not confirmed by faunal condensations (see the UA correlations given in Fig. 6.4a). They will be discussed in more details in Sect. 6.5.

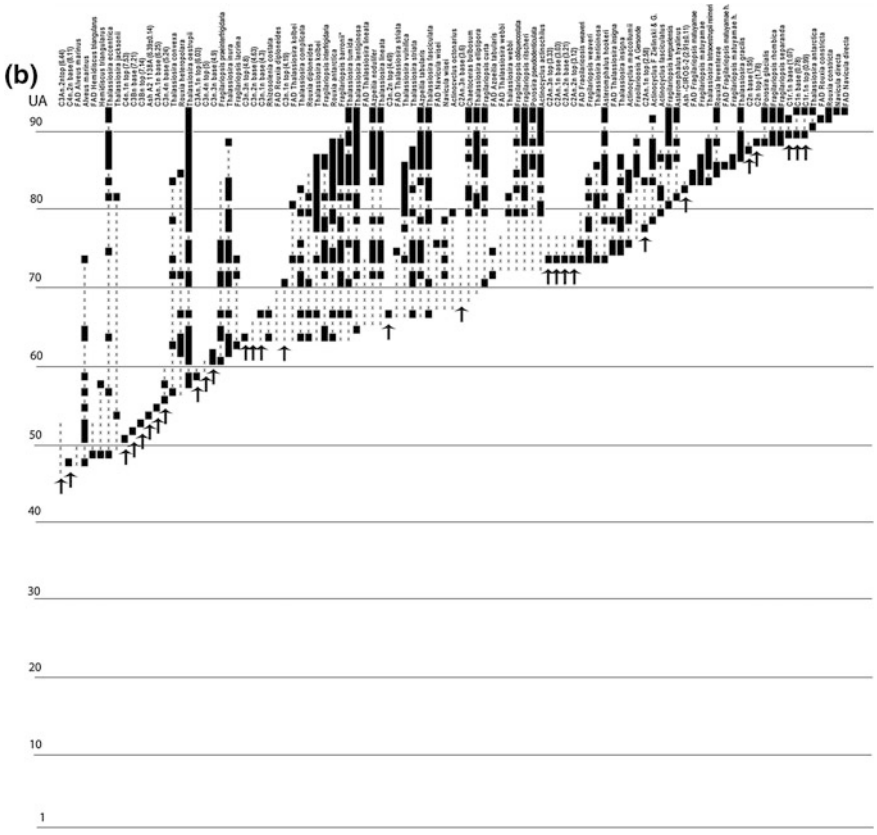

Fig. 6.2 (continued)

6.5 The Fence Diagrams Problem

Conop produces automated correlations between stratigraphic sections which are called "fence diagrams" (Sadler 2002), due to their special geometrical characteristics. These particular lines of correlations generate an alternating sequence of hiatuses (or stratigraphic condensations) followed by intervals of very expanded sedimentation.

We will demonstrate here the algorithmic reasons which are responsible for these alternations and show that in most cases these condensations are a misleading artefact due to the treatment of inter-events contradictions and have no real geological meaning.

As an example we will apply Conop's correlations to Deboo's problem studied in the previous chapter and which is characterized by a true sequence of

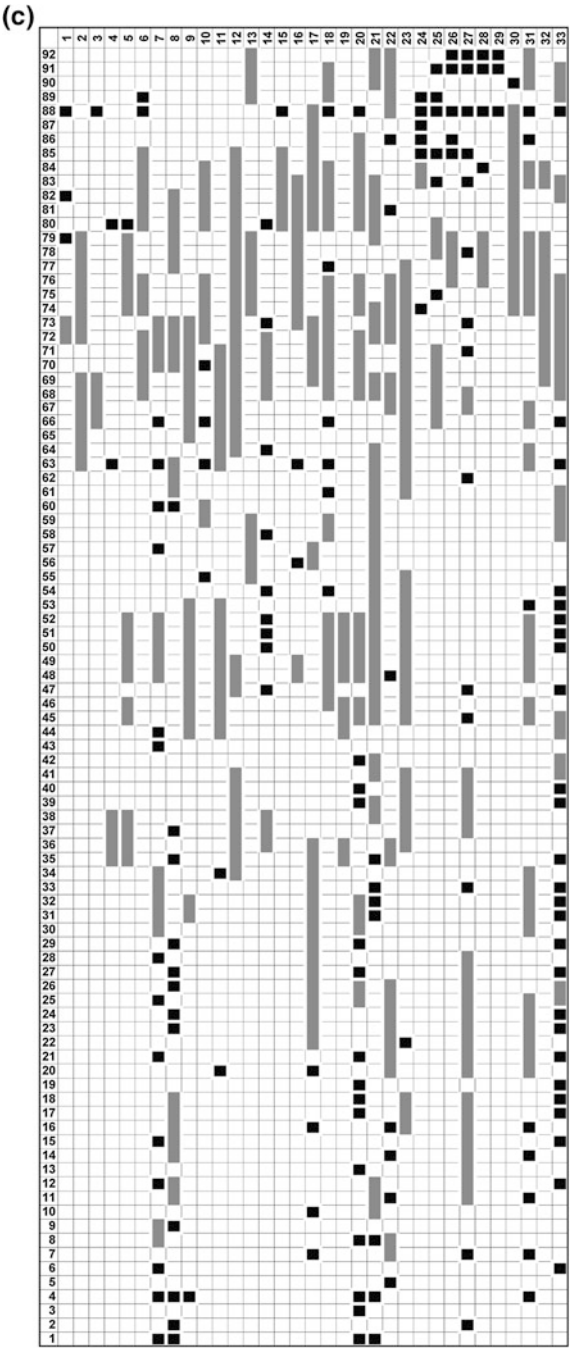

Fig. 6.2 (continued)

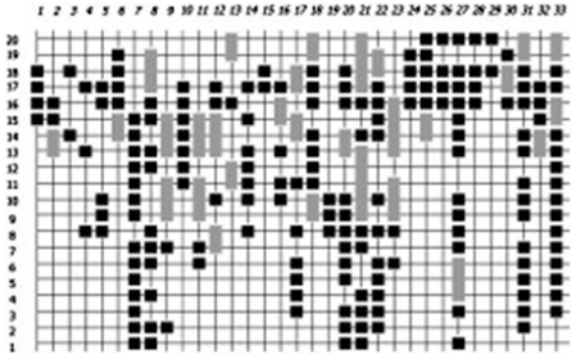

Fig. 6.3 Reproducibility of the 20 UAzones constructed based on Fig. 6.2c. Section 33 represents the sequence of magnetozones recognized by Cody et al. (2008). *Solid squares* are the identified UAs and *grey rectangles* are coalescences of identified UAs

regressive/transgressive cycles, indicated by the Unitary Associations as well as by the sedimentological observations of Siesser (1984).

As mentioned above, a first qualitative analysis of the "fence-diagram" obtained for Deboo's dataset produces the impression that the five sections are characterized by a large number of hiatuses, systematically alternating with periods of high sedimentation rate. We can note incidentally that the same kind of correlation was already observed in the Diatoms correlations established by Cody et al. (2008) and discussed above.

Concerning Deboo's problem, if we compare the correlations established by means of the UAs or if we evaluate the purely lithological correlations illustrated in Fig. 5.1, we note that the number of hiatuses or condensations is much greater in Conop's output than in the UAgraph's output (Fig. 6.5).

As already noted by Sadler (2002), it is well known that the large number of condensations proposed by this computer program is generated by an algorithmic artifact and not by the geological record itself.

First we will note that Conop proposes a correlation that is based on the expected positions of the events in the stratigraphic sections (see below). Conflictual inter-event stratigraphic relationships, in the sense of Conop, are solved by minimizing the net event-adjustments necessary to eliminate the contradictions. In other words it means that an event can freely be moved up-section (in the case of last occurrences) and down-section (in the case of first occurrences) once it reaches a new stratigraphic position that is not conflictual anymore with the other events. The choice to minimize such adjustments in terms of "jumped" samples, meters of section or cross-correlated events implies that the event's migration along the section stops at the first non contradictive position encountered, i.e. it stops once the migrating event encounters the stratigraphic position of the mutually conflictual events.

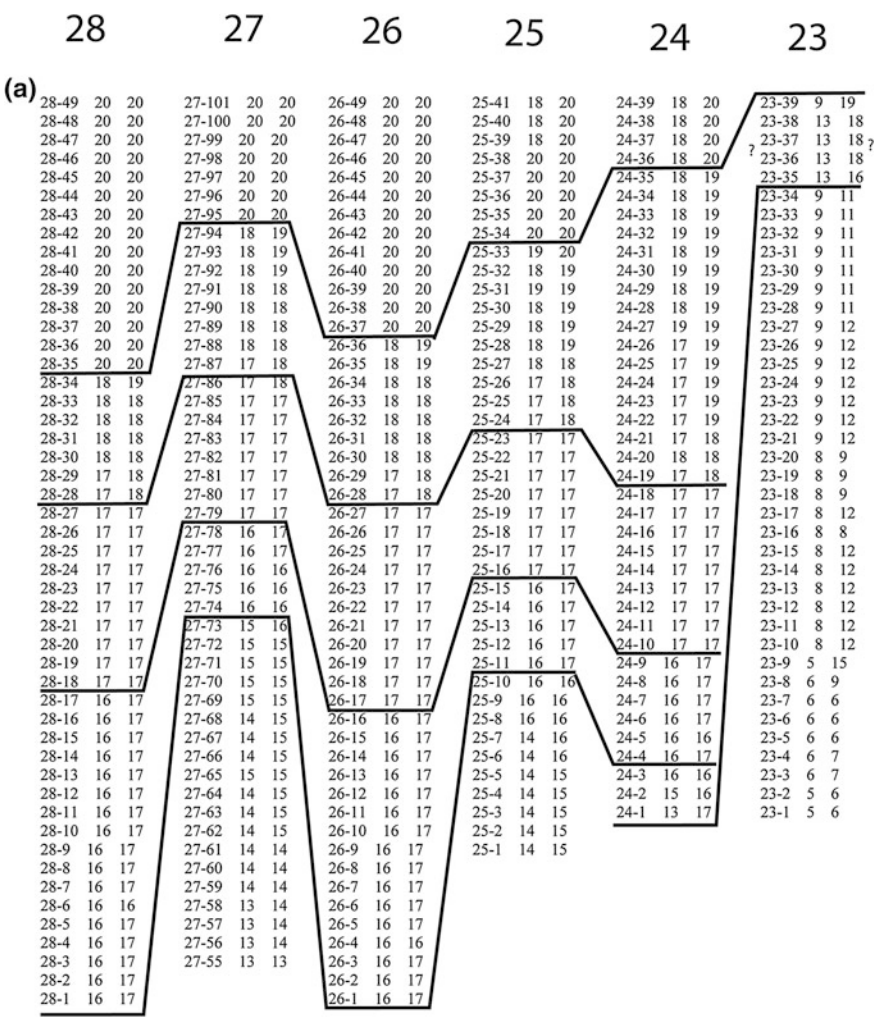

Fig. 6.4 **a** UA correlation of sections 23–28 compared with the C correlation established by Cody et al. (2008) (**b**). The top of section 23 is clearly condensed and the convergences of the correlations between the other sections are generated by the different sedimentary rates but some details of the fence correlation inside UA-zones are artificial

In the case of highly contradictive inter-event stratigraphic relationships such an approach unavoidably generates convergences of the correlation lines, resulting in time condensations.

A step by step explanation of the genesis of these condensations is given in Fig. 6.6, and a step by step description of the apparent condensation in bed 8 of section 3 is illustrated in Fig. 6.7.

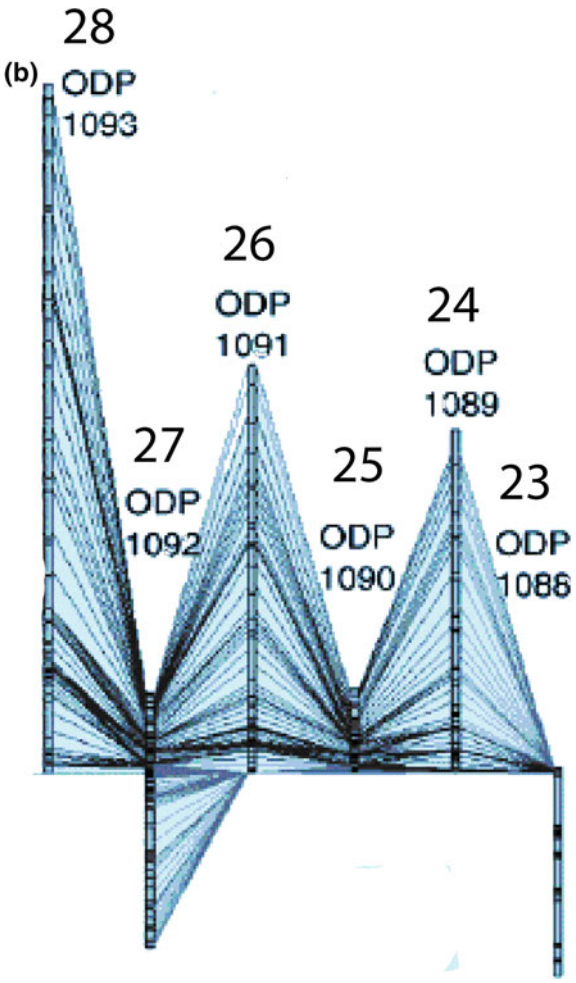

Fig. 6.4 (continued)

Figure 6.7 shows that in the philosophy of Conop all the events used in that figure are considered as potentially valid biochronological markers. The program assigns to all of them a precise stratigraphic level with the smallest uncertainty in a composite section and relocates the events in the local sections. Arc inversions are solved by displacing up-section the weakest edge rather than by enlarging the uncertainty on its assignment to a given stratigraphic level. The events that are not displaced (strong edges) are considered good markers and no information about the former inversions is considered to judge the uncertainty on its level assignment. This fact is completely disregarded by Conop in its estimation of uncertainty, as demonstrated below.

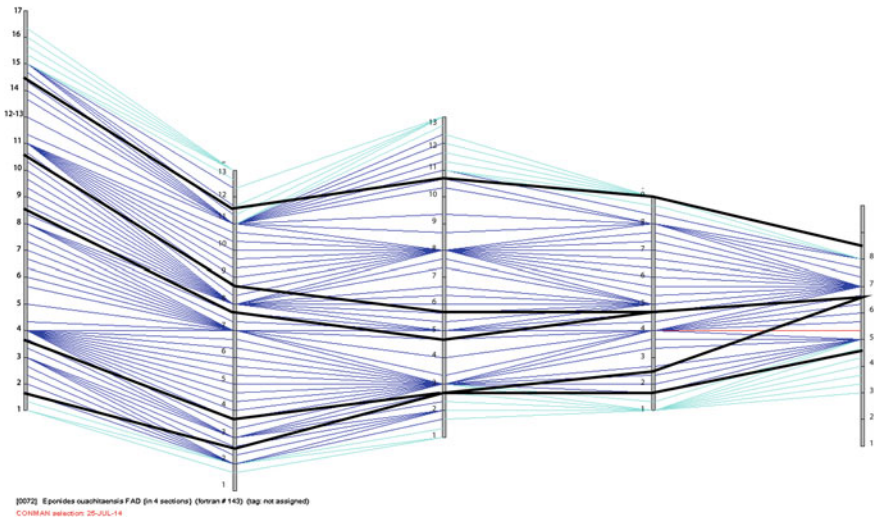

Fig. 6.5 Conop's correlations of Deboo's problem (in *blue*; *light blue* indicates the ranges which are truncated at their base or at their top) and UA zonal correlations showing the sedimentological condensations (in *black*) (see Fig. 6.3)

6.6 Uncertainities in Age Assigments and Apparent Resolution Power

UAgraph and Conop produce composite sequences of species that differ especially by their apparent resolution power, independently from the algorithms. If we define the resolution power of a method by the number of generated units, we observe that the resolution of the methods designed to establish sequences of datums have an apparent resolution which looks greater than the ones based of maximal associations of taxa. However, when reduced to such maximal intersections, datums and maximal association methods produce about the same number of units, as discussed in Galster et al. (2010). For example, if we consider the maximal intersections of the 232 events zonation of Cody et al. (original range chart: loc.cit.), we see that there are only 37 UAs generated by the compaction of that range chart (see Galster et al. 2010 Figs. 4a and 5c). From that new range chart we can extract empirically 14 zones which are chronologically significant, resulting from the merging of the UAs and based on their individual reproducibility. The UA numerical range chart showing the details of the zones is given in Appendix 3-F, and can be directly used in the UAgraph program to be edited graphically.

In practice, Conop estimates the uncertainties of the outputs by means of the "best-fit interval" values (see above and Sadler 2002) which account for the "degree of freedom" that each event's position has in a cluster of "best solutions" (best in the Conop's logic). An event position constrained in all "best-solutions" to the same level has a minimum best-fit interval and poorly constrained events have a

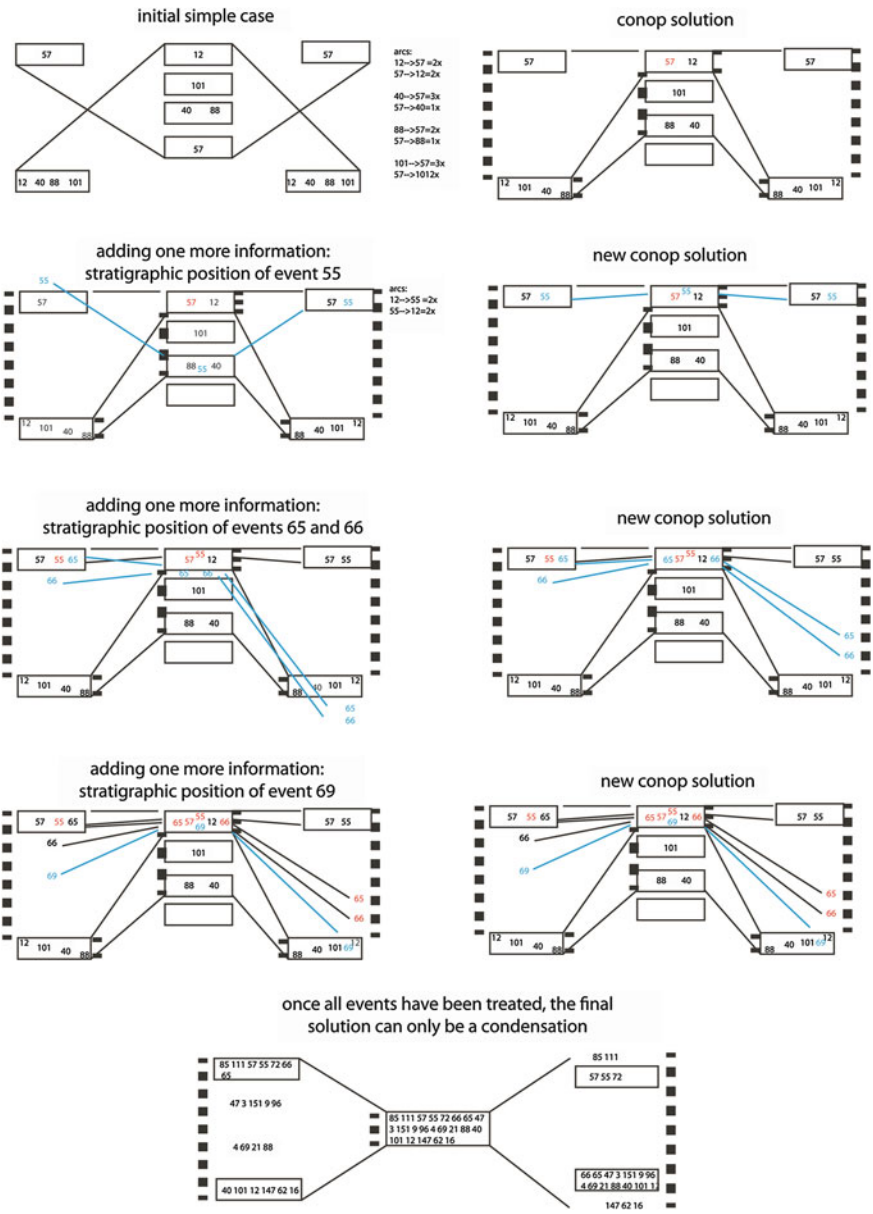

Fig. 6.6 Conop's step by step construction of the condensations generated by contradictive inter-event stratigraphic relationships

maximum uncertainty. Within a cluster of best solutions, we would expect that Conop should assign non-diachronous events to similar or identical levels in all composite solutions being part of the cluster, but it is not the case since occurrences

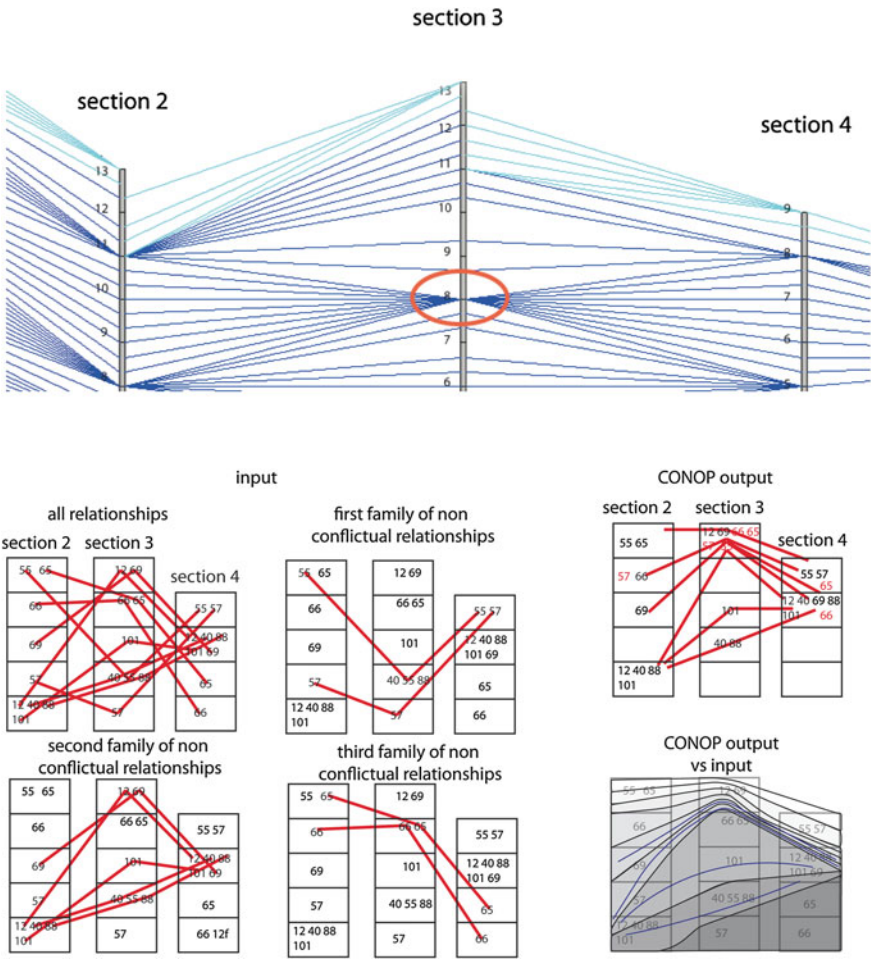

Fig. 6.7 Step by step construction of the artificial condensation at level 8 of section 3 of Deboo (see Figs. 6.5 and 5.1)

of diachronous events in the sections generate conflictual stratigraphic relationships even for the events considered as primary zonal markers by Conop, as demonstrated in Table 6.1 and in Fig. 6.8. In other words Conop tends to overestimate the uncertainty affecting non-diachronous events. Conversely, since highly diachronous occurrences are highly contradictive, their solution results in highly constrained events (Fig. 6.7). In this case Conop underestimates the uncertainty of diachronous events. This intuitive and qualitative discussion can be better explained with a practical example taken from the data of Cody et al. (original Table 3, 2008).

Figure 6.8 shows the local chronological occurrences of some events with the smallest best-fit interval (smallest uncertainty according to the Conop program) against the 14 UA zones extracted from Cody et al. original range chart (see above).

Table 6.1 Most reliable datums (=primary zonal markers) within the interval 2.6–3.6 Ma of Cody et al. (2008)

	Zone			
	Reprod	Base	Top	Diachr
127FAD	8	10	11	2
61FAD	6	10	11	2
80LAD	4	9	10	2
4FAD	6	10	12	3
13LAD	3	8	10	3
5FAD	6	10	11	2
11FAD	10	10	11	2
59LAD	7	8	9	2
45LAD	11	7	9	3
16FAD	8	9	14	6
116FAD	9	9	11	3
130FAD	21	9	12	4
111FAD	19	9	11	3
73FAD	18	9	11	3

Note that all of them are affected by a diachronism of at least 2 zones, up to 6 zones out of the 14 extracted from Cody's et al. original Conop range chart (see Appendix 3-F and 3-G, symbol "+")

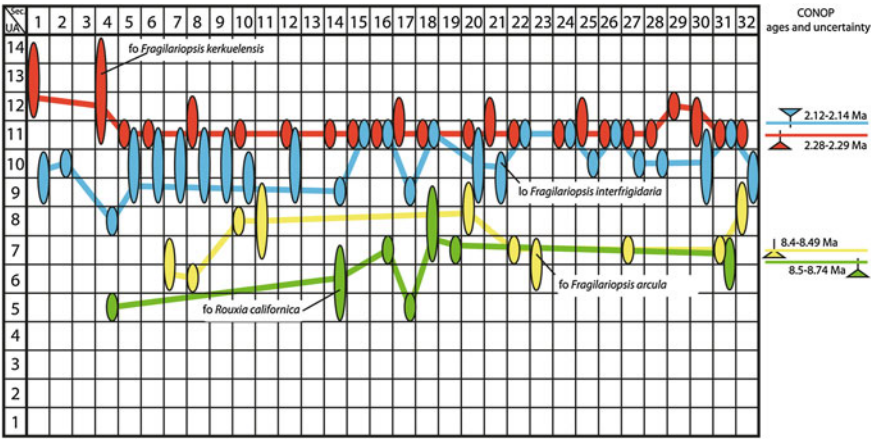

Fig. 6.8 Graph showing the diachronism of 4 taxa (FO or LO considered as primary zonal markers by Conop) within the 14 zones extracted from Cody et al. compacted range chart (see Appendix 3-F and text for discussion). Note that, in most localities, the FO of F. kerkuelensis (*red*) is located above the LO of F. interfrigidaria (*blue*) and not below, as calculated by Conop. The diachronism is compiled manually

The contradictions illustrated in that diagram clearly demonstrate that Conop cannot produce good predictions of the uncertainties for taxa which are considered as good markers.

Note that in theory Conop should have the ability to predict a precise degree of uncertainty for each event. This should be reflected by a wide coherence between occurrences in specific UA zones and "best-fit intervals". Events with large "best-fit intervals" should occur in samples assigned to different UA zones among the different sections, while events with very small values of uncertainty are expected to occur in samples systematically assigned to the same zones. However we note that it is not the case.

In conclusion the apparent high power of resolution of Conop results from the choice to use all datums combined with the impossibility to estimate the degree of uncertainty of single events.

6.7 Criteria of Comparison Between the UAgraph and Conop

The main constraint in the UA is to preserve a maximum of observed and reproducible superpositions while honouring the observed co-occurrences in the output. That condition was demonstrated long ago to be the most important constraint in biostratigraphic analysis (Guex 1977, 1979). To honour that condition, the UA algorithm is oriented towards the systematic destruction of cyclic structures present in the graph representing the inter-taxa stratigraphic relationships. The basic conditions adopted in the Conop program are similar but the approach for reaching an optimal solution is different from the one adopted for UAs, because the best-fit interval values (Sadler and Cooper 2003) used in Conop to characterize the uncertainty of event assignments are generally unrelated to the amount of implication of the taxa (and of the events) within cyclic relationships, such as the cycles of length 4 (Z4) and discontinuous stratigraphic distribution.

In contrast, the UA optimization procedure is designed to preserve a maximum of observed superpositions (=reproducibility of the arcs in G*) (output "Contradictions" in UAgraph), as discussed above (Chaps. 1 and 2).

6.8 Contradictions Between UAs and Conop's Output

According to Conop's output, the stratigraphic interval 2.58–3.6 Ma allows a very fine resolution thanks to the datums recorded during this interval and allows the use of very precise Interval Zones.

As noted previously, a zonation based on interval zones (where the units are defined as the intervals separating two events) makes sense only when the zones can be recognized in the stratigraphic sections: the local sequences must match the idealized FOs of the range chart defining the zones(bases). Comparing Conop's original chart (loc cit Fig. 6) with our 92 UAs sequence shows that two intervals seem to have a greater resolution in Conop's output.

1. The interval between UA 68 and UA 84 containing the paleomagnetic interval C2An-1ntop (2.58 Ma) to C2An.3nbase (3.6 Ma) has no precise superpositional resolution in the UAgraph output. We note in particular that paleomagnetic events C2An-3n top to C2An-1n top overlap without being distinguished from each other. The reasons for this are discussed below and the same remark applies to paleomagnetic events C5An.1n base and top.

During the interval 2.58–3.6 Ma, Conop's composite sequence versus the composite section curve (loc.cit. Fig. 5) presents a sequence of 29 increments characterized by FOs/LOs relationships and paleomagnetic events. This sequence is partly based on an interpolation between two paleomagnetic tie-points respectively located at 2.58 and 3.6 Ma. To explain this problematic situation we have constructed and analyzed the graph of the relationships between these events with the results illustrated in Figs. 6.9.

Figure 6.9a shows what we call the trivial virtual edges between the events considered as "primary zonal markers" by Conop and generated by specific sequences which are inverted from place to place: such coexistences are generated by the stratigraphic relationships where an event *i* is above an event *j* in one place

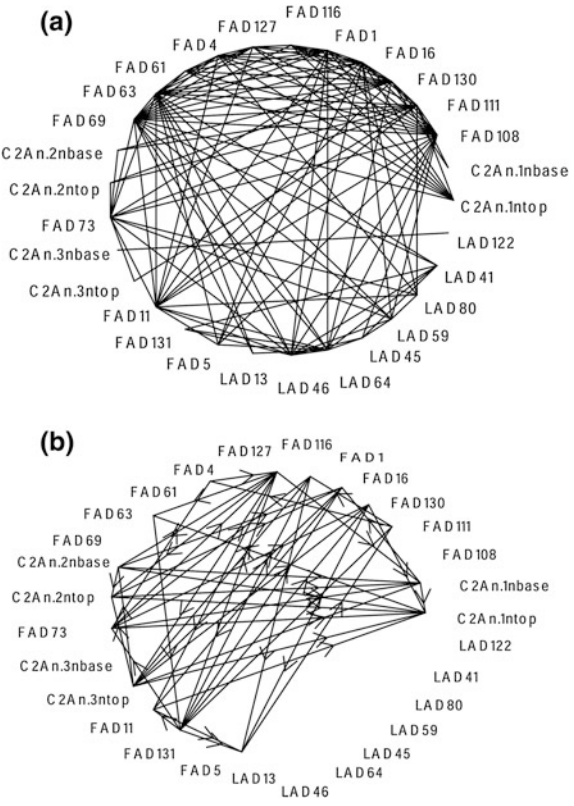

Fig. 6.9 *Above* trivial virtual edges between some selected events. Most of them are considered as "primary zonal markers" by Conop. *Below* cyclic relationships between the same events (Appendix 3-G)

and when the reverse relationship is observed in another section. Note that in this case, the virtual edges of the graph correspond to strictly real, but physically not observed, coexistences. A consequence of this is that computing maximal cliques is unequivocally allowed and provides a true sequence of non-contradictory arcs. Figure 6.9b shows the oriented graph of the 29 events with the cycles Cn, including paleomagnetic data, and Fig. 6.10 represents a selection of FOs local stratigraphic sequences in the different sections (1–32) and the contradictory age (Ma) assigned by Conop, explaining the origin of the cycles Cn in the lower graph of Fig. 6.9.

2. The first 23 FOs older than 18 Ma, located at the base of Cody's range chart: When analysing the Cody et al. problem, we realized that we were unable to reconstruct the initial sequence of 23 FOs (listed in Appendix 3-H) established by Conop (Cody et al. Table 3) where the FOs appear to be regularly separated by increments of 0.2 Ma. The difference between our sequence and the Conop's one is due to the fact that trivial virtual coexistences and cycles Cn, illustrated in Fig. 6.11a, b, are not taken into account by this program, even if they should be treated before the final output.

This implies the impossibility for UAgraph to compute the "true order" of these events because the order in which such cyclic events appear in any sort of calculated output is never reliable.

In summary we see that most of the sequence calculated by Conop does not correspond to any reproducible sequence of "datums" in the studied stratigraphic sections. To conclude this short discussion we can quote Fåhreus (1986, p. 150) who was a pioneer in criticising such ill-founded practices in biochronology: "In recent years many biostratigraphic zonations proposed in the literature either imply or directly state such a fine biostratigraphic resolution that in many cases has to be considered beyond the point of practical reproducibility, i.e. correlations attempted back onto such zonations carry with them little or no precision."

Another pioneer, Mamet (1977, p. 454), who is never quoted in the recent stratigraphic publications, used his biting humor to attack this inflation: "…1800 Visean "species" are known in the literature, hence the possibility of erecting 1800 first occurrence zones, 1800 last occurrence zones, and 1800 acme zones. This is common practice and gives a maze of incomplete ranges inducing pseudocorrelations."

Gradstein et al. (2012), in particular, strongly support the Conop and Rasc approaches which are discussed in the present chapter, and which produce precisely the kind of results criticized by Fåhreus and Mamet (loc.cit.). According to Gradstein et al. (2012) (GTS), in the UA theory "there is no inherent calibration to a time scale, unitary associations are not an exercise in biochronology as understood here" (i.e. in their book). However, Gradstein et al. (2012) overlooked the fact that their own calibration of U-Pb datings of the Triassic Jurassic boundary and that of the Hettangian Sinemurian boudary are precisely based on a biochronology established by means of the UAs (see Chap. 8).

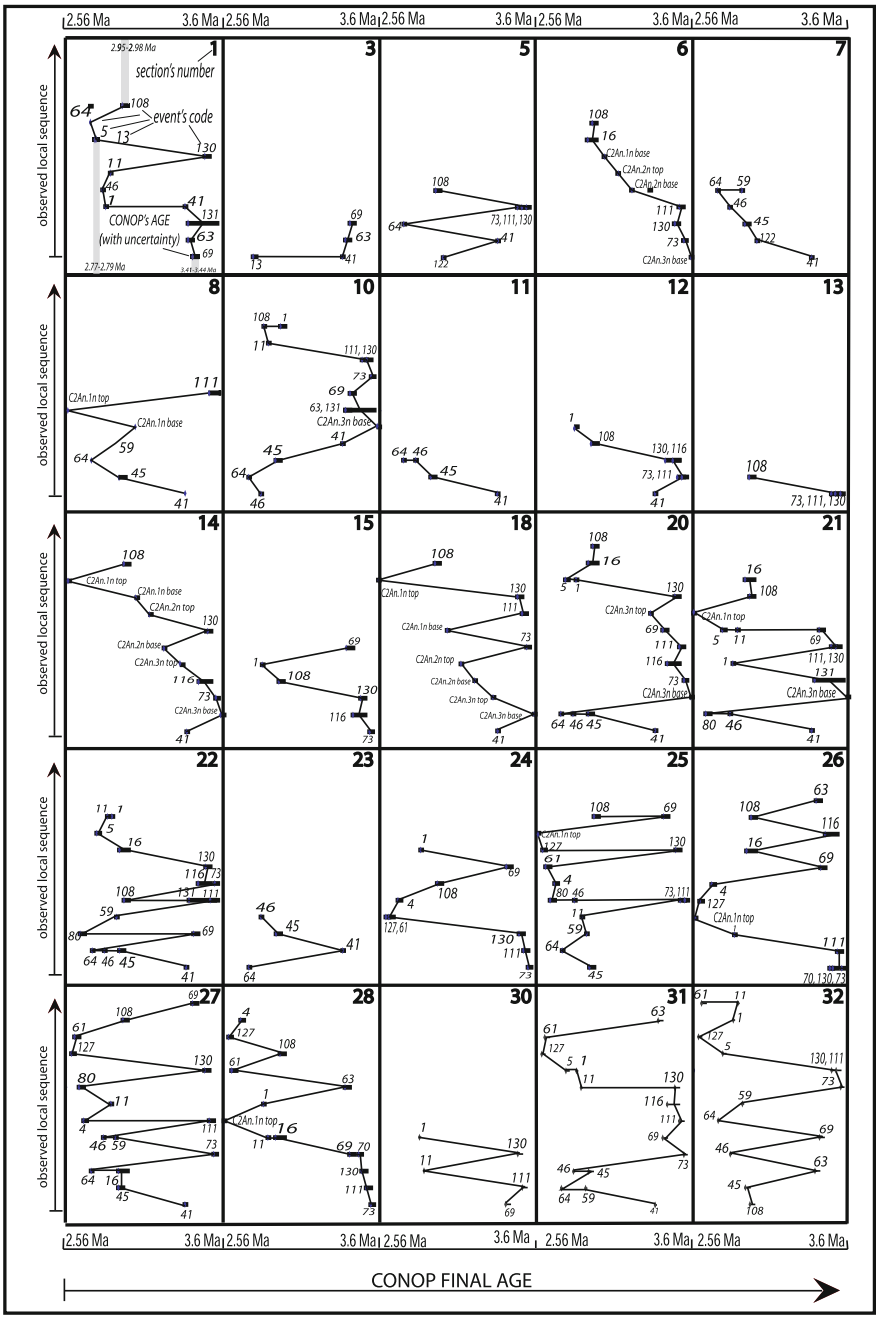

Fig. 6.10 Selected sequences of events in sections 1–32 considered as chronologically significant by Cody et al. (2008). These sequences are highly contradictory within each single stratigraphic section. *Codes* see Appendix 3-G

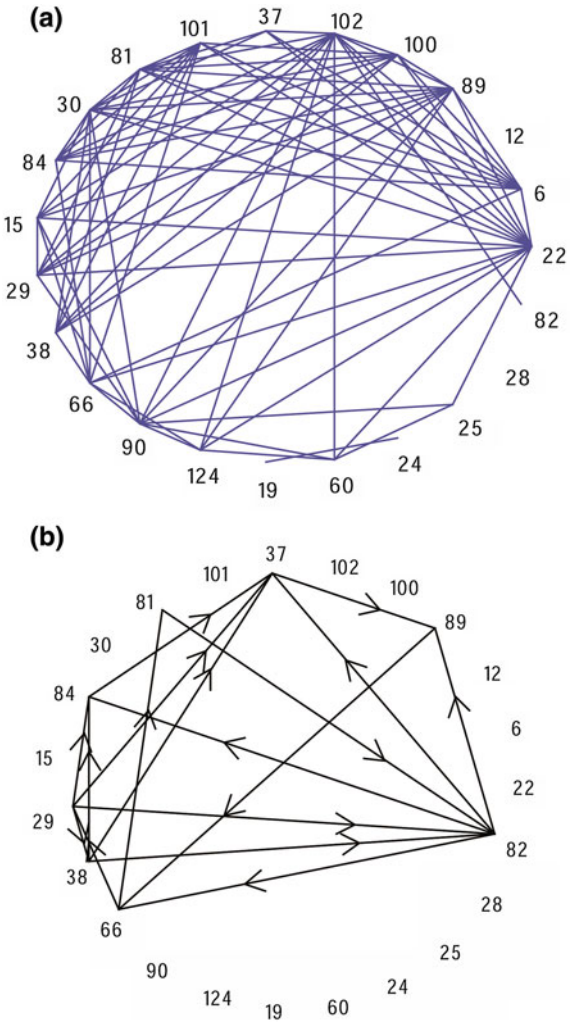

Fig. 6.11 **a** Trivial virtual coexistences between the FOs of the 23 first taxons considered in Cody's original range chart (Appendix 3-H). **b** Cycles Cn between the same "events"

6.9 Average Range Model

As noted above, some recent quantitative methods systematically produce ranges which are truncated while constructing zonations based on evolutionary first and last occurrences. To justify such truncations, some specialists introduced the "concepts" of *average range* or *hybrid range* to qualify them. The reader should realize that such ranges do not correspond to acmes or maximal evolutionary development of some taxons. In other words, average range zones are not synonym of "acme zones": they are just artefacts resulting from algorithms which do not take into account the rare inter-taxons coexistences, producing apparent ranges which

are much too short or which appear in the reversed order in the final outputs. That simple fact is sufficient to demonstrate that average ranges are not acme ranges (see below and Sect. 1.5).

For example Conop can be set up to relax the constraint against local range contraction and force the coexistences to be displayed in the output. As well noted by Cody et al. (loc.cit.) this is likely to contract many legitimate in situ range-ends arbitrarily and significantly underestimate the true temporal range of most taxa. According to Cody et al., such contractions provide a minimum to complement the Total Range Model's maximum estimate.

Comparing Cody's Average Range Chart with their original database by means of the UAgraph tools ("Biostratigraphic graph" and "Compare G*") we note that 670 coexistences were destroyed and 2 arcs have been reversed (See Appendix 3-E). Such results can be compared with the ones obtained by probabilistic approaches theoretically discussed by Guex (1991), Boulard (1993) and Baumgartner (1984). As an example we can note that Agterberg's program RASC (Ranking and Scaling: see Appendix 3-E), applied to Cody's data studied above in detail, destroys almost exactly the same edges as the Average Range option of Conop (667 truncated ranges: see Appendix 3-E): that huge range reduction produces an apparent pseudo-resolution accompanied by some inversions of taxa stratigraphic occurrences. This is another hard proof that average ranges do not represent the acmes of the truncated taxa.

6.10 Conclusions

The main difference between the UA theoretical model and Conop resides in the fact that the latter is essentially based on an algorithm which does not allow for an efficient treatment of the inter-FOs (respectively LOs) cyclic relationships (see Figs. 6.9, 6.10 and 6.11). In other words, the inter-events cycles have to be calculated separately (i.e. by means of another program such as UAgraph) to know which of Conop's FOs (or LOs) partial sequences are chronologically meaningful.

As an example we can consider the cyclic relationships linking the events listed in Fig. 6.9. All these taxa are considered as chronologically meaningful by Conop (see the corresponding list in Cody, loc.cit. Table 3, p. 102).

In the UA approach such contradictions are resolved by considering the events belonging to a given cycle as equivalent.

In contrast, the Unitary Associations theoretical model and the new program UAgraph (Hammer, Guex, Savary) are designed to produce a complete analysis of the complexity and structure of the paleontological data used to make correlations, and the computation is extremely rapid (a few minutes for the largest problems treated by means of UAgraph).

The following points are particularly important:

1. Analysis of the structure of the data and of its internal contradictions (list of cycles Z4 and Cn in G* and strongly connected components in G_k).
2. Individual comparison of the fossiliferous horizons showing conflicting stratigraphic relationships.
3. Display of the chronological discontinuities of the taxa distribution in the Range Chart.
4. Variety of tools allowing the analysis of the diachronism of the datums and the search for reworkings.
5. Analysis of the purely oriented graph of FOs (respectively LOs) containing all the virtual edges generated by the cross-over a > b and a < b.
6. Display of all the single co-occurrences associated with multiple superpositions in other localities.

To conclude, we note that the power of resolution of the UA method is contained in the data and not in the method. This is not true for every quantitative method because some systematically produce total ranges which are truncated, or arbitrarily constructed, generating non reproducible sequences of FOs and LOs that are implicated in cyclic and conflicting stratigraphic relationships. The UA theoretical model is unique in providing a full analysis of the internal complexity of any biochronological problem, and in this manner differs from all other quantitative methods available today.

References

Baumgartner, P. O. (1984). Comparison of Unitary Association and Probabilistic Ranking and Scaling as applied to Mesozoic Radiolarians. *Computers and Geoscience, 10*(1), 167–183.

Boulard, C. (1993). Biochronologie quantitative, concepts, methods et validité. *Docum. Lab. Géol. Lyon., 128*, 1–259.

Cody, R. D., Levy, R. H., Harwood, D. M., & Sadler, P. M. (2008). Thinking outside the zone High-resolution quantitative diatom biochronology for the Antarctic Neogene. *Palaeogeography, Palaeoclimatology, Palaeoecology, 260*, 92–121.

Edwards, L. E. (1978). Range chart and no-space graphs. *Computers and Geosc*ience*, 4*(3), 247–255.

Fåhreus, L. E. (1986). Spectres of biostratigraphic resolution and precision. Rock accumulation rates, processes of speciation and paleoecological constraints. *Newsletters on Stratigraphy, 15*(3), 150–162.

Galster, F., Guex, J., & Hammer, Ø. (2010). Neogene biochronology of Antarctic diatoms: A comparison between two quantitative approaches, CONOP and UAgraph. *Palaeogeography, Palaeoclimatology, Palaeoecology, 285*, 237–247.

Gradstein, F. M., Ogg, J. G., Schmitz, M., & Ogg, G. (2012). *The geologic time scale 2012* (Vol. 2). Amsterdam: Elsevier. ISBN 9780444594259.

Guex, J. (1977). Une nouvelle méthode d'analyse biochronologique. *Bulletin de la Société Vaudoise des Sciences Naturelles, 224*, 309–322.

Guex, J. (1979). Terminologie et méthodes de la biostratigraphie moderne. *Bull. Géol. Lausanne., 234*, 169–216.

Guex, J. (1991). *Biochronological correlations*. Berlin: Springer. 250 p.

Kemple, W. G., Sadler, P. M., & Strauss, D. J. (1995). Extending graphic correlation to many dimensions stratigraphic correlation as constrained optimization. In K. O. Mann & H. R. Lane (Eds.), *Graphic correlation* (pp. 65–82). SEPM Sp. Pap. 53.

Kirkpatrick, S., Gelatt, C. D., & Vecchi, M. P. (1983). Optimization by simulated annealing. *Science, 220*, 671–689.

Mamet, B. (1977). Foraminiferal zonation in the Lower Carboniferous. Methods and stratigraphic implications. In E.G. Kauffman & J.E. Hazel (Eds.), *Concepts and methods of biostratigraphy* (445–462). Dowden, Stroudsburg, Pennsylvania: Hutchinson and Ross Inc.

Sadler, P. M. (2002). *A users' guide and reference manual to the Conop program family* (Version 6.3). Riverside: Department of Earth Sciences, University of California.

Sadler, P. M. (2006). Constrained optimization approaches to the paleobiologic correlation and seriation problems: Part 1 (A Users Guide to the CONOP Program Family) and Part 2 (A Reference Manual to the Conop Program Family).

Sadler, P. M., & Cooper, R. A. (2003). Best-fit intervals and consensus sequences. In P. J. Harries (Ed.), *Approaches in high-resolution stratigraphic paleontology* (pp. 49–94). Netherlands: Kluwer Academic Publishers.

Sadler P. M., Cooper R. A., & Melchin, M. (2009). High-resolution, early Paleozoic (Ordovician–Silurian) time scales. *Geological Society of America Bulletin, 121*, 887–906. doi:10.1130/B26357.

Shaw, A. B. (1964). *Time in stratigraphy*. New York: McGraw Hill. 365 p.

Siesser, W. G. (1984). Paleogene sea level and climates USA eastern Gulf coastal plain. *Palaeogeography, Palaeoclimatology, Palaeoecology, 47*, 261–275.

Chapter 7
Lower Jurassic Radiolarian Biochronology and Evolutionary Rates

7.1 Introduction

In 2006 Gorican et al. published a comprehensive monograph on the systematics of Early Jurassic polycystine radiolarians which served as a coherent taxonomic base to establish a global radiolarian zonation for three stages that were poorly known before: the Pliensbachian, Toarcian, and Aalenian.

The goal of this major study was to examine the faunal turnovers and the biogeography through this critical time interval around a major ecologic and biotic crisis. The analysis was based on the distribution of 197 species belonging to 69 genera. Significant variations in the ratio between the number of originating and extinct species have been recognized. During the early Early Pliensbachian FADs greatly exceeded LADs and the maximum diversity was reached in the late Early Pliensbachian. The trend then reversed with the number of LADs exceeding FADs throughout the Late Pliensbachian and Early Toarcian (extinction interval). Recovery started in the Middle and Late Toarcian, when the number of FADs again surpassed the number of LADs.

The original results presented in this chapter were first elaborated by Carter et al. (2010) and Gorican et al. (2013) in collaboration with one of us (J.Gx).

7.2 The Radiolarian Zonation

The Pliensbachian to Aalenian zonation (Carter et al. 2010) was based on data from excellent sections at Haida Gwaii, British Columbia (BC), Williston Lake, north-eastern BC, east-central Oregon, Baja California Sur, southern Spain, Austria, Slovenia, Turkey, Oman, Japan and Argentina (see Appendix 4-C). Only the stratigraphically useful species were included in our computations of the data by means of UAgraph: those that were either rare, long ranging or non-diagnostic with

J. Guex et al., *Discrete Biochronological Time Scales*,
DOI 10.1007/978-3-319-21326-2_7

wide limits of variability and others that occur sporadically because their skeletons are very delicate and are rarely preserved were omitted. The ammonites from British Columbia were included to facilitate the calibration between the radiolarian zonation and the Lower Jurassic standard zones. Note that the Queen Charlotte Islands sections were merged to make a unique composite section, thanks to the regional ammonite correlations. The different regions were first studied separately and then transformed into composite sections with the help of UAgraph before the final computation of the global data file.

The database, treated by means of UAgraph, resulted in a referential consisting of 41 successive UAs (Fig. 7.1). The first and the last UAs represent composite samples of the Upper Sinemurian and the Lower Bajocian respectively, used to frame the main Pliensbachian to Aalenian new data. The remaining 39 UAs were merged into zones according to prominent radiolarian faunal breaks and ammonite data, mostly from sections located in the Haida Gwaii. Nine Unitary Association Zones (UAZ) were defined: four Lower Pliensbachian, one Upper Pliensbachian, one Lower Toarcian, one Middle–Upper Toarcian, and two Aalenian.

The Pliensbachian and Toarcian were then analysed in terms of faunal turnovers and paleobiogeography. The Aalenian was not included in this analysis because the data are too scarce to allow a reliable interpretation. The Aalenian contains only the most stratigraphically important species that have already been used for biostratigraphy in previous works and could serve as a link with the Middle Jurassic to Lower Cretaceous UA-zonation of Baumgartner et al. (1995). Many species, even those that first appear in the Aalenian have been neglected.

For the Pliensbachian and Toarcian the zonation integrates virtually all available data on the global distribution of radiolarians (see appendix 4-C). Stratigraphic ranges of 167 Pliensbachian and Toarcian species are incorporated (Fig. 7.1). The data include occurrences in middle to high palaeolatitudes (Haida Gwaii, Williston Lake in north-eastern British Columbia, east-central Oregon) and several west–east

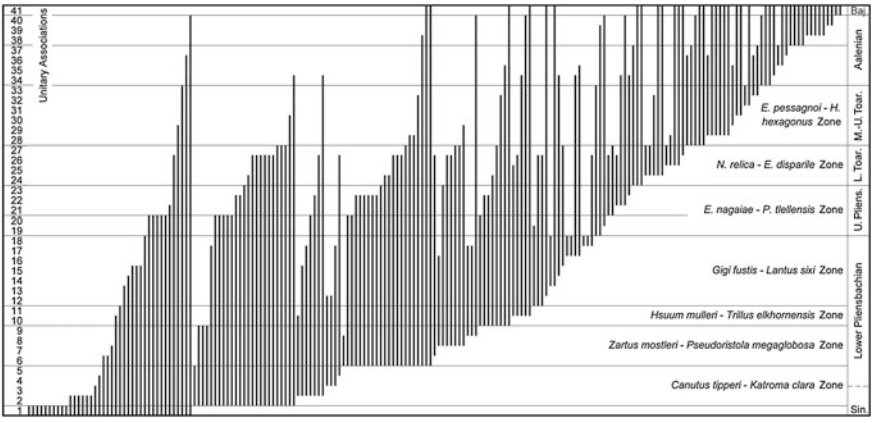

Fig. 7.1 Lower Jurassic radiolarian UA range chart. For the names see Appendix 4-B

distributed occurrences in low palaeolatitudes (Baja California Sur, Tethyan realm, Japan). One locality from the southern hemisphere (Argentina) is also included.

The sections studied record a great variety of facies and depositional environments. In the Haida Gwaii and Baja California Sur, they are mostly sandstone and siltstone with limestone concretions and have high sedimentation rates. The Tethyan sections were deposited on a subsided continental margin (Austria, Slovenia, Turkey, Oman) with facies ranging from almost purely calcareous to highly siliceous pelagic limestone and in Oman, bedded radiolarian chert and siliceous mudstone. The sections from Japan are typically oceanic and are composed almost entirely of bedded radiolarian chert in which sedimentation rates do not exceed 2 m/my (details in Carter et al. 2010, and references therein). The zonation calculated by means of UAgraph thus satisfactorily reflects the global magnitude of evolutionary rates but the observed faunal changes cannot be directly tied to short-term local facies/environmental changes.

Resolution for the Lower Pliensbachian is the most precise and equals that of the ammonite zones, i.e. the four radiolarian zones are correlative to the Tetraspidoceras, Imlayi, Whiteavesi and Freboldi ammonite zones (see Fig. 6 in Carter et al. 2010). Except for the *Hsuum mulleri—Trillus elkhornensis* radiolarian zone (equivalent of the Whiteavesi ammonite Zone), which was recognized in the Haida Gwaii only, all other zones were recognized in other areas. Resolution for the Upper Pliensbachian, Lower Toarcian and Middle–Upper Toarcian is less precise. The Upper Pliensbachian was not subdivided because the data outside Haida Gwaii were too poor to demonstrate worldwide reproducibility. However, the superpositional control in these sections is obvious and well constrained with the ammonites. Thus in Haida Gwaii a subdivision into two subzones, corresponding to the Kunae (UAs 19–20) and Carlottense (UAs 21–23) ammonite zones is possible. The refined resolution in the Upper Pliensbachian is considered in this chapter for the analysis of evolutionary rates.

7.3 Evolutionary Patterns

The rate of faunal turnover is expressed as the number of species with FAD (first appearance datum) against the number of species with LAD (last appearance datum) in a given unitary association. A specially designed tool, i.e. 'Cumulated FADs/LADs' of the UAgraph program was used for the following analysis. The numerical data (Appendix 4-C) are graphically presented in Fig. 7.2, where the cumulative number of FADs is plotted against cumulative number of LADs. Each UA is represented by a point on the curve. Gentle slopes of the curve indicate high diversification rates (great number of FADs versus low number of LADs) and steep slopes indicate high extinction rates (low number of FADs versus great number of LADs). The beginning and the end of such a curve are biased by the fact that the base and the top of the original range chart record truncated ranges—all taxa in the lowest UA may range downward and all taxa in the highest UA may

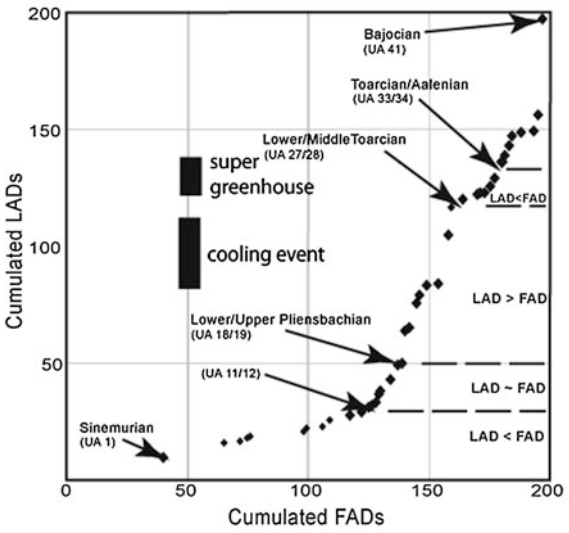

Fig. 7.2 Cumulated FADs versus cumulated LADs during the Lower Jurassic

range upward. These parts of the curve must obviously be ignored. This method has been applied successfully for Jurassic and Cretaceous radiolarians (Guex 1991; Savary and Guex 1999; O'Dogherty and Guex 2002), and for Jurassic nannoplankton (Mailliot et al. 2006).

The advantage of this method is that it analyses the relationship between FADs and LADs and not only their absolute numbers. This means that the analysis is not biased by exceptional preservation, which is a common phenomenon in the radiolarian fossil record. An exceptionally well-preserved assemblage would be characterized by an increase in the total diversity, i.e. by an exceptionally high number of FADs as well of LADs, but the FAD/LAD relationship would not change significantly. In our case this is important, because some species were deliberately eliminated from the calculation of unitary associations as explained above.

Through the Pliensbachian and Toarcian three distinctive intervals that differ significantly in their radiation/extinction patterns were recognized (see Fig. 7.2 and 7.3). These are: Early Pliensbachian (pronounced diversification), Late Pliensbachian to Early Toarcian (extinction interval), and Middle to Late Toarcian (recovery).

The overall trend of radiolarian diversity is in a fairly good agreement with that of other marine faunas (ammonites and also benthos), but shows an inverse correlation with diversity trends of phytoplankton.

Correlation with concomitant environmental changes indicates that radiolarian radiation/extinction rates were not consistently linked with temperature fluctuations or sea-level changes. It is also evident that the diversity decrease started well before the Early Toarcian negative $\delta^{13}C$ peak and the Oceanic Anoxic Event (OAE) (see Fig. 7.2 and 7.3). The extinction interval corresponds to the duration of a short-term anomaly in the strontium-isotope record, including the rapid decrease of $^{87}Sr/^{86}Sr$

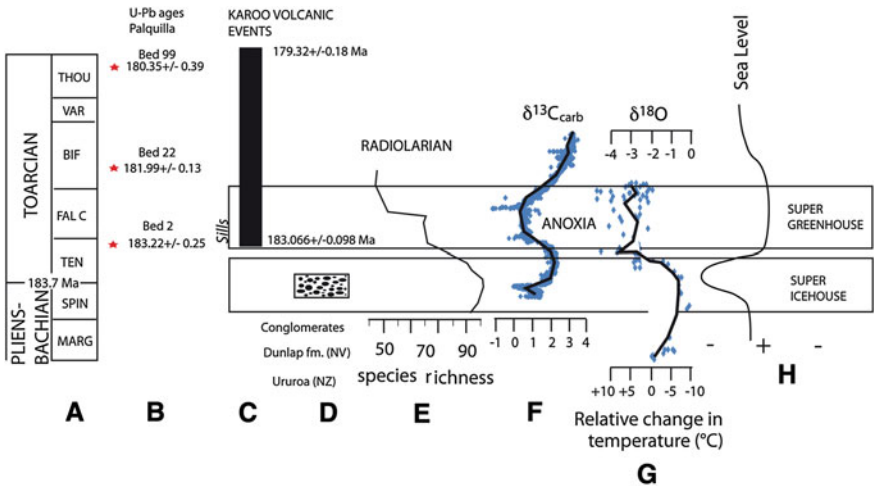

Fig. 7.3 A model for the Pliensbachian-Toarcian crisis. (*A*) Standard ammonite zonation of the Upper Lias (Margaritatus, Spinatum, Tenuicostatum, Falciferum, Bifrons, Variabilis, Thouarsense). (*B*, *C*) Numerical ages of beds 2, 22 and 99 at Palquilla (Peru) and of the Karoo basalts. Redrawn from Guex et al. (2012a), Sell et al. (2014). (*D*) Conglomerates present at the Pliensbachian—Toarcian boudary in New Zealand and Nevada. From Guex et al. (2012a). (*E*) Species richnes of Radiolarians in the Upper Pliensbachian and Early Toarcian. From Gorican et al. (2013). (*F*) Variation of the $\delta^{13}C$ around the Pliensbachian—Toarcian boundary. Redrawn from Hesselbo et al. (2007). (*G*) Variation of the $\delta^{18}O$ and paleotemperatures around the Pliensbachian—Toarcian boundary. Redrawn from Dera et al. (2010). (*H*) Variations of sea level around the Pliensbachian—Toarcian boundary. From Guex et al. 2001

values in the Late Pliensbachian as well as the rapid increase in the Early Toarcian. This coincidence supports the hypothesis that the predominance of extinctions over originations was caused by a series of climatic and environmental changes related to intensified magmatic activity.

Some distinct biogeographic differences have also been observed in the distribution of the radiolarians. Generic differences are most strongly displayed by the presence or absence of a particular genus or by changes in abundance. Two groups of genera are distinguished: those that are common to abundant in the Tethys (low latitudes) and rare to absent in mid to high latitudes, and those common to abundant in mid to high latitudes and rare to absent in the Tethys.

7.4 A Model of the Pliensbachian-Toarcian Environmental Perturbation

Environmental perturbations related to the early Jurassic Pliensbachian-Toarcian boundary have long been related to the onset of the Karoo-Ferrar large igneous province (Pálfy and Smith 2000). Recent high precision U-Pb dating on zircons of

major sill intrusions in the Karoo basin can be directly correlated with the well known Toarcian Oceanic Anoxic Event (OAE) and is concomitant with these sill intrusions into organic rich sediments of that basin (Guex et al. 2012a, b; Sell et al. 2014). In Fig. 7.3 we present a compilation of major isotopic variations, the available geochronological data and major sea level variations to investigate whether and how the geochemical and biochronological data can be correlated with the magmatic activity of the Karroo-Ferrar LIP.

The end-Pliensbachian extinction, preceding the Toarcian AOE by a few hundred of kyr (Dera et al. 2010), is marked by an important diversity drop (disappearance of 90 % of the ammonite taxa) associated with a generalized sedimentary gap linked to a marked regression event in NW-Europe and the Pacific area.

This regression was interpreted as due to a major short lived glaciation (Guex et al. 2001, 2012a, b) coeval with the main extinction and preceding the main basalt eruptions. Our major arguments refer to an important emersion topography observed on seismic images of the North Sea (Marjanac and Steel 1997), to the evidence for polar ice storage (Price 1999) and to the deposition of thick conglomerates Dunlap Formation in Nevada (USA) (Muller and Ferguson 1939) and Ururoa-Kawhia area, New Zealand (Hudson 2003). The cooling model is supported by recent $\delta^{18}O$ data on belemnites (Gomez et al. 2008a, b; Harazim et al. 2012) and by the discovery of glendonites in the upper part of the Pliensbachian (Suan et al. 2011). The origin of the major cooling is probably related to huge volcanogenic SO_2 degassing during the Late Pliensbachian preceding the major CO_2 emissions of the Early Toarcian (Guex et al. 2001; see also Sect. 8.5).

The regressive phase is followed, after a few hundred thousand years, by a worldwide transgression during the Early Toarcian, with the deposition of black shales associated to the Toarcian OAE (Jenkyns 1988). The Toarcian OAE itself is responsible for a second extinction affecting mainly benthic foraminifera populations (Bartolini et al. 1990) and brachiopods (García-Joral et al. 2011. Radiolarians were also affected (Fig. 7.3) but their extinction was apparently slightly delayed with respect to benthos and probably coincided with a drastic fertility drop just after the OAE.

References

Bartolini, A., Nocchi, M., Baldanza, A., & Parisi, G. (1990). Benthic life during the early Toarcian anoxic event in the Southwestern Tethyan Umbria-Marche basin, Central Italy (pp. 323–338). Benthos '90, Sendai, Japan: Tokai University Press.

Baumgartner, P. O., Bartolini, A., Carter, E. S., Conti, M., Cortese, G., Danelian, T., et al. (1995). Middle Jurassic to early Cretaceous radiolarian biochronology of Tethys based on Unitary Associations. In P. O. Baumgartner, L. O'Dogherty, Š. Gorican, E. Urquhart, A. Pillevuit, P. De Wever (Eds.), *Middle Jurassic to lower Cretaceous radiolaria of Tethys occurrences, systematics, biochronology* (pp. 1013–1038). Mémoires de Géologie Lausanne 23.

Carter, E. S., Gorican, Š., Guex, J., O'Dogherty, L., De Wever, P., Dumitrica, P., et al. (2010). Global radiolarian zonation for the Pliensbachian, Toarcian and Aalenian. *Palaeogeography, Palaeoclimatology, Palaeoecology, 297*, 401–419.

Dera, G., Neige, P., Dommergues, J.-L., Fara, E., Laffont, R., & Pellenard, P. (2010). High-resolution dynamics of Early Jurassic marine extinctions the case of Pliensbachian-Toarcian ammonites (Cephalopoda). *Journal of the Geological Society, 167*, 21–33. doi:10.1144/0016-76492009-068.

García-Joral, F., Gómez, J. J., & Goy, A. (2011). Mass extinction and recovery of the Early Toarcian (Early Jurassic) brachiopods linked to climate change in Northern and Central Spain. *Palaeogeography, Palaeoclimatology, Palaeoecology, 302*, 367–380.

Gómez, J. J., Goy, A., & Canales, M. L. (2008a). Seawater temperature and carbon isotope variations in belemnites linked to mass extinction during the Toarcian (Early Jurassic) in Central and Northern Spain. *Comparison with other European sections Palaeogeography, Palaeoclimatology, Palaeoecology, 258*, 28–58.

Gómez, J. J., Goy, A., & Canales, M. L. (2008b). Seawater temperature and carbon isotope variations in belemnites linked to mass extinction during the Toarcian (Early Jurassic) in Central and Northern Spain. *Comparison with other European sections Palaeogeography, Palaeoclimatology, Palaeoecology, 258*, 28–58.

Gorican, Š., Carter, E. S., Guex, J., O'Dogherty, L., De Wever, P., Dumitrica, P., et al. (2013). Evolutionary patterns and palaeobiogeography of Pliensbachian and Toarcian Radiolaria. *Palaeogeography, Palaeoclimatology, Palaeoecology, 386*, 620–636.

Guex, J. (1991). *Biochronological correlations*. Berlin: Springer. 250 p.

Guex, J., Morard, A., Bartolini, A., & Morettini, E. (2001). Découverte d'une importante lacune stratigraphique à la limite Domérien-Toarcien: implications paléo-océanographiques. Bulletin de la Société vaudoise des Sciences Naturelles, *87*(3), 277–284

Guex, J., Bartolini, A., Spangenberg, J., Vicente, J.-C., & Schaltegger, U. (2012a). Ammonoid multi-extinction crises during the late Pliensbachian—Toarcian and carbon cycle instabilities. *Solid Earth Discussions, 4*, 1205–1228. doi:10.5194/sed-4-1205-2012.

Guex, J., Schoene, B., Bartolini, A., Spangenberg, J., Schaltegger, U., O'Dogherty, L., et al. (2012b). Geochronological constraints on post-extinction recovery of the ammonoids and carbon cycle perturbations during the Early Jurassic. *Palaeogeography, Palaeoclimatology, Palaeoecology, 346–347*, 1–11.

Harazim, D., Van de Schootbrugge, B., Sorichter, K., Fiebig, J., Weug, A., Suan, G., et al. (2012). Spatial variability of watermass conditions within the European Epicontinental Seaway during the Early Jurassic (Pliensbachian–Toarcian). Sedimentology. doi:10.1111/j.1365-3091.2012.01344.x.

Hesselbo, S. P., Jenkyns, H. C., Duarte, L. V., & Oliveira, L. C. V. (2007). Carbon-isotope record of the Early Jurassic (Toarcian) Oceanic Anoxic Event from fossil wood and marine carbonate (Lusitanian Basin, Portugal). *Earth Planetary Science Letters, 253*, 455–470.

Hudson, N. (2003). Stratigraphy and correlation of the Ururoan and Temaikan Stage (Lower-Middle Jurassic, Sinemurian-Callovian) sequences, New Zealand. *Journal of the Royal Society of New Zealand, 33*(1), 109–147.

Jenkyns, H. C. (1988). The Early Toarcian (Jurassic) anoxic event stratigraphic, sedimentary and geochemical evidence. *American Journal of Science, 288*, 101–151.

Mailliot, S., Mattioli, E., Guex, J., & Pittet, B. (2006). The early Toarcian anoxia, a synchronous event in the Western Tethys? An approach by quantitative biochronology (Unitary Associations), applied on calcareous nannofossils. *Palaeogeography, Palaeoclimatology, Palaeoecology, 240*, 562–586.

Marjanac, T., & Steel, R. J. (1997). *Dunlin group sequence stratigraphy in the northern North Sea. A model for Cook sandstone deposition*. AAPG Bulletin, 81(2), 276–292.

Muller, S. W., & Ferguson, H. G. (1939). Mesozoic stratigraphy of the Hawthorne and Tonopah quadrangles, Nevada. *Geological Society of America Bulletin, 50*, 1573–1624.

O'Dogherty, L., & Guex, J. (2002). Rates and patterns of evolution among Cretaceous radiolarians, relations with global paleoceanographic events. *Micropaleontology, 48*(1), 1–22.

Pálfy, J., & Smith, P. L. (2000). Synchrony between Early Jurassic extinction, oceanic anoxic event, and the Karoo-Ferrar flood basalt volcanism. *Geology, 28*, 747–750.

Price, G. D. (1999). The evidence and implications of polar ice during the Mesozoic. *Earth-Science Reviews, 48*, 183–210.

Savary, J., & Guex, J. (1999). Discrete biochronological scales and unitary associations description of the biograph computer program. *Mémoires de Géologie Lausanne, 34*, 1–282.

Sell, B., Ovtcharova, M., Guex, J., Bartolini, A., Jourdan, F., Spangenberg, J. E., et al. (2014). Evaluating the causal link between the Karoo LIP and climatic-biologic events of the Toarcian Stage with high-precision geochronology. *Earth and Planetary Science Letters, 408*, 48–56.

Suan, G., Nikitenko, B. L., Rogov, M. A., Baudin, F., Spangenberg, J. E., Knyazev, V. G., et al. (2011). Polar record of Early Jurassic massive carbon injection. *Earth and Planetary Science Letters, 312*, 102–113.

Chapter 8
Calibrating Biochronological Zones with Geochronology

8.1 Introduction

One fundamental problem in geology is to calibrate precisely the Phanerozoic geological stages based on fossils with accurate geochronological data. To proceed to such a calibration we need essentially to use marine time diagnostic fossils like Graptolites, Trilobites, Ammonites or planctonic Foraminifera associated with coeval volcanic ashes or lava flows containing radiogenic minerals like zircons for U-Pb dating or K-feldspars for Ar–Ar dating. Ideal situations are where marine basins are closely associated with volcanic arcs such as the Mesozoic basins of the Pacific cordilleras in South and North America. Such basins usually provide marine organisms associated with ash beds (tephras) containing zircons or other silicates which can easily be dated with routine radiochronologic methods.

In this chapter we will present a quantitative study of the early Jurassic recovery of ammonoids after the end-Triassic mass extinction based on detailed U-Pb ID-TIMS geochronology from ash bed zircons placed within a clear phylogenetical and biochronological framework at the subzonal and species level. This study was triggered by our discovery of a rich Peruvian sequence of ammonites, deposited concomitantly with an unusually large number of ash beds (Guex et al. 2012). We also show the first ammonoid calibration of a complete $\delta^{13}C_{org}$ curve spanning the Hettangian in the Pacific realm. This allows us to integrate the ammonoid recovery pattern with the carbon isotope data. We observe two major phases of rediversification during the Hettangian ammonite *P.spelae* (syn. *P.spelae tirolicum*) and Angulaticeras zones that correspond to positive peaks in our new $\delta^{13}C_{org}$ curve, providing a possible link between biodiversity and the global carbon cycle.

J. Guex et al., *Discrete Biochronological Time Scales*,
DOI 10.1007/978-3-319-21326-2_8

8.2 Biochronology and Geochronology of the Hettangian Stage

Despite the importance of mass extinction events on biological evolution, global climate and geochemical cycling, we still need to establish quantitative models for the rates, causes, and consequences of biotic re-proliferation following these catastrophic events. Our discovery of a rich Peruvian sequence of ammonites, deposited concomitantly with ash beds containing zircon has allowed establishing high-precision U/Pb time constraints around the Triassic-Jurassic (TJ) transition within a clear phylogenetical framework and a biochronological analysis at the subzonal level and species level (Guex et al. 2012).

In the case of the TJ recovery, we note that the explosion of the earliest Hettangian ammonites occurs within the genus *Psiloceras*. That genus literally exploded a few tens of thousands of years after the TJ crisis and occupied massively all the possible ecological niches all over the world, from the Pacific deep waters to the NW European shallow deposits and also in some few known Tethyan occurences like at Germig in Tibet (Yin et al. 2007). The worldwide dispersion allowed the differentiation of the group in several major "phyla", the Schlotheimiidae, Discamphiceratinae, Arietitidae and Lytocerataceae, which were the roots of all other Jurassic and Cretaceous ammonites. That rapid differentiation was probably enhanced by the appearance of multiple epicontinental basins during the fragmentation of the Pangea.

It is well known that the Triassic-Jurassic boundary represents one of the most important biotic crises in Earth history: that mass extinction involved the disappearance of some 80 % of all known species on land and in the sea. Widespread magmatic activity of the Central Atlantic Magmatic Province (CAMP) has been invoked as a cause for this catastrophic biotic event (Courtillot et al. Courtillot 1999; Hesselbo et al. 2002; Marzoli et al. 2011). The relationship between the extinction and its probable volcanic cause can only be established by demonstrating the synchrony of the two events. This requires accurate and precise age determinations for both the TJB strata in a perfectly calibrated marine section and of volcanic rocks of the CAMP. New zircon U-Pb ages of highest precision and accuracy have been published recently (Schoene et al. 2010), demonstrating an identical age of the earliest Jurassic ammonite *Psiloceras spelae* in Peru and in Nevada, synchronous within geochronological uncertainty of ca. 150 ka to the oldest volcanic rocks of the CAMP in North America. In other words, the massive CAMP volcanism seems to be slightly younger than the catastrophic extinction.

The Pucara Formation in the Utcubamba Valley (northern Peru; see Fig. 8.1) hosts one of the best sedimentary records straddling the TJ boundary in the world. A complete deep marine sedimentary sequence from mid Rhaetian to Early Sinemurian was studied in detail, in which the position of the Triassic-Jurassic boundary (TJB), defined as the first appearance of ammonite *P. spelae*, has been identified. Numerous volcanic ash beds interspersed throughout a section named after the closeby village of Levanto and containing zircon have also been

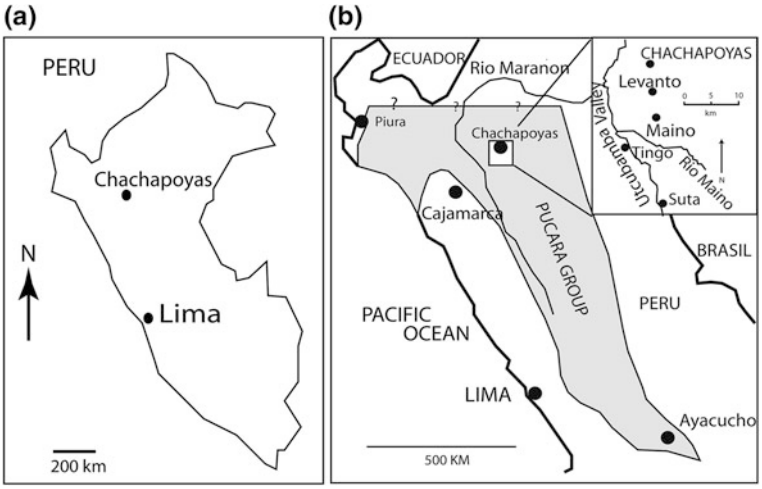

Fig. 8.1 Map showing the location of the Levanto section (N-Peru)

discovered during these investigations, allowing temporal calibration of the biostratigraphy with precise and accurate U-Pb zircon ages. These geochronological tie-points allow calibration of the rates of Rhaetian to Sinemurian ammonite fauna evolution during the critical pre- to post-extinction interval.

The Levanto section is a thick monotonous sequence of siltstones alternating with slightly more calcareous silty beds. More than 20 fossiliferous beds have been excavated, allowing a very precise correlation with the standard ammonoid zonations used in the Upper Rhaetian and Lower Jurassic (Guex 1995; Guex et al. 2004; Taylor et al. 2001). The Rhaetian/Hettangian boundary (TJB) is defined by the first occurrence of *Psiloceras spelae*, bracketing a barren interval of some 6 meters for the extinction interval, the Hettangian/Sinemurian boundary is bracketed by *Badouxia canadensis* and *Coroniceras*, leaving a c.15 meter thick barren interval for this boundary. Four major ammonite faunas have been located between these boundaries in that Peruvian sequence: *Psiloceras tilmanni, Kammerkarites, Alsatites* and first abundant *Angulaticeras*, allowing a precise calibration of that Peruvian sequence with the sequences described in Nevada and Oregon (Guex 1995; Taylor et al. 2001).

The Peruvian U-Pb data have been used to build an age model for the deposition of the Rhaetian-Sinemurian section from the Pucara basin in Peru. We have shown that the youngest zircon age from the main population of zircons from an ash bed was our best estimate for the timing of deposition, excluding sample LM4-185A which is reworked (Fig. 8.2). We have then assumed a linear deposition rate between our samples, which yields deposition rates between 13 and 68 mm/ka, with an average of 36 ± 18 mm/ka (±1 standard deviation).

Because of such low sedimentation rates and an abundance of ashbeds, many ages for ash beds overlap with those above and below them, resulting in large

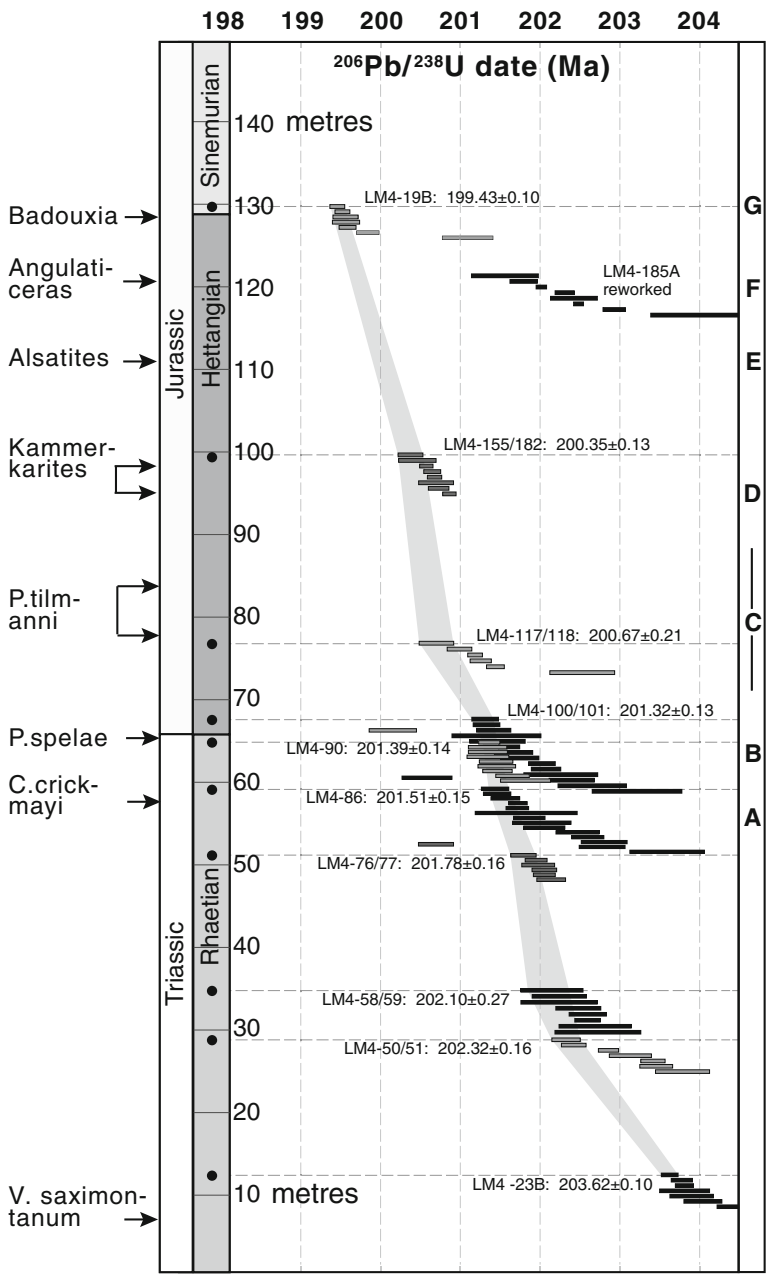

Fig. 8.2 Geochronologic ages of the ash beds coeval with the ammonite bearing sediments (From Guex et al. 2012) *Column A–G* biochronologic ages used in Figs. 8.3 and 8.4

uncertainties in deposition rates. This can be partly reduced if we take into account the constraint that an ashbed higher in the sequence must be younger than the one beneath it. To build this constraint into the age model, we ran a simple Monte Carlo simulation. This model produces 10^6 normally distributed numbers for each ash bed that correspond to the age and uncertainty of the youngest zircon from an ashbed. It then randomly pulls a value from each ash bed distribution to produce an age model for age versus height, resulting in 10^6 age models. If any ash bed is older than the one beneath it, that age model is discarded. The remaining age models ($\sim$400,000 were kept) are used to generate a new deposition age for each ash bed. In most cases, the resulting deposition age is identical to the input, though improved precision is seen in areas of dense ash bed sampling (e.g. near the TJ boundary) or for example with the relatively imprecise data of sample LM4-58/89—a result of very low U content in those grains. The resulting age versus height model and recalculated deposition ages for ash beds are plotted in Fig. 8.2 with a gray band. This age model can also be used to calculate estimates for the time of important events in ammonite evolution. The main goal of our geochronologic and palaeontological study was to establish the rate of recovery of the ammonites at the genus and species level in the two main realms, where Hettangian ammonites are well recorded and have been studied in great detail: the North and South American and the NW European sequences. In the Tethyan realm, the classical Alpine sequences described by Waehner (1882–1898) and other pioneers (Lange 1952) are condensed and do not satisfy the conditions of continuity necessary to quantify the recovery rates.

The age model determined in the previous section can be used to calibrate the timing of classical ammonite zones. For practical reasons, we provide a simplified non-standard zonation (Fig. 8.3) allowing a clear representation of the large scale

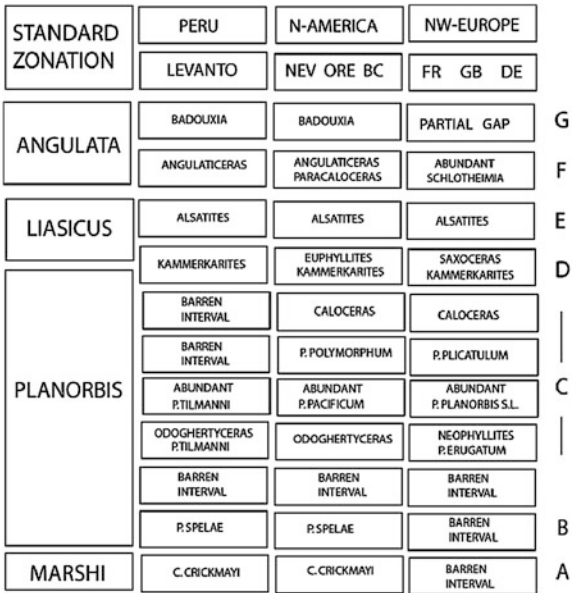

Fig. 8.3 Informal zonation of the stratigraphic interval Late Rhaetian–Late Hettangian

correlations applied in the present work and resulting from the large biochronological syntheses presented below.

Biostratigraphic data from the Pacific Realm (western South and North America), including some data from Kuhjoch in the Austrian Alps have been in part empirically analyzed using the Unitary Associations to illustrate the maximal associations of the ammonites. In this case our treatment of the data by means of the UAgraph program was not standard because we used a composite stratigraphic range chart made by Taylor et al. (2001) (see Sect. 3.6). The original data used in our synthesis included the distribution of more than 90 taxa, species and genera where dubious data were excluded.

The range chart resulting from those synthetic data is given in Fig. 8.4, showing the details of the diversification of the ammonites during that interval of time, following the Late Triassic major extinction.

8.3 Variations of the Taxonomic Richness Versus $\delta^{13}C_{org}$ and $^{87}Sr/^{86}Sr$ Variations

A calibration of the Hettangian $\delta^{13}C_{org}$ established at New York Canyon (Nevada) with the above biochronological scale is given in Fig. 8.5. The lower part of the stratigraphic section is based on Guex et al. (2004, 2008). Our original curve (Guex et al. 2004) of the transition between the Triassic and Early Hettangian has been the subject of some thermal alteration of the organic matter inducing noise in the measurements and for that reason we applied a simple moving average to the original measurements (Guex et al. 2008). The large scale correlations of that new curve and the technical description of the analytical part are discussed in Bartolini et al. (2012) and Guex et al. (2011) and will not be repeated here.

The different excursions (negative and positive) of this curve are labelled by the names of the ammonites that are characteristic of the timing of each excursion. The first negative shift (initial negative anomaly of Hesselbo et al. 2002) is named the Crickmayi negative excursion. It is followed by the Spelae positive, Pacificum negative and Angulaticeras-Sunrisites positive excursions.

The variations of the ammonite species richness (Sobs) is expressed as the total taxonomic richness observed in the interval corresponding to the geochronometrical tie point. That variation (Sobs) throughout the Hettangian, calibrated to our new geochronological data and constructed from the UA-range chart of Fig. 8.4 is given in Fig. 8.5.

That diagram shows a partial correlation between the $\delta^{13}C_{org}$ curve and the diversity fluctuations. This figure shows that the well known first negative excursion of the organic carbon is correlated with the peak of the Rhaetian extinction. The second negative excursion is restricted to the Psiloceras pacificum zone. The mid-Hettangian slow-down of the diversification is followed by an explosion of the diversity in the Upper Hettangian and by a new positive excursion of the organic

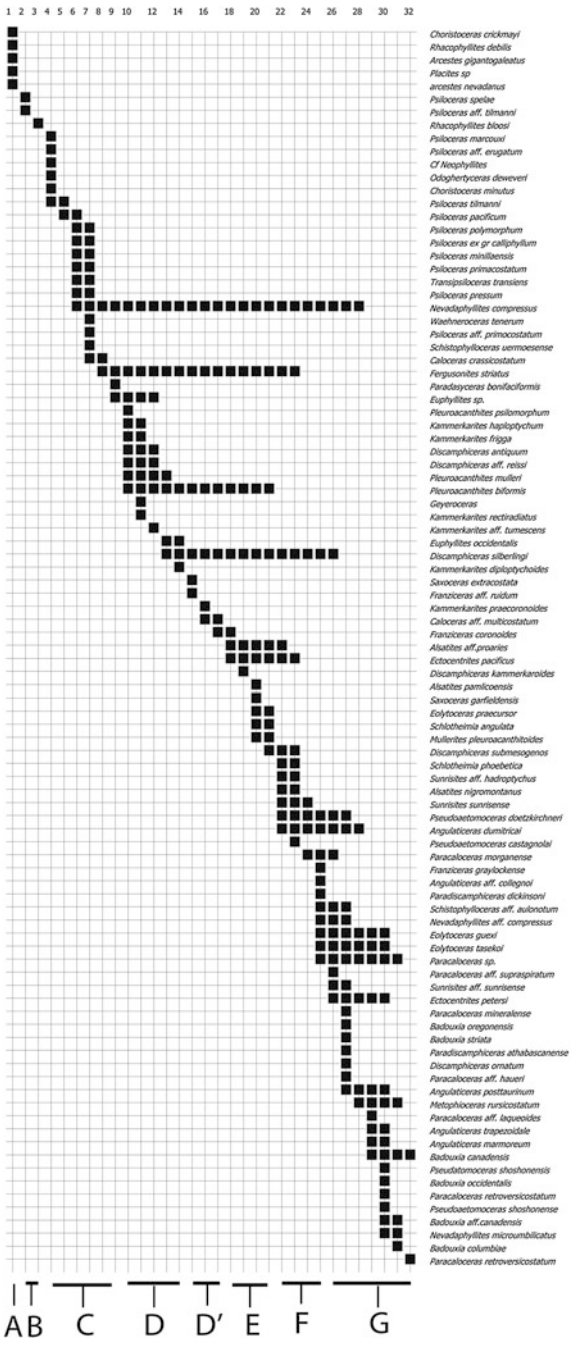

Fig. 8.4 Late Rhaetian to Late Hettangian ammonites biochronological distribution. From Guex et al. (2012)

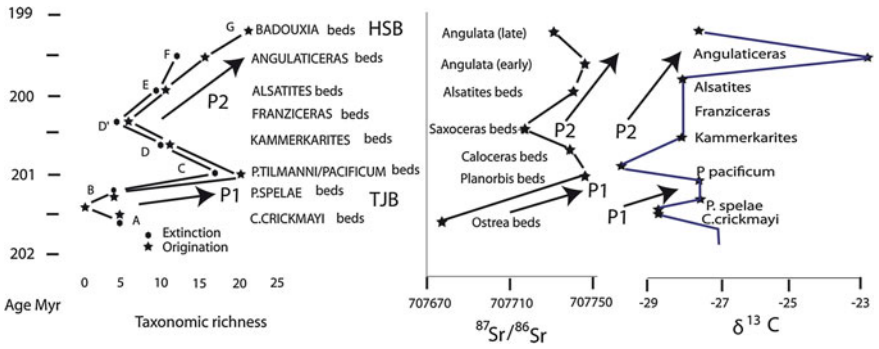

Fig. 8.5 Taxonomic richness of the ammonite species (=diversity, not disparity) correlated with the isotopic variations of $\delta^{13}C_{org}$ and $Sr^{87/86}$ (From Guex et al. 2012)

carbon. However we note that the minimum of the ammonite diversity (D′) occurs later than the minimum of the $\delta^{13}C_{org}$ curve which is located between the P.pacificum and Kammerkarites beds. The strontium data, based on Jones et al. (1994) measurements in Great Britain (see also Cohen and Coe 2007) are plotted as the mean-values of the original measurements per subzone. There is an apparent correlation between the taxonomic richness and the variation of the $^{87}Sr/^{86}Sr$ ratio. Such a correlation was already observed and discussed by Cardenas and Harries (2010) at a very large scale in the marine Phanerozoic genera. According to these authors, this correlation is basically controlled by the availability of marine nutrients.

8.4 Rate of Evolutionary Changes in Ammonoids Evolutionary Trends

8.4.1 Phylogeny

The general pattern of the phylogeny of the Lower Jurassic ammonites is shown in Fig. 8.6

The most frequent evolutionary trend observed in Mesozoic ammonites is where the ancestral group has an open umbilicus (i.e. evolute form) and where the descendants are involute (i.e. tightly coiled, oxycone or sphaerocone). This trend was first described in Liassic ammonites (Hyatt 1889) and later recognized in Devonian ammonites, at the beginning of the history of the group (Erben 1966).

The trend towards increasing involution of originally evolute shells leads either to lenticular (oxycones) or more or less spherical shells (sphaerocones). The recurrent character of this trend was discussed in the early 1940's to explain the multitude of heterochronous homeomorphies observed within this group (Schindewolf 1950; Haas 1942). Some ammonite lineages also show a broad trend towards increased sinuosity of the growth-lines and, on a large time scale, this group show an overall increase in suture line complexity.

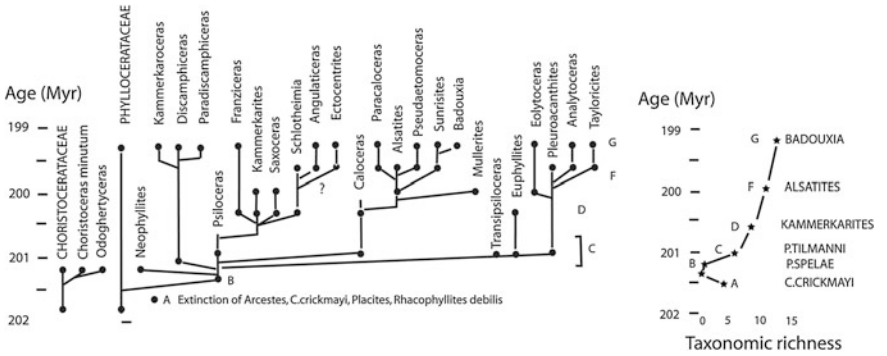

Fig. 8.6 Phylogeny of the last Rhaetian ammonite genera (*A*–*G* see Fig. 8.4) and taxonomic richness of genera (=reflecting the morphological disparity) calculated after the phylogenetic diagram (modified from Guex et al. 2012)

Such trends are well represented in most lineages of our Fig. 8.6. They all derived from smooth *Psiloceras* of the Lower Hettangian: *Kammerkaroceras* via *Discamphiceras* (*Discamphiceratinae, Psiloceratacеae*), *Angulaticeras* via *Saxoceras* and *Kammerkarites* (*Schlotheimiidae, Psiloceratacеae*), *Pseudaetomoceras* via *Caloceras* and *Alsatites* (*Arietitidae, Arietitaceae*), *Badouxia* via *Caloceras* and *Sunrisites*.

It is quite obvious that allometries characterizing the geometrical/morphological evolution of shelly invertebrates show that size (i.e. diameter or length), volume and surface vary independently. Within ammonites, an increase in volume, which is not accompanied by an increase in size (i.e. the diameter) will result in an increase of involution. Similarly, a decrease in size which is not accompanied by a decrease in volume will also lead to a drastic increase of involution. Such a process certainly accounts for the geometry of the lower Triassic small cryptogenic sphaerocone ammonites, for example the Isculitids deriving from *Columbites*. We also note that an increase in the mantle's surface area, if not compensated by a simultaneous increase in volume of the animal, results in an increase in suture complexity and/or flexuosity of growth-lines at the aperture (see Guex 2003 for details).

Thanks to the new geochronological data produced in our recent papers, we can quantify the rate of change in the involution, expressed by the variation of the ratio U/D (=umbilicus vs diameter) in some typical phylogenetical sequences mentioned above (Fig. 8.7).

8.4.2 Stress and Uncoiling

The relation between stress and uncoiling in ammonites is widely observed and we demonstrated that such evolutionary simplifications of the geometry of ammonites were generally correlated with $\delta^{13}C_{org}$ negative anomalies in the stratigraphical

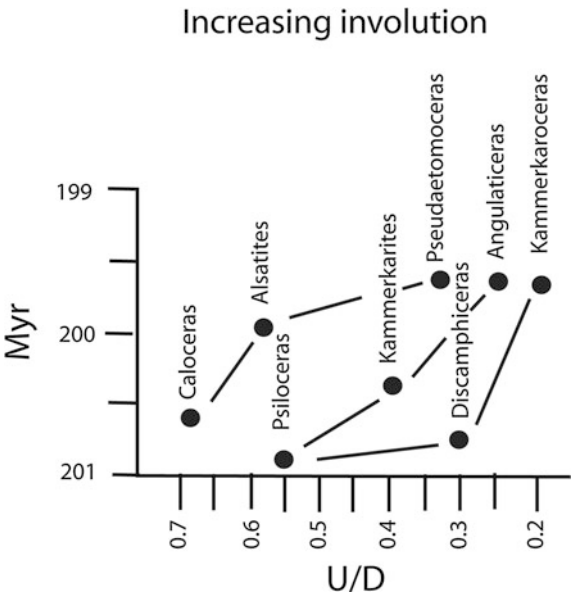

Fig. 8.7 Absolute rate of variation of the degree of involution within 3 major hettangian ammonite lineages

record (O'Dogherty et al. 2006; Guex 2003, 2006). In the present case we observe two major abnormal developments of serpenticone ammonites during the Hettangian. The first is characterized by the appearance of serpenticone Caloceratids such as *C.multicostatum* in the Planorbis Zone which occurs in the early part of the second negative carbon excursion of Guex et al. (2004). The second occurrence of serpenticone ammonites occurs in the Badouxia Zone (see Taylor et al. 2001) with the appearance of serpenticone Vermiceratids such as *V.morganense* and *Paradiscamphiceras*. These Vermiceratids are perfectly homeomorph with the most evolute representative of Alsatitids of the Middle Hettangian.

These two cases of relative "uncoiling" are concomitant with important sedimentary gaps in the Caloceras beds in Nevada and in the interval spanning the HSB in NW Europe.

8.5 A Model for the End Triassic Extinction

As demonstrated above, we have correlated the geochronological ages of the CAMP volcanism with the biochronological scale established in the American Cordilleras thanks to the discovery of ash beds deposited in the same beds as our ammonites (Schoene et al. 2010; Guex et al. 2012). These discoveries allowed us to propose an original model explaining the precise timing of the end Triassic extinction (ETE).

There are currently two main hypotheses to explain the ETE catastrophic event. The first invokes super-greenhouse conditions due to extreme atmospheric CO_2 concentrations (McElwain et al.1999; Schaller et al. 2011). This enrichment is often interpreted as degassing of magmatic CO_2 from huge volcanic basalt provinces (e.g. Sobolev et al. 2011) and/or from the degassing of carbonaceous or organic material-rich sediments (e.g. Svensen et al. 2009). The second scenario invokes a short period of global icehouse conditions caused by degassing of huge volumes of volcanic SO_2, atmospheric poisoning, cooling and eustatic regression coeval with the main extinction (ETE) but probably older than the main basalt emissions (Guex et al. 2001, 2004 and 2012b).

A nice petrological model has been elaborated by our colleagues Sebastien Pilet and Othmar Muntener to explain the SO_2 dominated vs CO_2 dominated degassing couplet generating the successive ice house and super green house conditions, and the decoupling of the ETE marine extinction followed by the later major plant turnover (Guex et al. 2004 and 2012b). The model invokes a thermal erosion of the cratonic lithosphere inducing giant H_2S/SO_2 release from sulfur bearing basal continental crust before CO_2 becomes the dominant gas associated to the giant basalt emission (Guex et al. 2015 submitted).

Although both hypotheses are compatible with massive volcanic degassing related to the emission of large volumes of flood basalts, they must also be able to explain the paleontological record in complete stratigraphic sections that displays decoupling between the (marine) ammonoids versus (terrestrial) plant extinctions (Guex et al. 2012b). Correlating the sedimentary and the fossil record with carbon and oxygen isotope variations and sea level changes from the T-J and Pl-To boundaries indicates that both boundaries are related to a regressive event followed by major sea level rise.

The data allowing us to discuss the various hypotheses of recent extinction models and the timing concerning the End-Triassic Extinction (ETE) and the T-J boundary are shown in Fig. 8.8 (for references see figure caption). This compilation synthesizes the timing of sea level changes, and $\delta^{13}C_{org}$, $\delta^{18}O$, and pCO_2 variations in relation with paleotemperatures, the age of the onset of the CAMP-related basaltic volcanism in the northeastern United States (Newark Supergroup) and Morocco (Argana Basin), and the ages of the two distinct End Triassic (ammonoids) and Earliest Jurassic (terrestrial plants) extinctions. The base of the Jurassic is officially defined by the first occurrence of *Psiloceras spelae* Guex, which has been found in Hettangian marine basins in Nevada (Sunrise Formation, New York Canyon section) and Peru (Pucara group, Levanto section), and the Northern Calcareous Alps, Austria (T/J GSSP Kuhjoch section). The first occurrence of *Psiloceras spelae* is bracketed by volcanic ash beds, which were shown on the basis of high-precision U-Pb zircon dates to be subcontemporaneous of the base of the North Mountain Basalt (Newark Basin), which is the oldest known CAMP basalt in North America (Schoene et al. 2010; Guex et al. 2012b). The chronology, established by ammonoids and U-Pb dating implies that the Newark supergroup basalts clearly postdates the ETE and the disappearance of the latest Triassic ammonite Choristoceras crickmayi (Guex et al. 2004; Schoene et al. 2010). The delay between the recovery

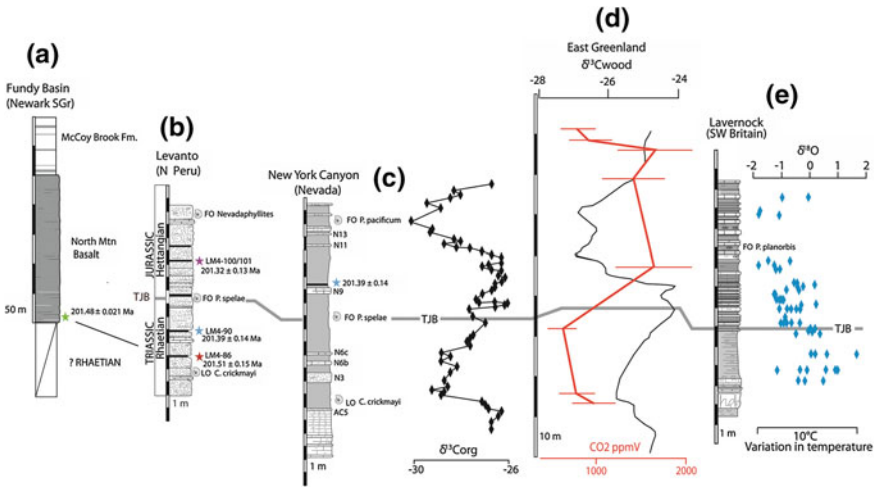

Fig. 8.8 **a–c** Numerical ages of the base of the North Moutain basalt and of the TJB in Peru and Nevada. $\delta^{13}C$ curve at New York Canyon (Nevada). From Schoene et al. (2010), Guex et al. (2004), Bartolini et al. (2012). **d** Variation of the CO_2 ppmV and $\delta^{13}C$ in Greenland. Redrawn from McElwain et al. (2009). **e** Variation of the $\delta^{18}O$ in SW Britain. Redrawn from Korte et al. (2009)

of the Jurassic ammonites and the extinction of the very last Triassic ammonoids lasted at least 200 kyr (probably more), based on sedimentary rates in Northern Peru and Nevada. The extinction of the last Triassic ammonoids in the uppermost Rhaetian is correlated with a strong negative excursion of $\delta^{13}C$ and a marine regression (Guex et al. 2004). The $\delta^{18}O$ record (Clémence et al. 2010; Korte et al. 2009) indicates a cooling episode (Fig. 8.8), which could explain the regressive event recorded in the upper Rhaetian of Austria, England and Nevada. Figure 8.8 indicates that the initial regression is followed by a significant sea level rise potentially associated to large volcanic CO_2 emissions related to the CAMP basaltic volcanism (McElwain et al. 1999, 2009; Schaller et al. 2011; Bartolini et al. 2012). A major plant extinction is correlated with the greenhouse conditions that postdates the ETE by at least a few hundred thousand years. The plant extinction is recorded in Greenland (McElwain et al. 1999, 2009) and is associated with a second negative $\delta^{13}C$ recorded in the Hettangian Psiloceras planorbis beds (coeval with P.pacificum). In the Newark basin this second extinction, mainly continental, occurs higher than the youngest Triassic-looking sporomorphs embedding Lower Jurassic CAMP basalts: These floras are still of Triassic affinity (Cirilli et al. 2009) and are coeval with the flora of "Rhaetian" affinity recorded in the Tiefengraben Member of the Lower Jurassic in the TJB stratotype at Kuhjoch (Austria, Bonis et al. 2009): all the sporomorphs present in the Lower Jurassic of that section already exist in the Triassic. In other words they are not serious markers for the base of the Jurassic. Concerning the marine ecosystem, severe anoxia developed in various basins and the

last Triassic style ammonoids surviving the ETE, were definitely extinct at the same time during the P. planorbis negative $\delta^{13}C$ (Guex et al. 2012b).

References

Bartolini, A., Gardin, S., & Guex, J. (2012). La limite Trias Jurassique: une crise biologique enigmatique. *Géochronique, Société Géologique de France, 122*, 30–33.

Bonis, N. R., Ruhl, M., & Kürschner, W. M. (2009). Climate change driven black shale deposition during the end-Triassic in the western Tethys. *Palaeogeography, Palaeoclimatology, Palaeoecology, 290*, 151–159.

Cárdenas, A. L., & Harries, P. J. (2010). Effect of nutrient availability on marine origination rates throughout the Phanerozoic eon. *Nature Geoscience, 3*, 430–434. doi:10.1038/ngeo869.

Cirilli, S., Marzoli, A., Tanner, L., Bertrand, H., Buratti, N., Jourdan, F., et al. (2009). Latest Triassic onset of the Central Atlantic Magmatic Province (CAMP) volcanism in the Fundy Basin (Nova Scotia) New stratigraphic constraints. *Earth and Planetary Science Letters, 286*, 514–525. doi:10.1016/j.epsl.2009.07.021.

Clemence, M., Gardin, S., Bartolini, A., Paris, G., Beaumont, V., & Guex, J. (2010). Bentho-planktonic evidence from the Austrian Alps for a decline in sea-surface carbonate production at the end of the Triassic. *Swiss Journal of Geology, 103*, 293–315.

Cohen, A. S., & Coe, A. L. (2007). The impact of the Central Atlantic Magmatic Province on climate and on the Sr- and Os-isotope evolution of seawater. *Palaeogeography, Palaeoclimatology, Palaeoecology, 244*, 374–390.

Courtillot, V. E. (1999). *Evolutionary catastrophes: The science of mass extinction* (p. 173). Cambridge: Cambridge University Press.

Erben, H. K. (1966). Über den Ursprung der Ammonoidea. *Biological Reviews*, *41*, 641–658.

Gorican, Š., Carter, E. S., Dumitrica, P., Whalen, P. A., Hori, R. S., De Wever, P., et al. (2006). *Catalogue and systematics of Pliensbachian, Toarcian and Aalenian radiolarian genera and species*. Ljubljana: Založba ZRC/ ZRC Publishing, ZRC SAZU.

Guex, J. (1995). *Ammonites hettangiennes de la Gabbs valley range (Nevada, USA)* (Vol. 27, pp. 1–131)., Mémoires de géologie Lausanne Lausanne: Université de Lausanne.

Guex, J. (2003). A generalization of Cope's rule. Bulletin de la Société géologique de France 174, 449–452.

Guex, J. (2006). Reinitialization of evolutionary clocks during sublethal environmental stress in some invertebrates Earth and Planetary Science Letters 240, 242–253.

Guex, J., Bartolini, A., Atudorei, V., & Taylor, D. (2004). High-resolution ammonite and carbon isotope stratigraphy across the Triassic-Jurassic boundary at New York Canyon (Nevada). *Earth and Planetary Science Letters, 225*, 29–41. doi:10.1016/j.epsl.2004.06.006.

Guex, J., Bartolini, A., Spangenberg, J., Schoene, B., Atudorei, V., & Schaltegger, U. (2011). The age of the major $\delta^{13}C_{org}$ and $\delta^{34}S$ Hettangian excursions at Kennecott Point (Queen Charlotte Islands, Canada). *Geophysical Research*, 13, EGU2011-1696, 2011.

Guex, J., Bartolini, A., Taylor, D., Atudorei, V., Thelin, P., Bruchez, S,. et al. (2008). Comment on: "The organic carbon isotopic and paleontological record across the Triassic-Jurassic boundary at the candidate GSSP section at Ferguson Hill, Muller Canyon, Nevada, USA" by Ward et al (2007). *Palaeogeography, Palaeoclimatology, Palaeoecology*, 273, 200–204.

Guex, J., Morard, A., Bartolini, A., & Morettini, E. (2001). Découverte d'une importante lacune stratigraphique à la limite Domérien-Toarcien: implications paléo-océanographiques. Bulletin de la Société vaudoise des Sciences Naturelles, *87*(3), 277–284 and *Bulletin Géologiques Lausanne, 345*, 277–284.

Guex, J., Pilet, S., Muntener, O., Bartolini, A., Spangenberg, J., Schoene, B., et al. (2015). Thermal erosion of cratonic lithosphere as a trigger for mass-extinction (submitted).

Guex, J., Schoene, B., Bartolini, A., Spangenberg, J., Schaltegger, U., O'Dogherty, L., et al. (2012). Geochronological constraints on post-extinction recovery of the ammonoids and carbon cycle perturbations during the Early Jurassic. *Palaeogeography, Palaeoclimatology, Palaeoecology, 346–347*, 1–11.

Haas, O. (1942). Recurrence of morphologic types and evolutionary cycles in Mesozoic ammonites. *Journal of Paleontology*, *16*, 643–650.

Hesselbo, S. P., Robinson, S. A., Surlyk, F., & Piasecki, S. (2002). Terrestrial and marine extinction at the Triassic-Jurassic boundary synchronized with major carbon-cycle perturbation a link to initiation of massive volcanism? *Geology, 30*, 251–254.

Hyatt, A. (1889). Genesis of the Arietitidae. Smithsonian contribution to knowledge 73, xi +238 pp.

Jones, C. E., Jenkyns, H. C., & Hesselbo, S. P. (1994). Strontium isotopes in Early Jurassic seawater. *Geochimica et Cosmochimica Acta, 58*, 1285–1301.

Korte, C., Hesselbo, S. P., Jenkyns, H. C., Rickaby, R. E. M., & Spotl, C. (2009). Palaeoenvironmental significance of carbon- and oxygen-isotope stratigraphy of marine Triassic-Jurassic boundary sections in SW Britain. *Journal of the Geological Society, 166*, 431–445. doi:10.1144/0016-76492007-177.

Lange, W. (1952). Der untere Lias am Fonsjoch (östliches Karwendelgebirge) und seine Ammonitenfauna. *Palaeontographica, (A)*, *102*, 49–162.

Marzoli, A., Jourdan, F., Puffer, J. H., Cuppone, T., Tanner, L. H., Weems, R. E., et al. (2011). Timing and duration of the Central Atlantic magmatic province in the Newark and Culpeper basins, eastern U.S.A. *Lithos, 122*, 175–188.

McElwain, J. C., Beerling, D. J., & Woodward, F. I. (1999). Fossil plants and global warming at the Triassic-Jurassic Boundary. *Science, 285*, 1386–1390.

McElwain, J. C., Wagner, P. J., & Hesselbo, S. P. (2009). Fossil plant relative abundances indicate sudden loss of Late Triassic biodiversity in East Greenland. *Science, 324*, 1554–1556. doi:10.1126/science.1171706.

Schaller, M. F., Wright, J. D., & Kent, D. V. (2011). Atmospheric PCO2 perturbations associated with the Central Atlantic Magmatic Province. *Science*, *331*. doi:10.1126/science.1199011.

Schindewolf, O. H. (1950). *Grundlagen und Methoden der Palaeontologischen Chronologie*. Berlin: Borntraeger. 152 p.

Schoene, B., Guex, J., Bartolini, A., Schaltegger, U., & Blackburn, T. J. (2010). Correlating the end-Triassic mass extinction and flood basalt volcanism at the 100 ka level. *Geology, 38*, 387–390. doi:10.1130/G30683.1.

Sobolev, S. V., Kuzmin, D. V., Krivolutskaya, N. A., Petrunin, A. G., Arndt, N. T., Radko, V. A., & Vasiliev, Y. R. (2011). Linking mantle plumes, large igneous provinces and environmental catastrophes. *Nature, 477*, 312–316.

Svensen, H., Planke, S., Polozov, A. G., Schmidbauer, N., Corfu, F., Podladchikov, Y., Jamtveit, B. (2009). Siberian gas venting and the end-Permian environmental crisis. *Earth and Planetary Sciences Letters*, *277*, 490–500.

Taylor, D. G., Guex, J., & Rakus, M. (2001). Hettangian and Sinemurian ammonoid zonation for the western Cordilleran of North America. *Bulletin de la Société vaudoise des Sciences naturelles, 87*(4), 381–421.

Waehner, F. (1882–1898). Beiträge zur Kenntnis der tieferen Zonen des unteren Lias in nordöstlichen Alpen. I-VIII, Beitr. Pal. Geol. Österr.-Ung. Orients, 2-11, 1- 291.

Yin, J., Smith, P. L., Palfy, J., & Enay, R. (2007). Ammonoids and the Triassic/Jurassic boundary in the Himalayas of Southern Tibet. *Palaeontology, 50*, 711–737.

Chapter 9
Statistical Pseudo-improvements of the UA Method

In a recent Lethaia paper, Monnet et al. (2011) propose a series of refinements intended to ameliorate the performances of the Unitary Association Method (UAM) and of the UAgraph program. Monnet et al. (loc.cit) main criticisms will quickly be reevaluated in the present chapter.

Monnet et al. (2011) first suggest to use the statistical technique known as bootstrapping in order to evaluate the robustness the UAgraph solutions by means of "confidence intervals". The bootstrapping is a well known technique of re-sampling using iterations resulting from the application of a Monte-Carlo method. Monnet et al. propose to use that technique but they do not say on what the re-sampling should be done: should one bootstrap the occurrences of the taxa, the samples, the sections? The identity and ordering of the UAs will of course partially break down in the bootstrap replicates—how should the "confidence intervals" then be reported? In our view, the use of such a technique would add nothing to current results of the UAs: the robustness of the solutions, as said before, depends strictly on the reproducibility and inter-units superpositional control. They are the only criteria allowing a serious evaluation of the internal coherence of the UA results.

Concerning the strongly connected components of the G_k graph, Monnet et al. write: "UAgraph currently solves these contradictions by using the 'weakest link' rule (i.e. the clique superposition supported by the fewest inter-taxon relationships is destroyed; see Guex 1991, p. 82). Given the uncertainties related to this type of resolution, the unique result produced by the UAM is likely to be partly wrong (sic). Figure 9 (NB: of Monnet et al.) reports an imaginary example (Fig. 9.1a) containing cycles between its maximal cliques where the automatic resolution by the software UAgraph yields a result (Fig. 9.1b), which is clearly not the most parsimonious compared to what can be found empirically (Fig. 9.1c). This example clearly illustrates and demonstrates that the 'weakest link' rule is not adequate in such cases." Monnet et al. Figure 9 is redrawn here in our Fig. 9.1, showing the different outputs of UAgraph useful to solve Monnet's problem.

First we note that the biostratigraphic graph G* contains 3 cycles, all generated by taxon 1: this means that this taxon can be misidentifed or out of place (possible reworking). If we remove taxon 1, UAgraph produces automatically the solution that Monnet calls "empirical", with three units. We also note that the strongly

J. Guex et al., *Discrete Biochronological Time Scales*,
DOI 10.1007/978-3-319-21326-2_9

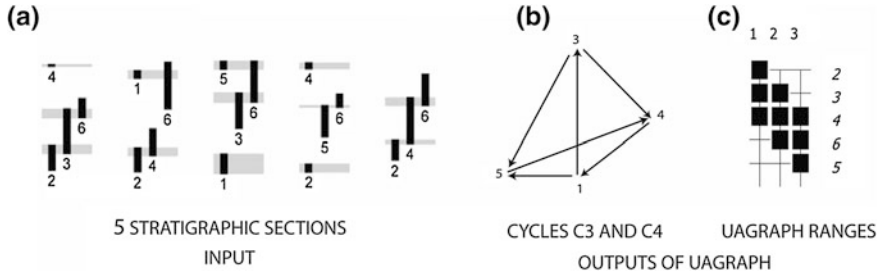

Fig. 9.1 **a** Input redrawn from Monnet's Fig. 9; **b**, **c** outputs of the UAgraph program; **b** cycles in the G* graph showing that all the cycles and strongly connected components of G_k are generated by taxon 1; **c** output of the UAgraph obtained after removing taxon 1: that solution is identical to that proposed by Monnet after a complicated operation

connected component of G_k disappears if we remove that taxon, present in the maximal clique mc2.

Monnet et al. continue their critical remarks as follows: "One way to avoid this problem is to calculate all possible minimal sets of clique superpositional relationships necessary to break the cycles and then select the most parsimonious solution in terms of reconstructed virtual coexistences." As the enumeration of all possible minimal sets of cliques superpositional relationships is NP complete (see Galster et al. 2010), the proposal does not makes sense, even in small databases like the standard alveolinid example used at the beginning of the present book.

Monnet et al. use another example (their Fig. 10, loc.cit.) to illustrate their theoretical thinking. That figure is reproduced in our Fig. 9.2. Thanks to their example, Monnet et al. want to show that "better" solutions than the ones directly produced by UAgraph can be obtained empirically (their Fig. 10c, showing two additional solutions). Analysing their figure, we immediately note that taxon 8 is located below the coexistence interval of (3, 1) in one solution and above that interval in the other solution: this is called a trivial virtual coexistence. Monnet's two "empirical" solutions (M1 and M2 in Fig. 9.2) are therefore wrong because they do not take that forced virtual coexistence into account. In other words, it means that the correct solution is the one produced by UAgraph, with taxon 8 virtually coexisting with (3, 1). That solution can be directly obtained by pushing the button "Null endemic taxa" of UAgraph, because taxon 8 is indeed present in only one section. Doing so, we obtain the UAgraph range chart with 5 units in which the singleton 8 is ignored (see Fig. 9.2).

It should be noted that Monnet et al. do not explain how they obtain their empirical solutions (they possibly use some kind of black box, to return the words they use in their critical discussion). We will finally note that they state that the UAM disregards all the informations relative to datums' sequences. This is totally incorrect, as discussed at length in Guex (1991) and in Galster et al. (2010).

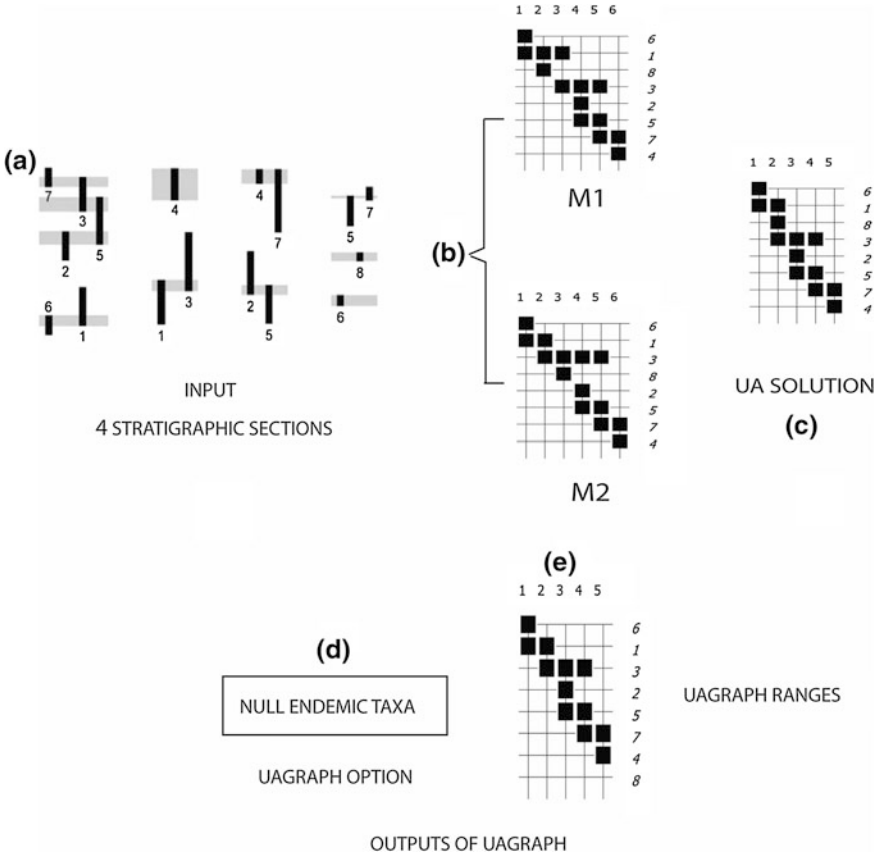

Fig. 9.2 **a** Input redrawn from Monnet's Fig. 10; **b** the two empirical solutions, *M1* and *M2*, proposed by Monnet et al., ignoring the trivial virtual coexistence between 8 and (3, 1); **c** the UAgraph solution of the conflict between *M1* and *M2*; **d** the UAgraph option that Monnet et al. should have used; **e** Output of the UAgraph program ignoring taxon 8 present only in section 4: the output has no conflicting solutions

References

Galster, F., Guex, J., & Hammer, Ø. (2010). Neogene biochronology of Antarctic diatoms: A comparison between two quantitative approaches, CONOP and UAgraph. *Palaeogeography Palaeoclimatology Palaeoecology, 285*, 237–247.

Guex, J. (1991). *Biochronological correlations* (250 p.). Berlin: Springer.

Monnet, C., Klug, C., Goudemand, N., De Baets, K., & Bucher, H. (2011). Quantitative biochronology of Devonian ammnoids from Morocco and proposals for a refined unitary association method. *Lethaia,*. doi:10.1111/j.1502-3931.2010.00256.1-21.

Chapter 10
Conclusions

10.1 Stratigraphic Terminology

Many authors have complained about the chaotic nature of stratigraphic terminology. One of the historical reasons for this is that the term biostratigraphy has been mostly used in a chronological sense. In fact this is a very general term which applies to everything that concerns the study of the fossil content of sedimentary rocks (paleontological inventory, study of biofacies, determining ecozones, etc.). When discussing the chronological significance of some fossils, we should use the term biochronology which is restricted to identifying the taxa in a fossil assemblage that are characteristic of the relative age of this assemblage.

More than 40 years ago, in 1970, for example, Schindewolf listed almost 100 different biostratigraphic terms, and several dozen of classical articles, some of them excellent (e.g. Eldredge and Gould 1977; Gabilly 1971; Mamet 1977; Miller 1977; Tozer 1967) discuss the famous concept of zone.

This profusion is partially due to the difficulty of establishing a precise relationship between a biochronologic zone and the corresponding time interval.

It is also due to the fact that the logical steps followed in constructing biochronologic scales and in establishing correlations vary considerably both with the taxonomic group under study and with the concrete stratigraphic situation (nature of the sedimentation, quality of the fossil record, etc.).

Three major categories of biochronologic scales were differentiated in Chap. 1.

1. Scales whose subdivisions are discrete (non-contiguous) and characterized by unique and mutually exclusive associations of species.
2. Continuous scales whose subdivisions are Interval ZonesInterval zones defined by the intervals separating the evolutionary events embodied by the first phyletic appearances (or disappearances) of species.
3. Continuous scales whose subdivisions are Peak Zones or Acme Zones, defined by the relative abundances of taxa.

J. Guex et al., *Discrete Biochronological Time Scales*,
DOI 10.1007/978-3-319-21326-2_10

Up to now our discussion has been limited to the problems involved in constructing discrete biochronologic scales and using them in stratigraphic correlations.

In this concluding chapter we will make some general remarks about the different kinds of zonations currently used in the recent literature. We will discuss in particular the factors affecting their validity.

10.2 Oppel Zones and Unitary Associations

In 1856, Oppel gave the first general description of what would later be called the Oppel Zone: "Comparison has often been made between whole groups of beds, but it has not been shown that each horizon, identifiable in any place by a number of peculiar and constant species, is to be recognised with the same degree of certainty in distant regions. This task is admittedly a hard one, but it is only by carrying it out that an accurate correlation of a whole system can be assured. It necessarily involves exploring the vertical range of each separate species in the most diverse localities, while ignoring the lithological development of the beds; by this means will be brought into prominence those zones which, through the constant and exclusive occurrence of certain species, mark themselves off from their neighbors as distinct horizons. In this way is obtained an ideal profile, of which the component parts of the same age in the various districts are characterized always by the same species." (Oppel 1856, p. 3, translated by Arkell 1933, p. 16).

We note the following points about Oppel's discussion.

1. The petrographic nature of the strata is not taken into consideration when establishing the existence of a zone.
2. The zone is characterized by the constant and exclusive occurrence of certain species that are homotaxic over vast geographic ranges.
3. The end product of Oppelian analysis is an ideal sequence whose subdivisions are approximately the same age in all the regions where they are recognized.

These remarks show that a zone constructed by means of the unitary associations has the same attributes as an Oppel Zone.

1. It is defined and entirely characterized by the existence interval of one (or more) species and/or by the coexistence interval of n species.
2. This interval is unique and distinct from all others.
3. The zone is identifiable in a reproducible way by the species that characterize it.
4. Such a zone is at first an abstract construction and only secondarily a body of rock.
5. It is strictly an order relation in the mathematical sense.

From a historical point of view, it is interesting to note that this last point inspired amusing polemics. More than hundred years after Oppel deep and influential thoughts, Hancock (1977, p. 21) wrote: "Some German stratigraphers (e.g. Schindewolf 1950, …) have even interpreted a zone as a time term to

designate an interval during which was deposited the sediment that contains certain index fossils. Such a mystical inexactitude has dissatisfied twentieth-century American pragmatic stratigraphers."

In 1956 Arkell (p. 5) proposed a pragmatic solution to these mystical problems:

"British geologists have always envisaged a zone as a bed or stratum, a tangible object accessible to the hammer, though differing lithologically from place to place. Consequently some have thought it necessary to construct a parallel terminology to express the time units to which the various kinds of zones correspond.

The need to keep time and rock distinct in our thoughts is obvious, and to the extent that this elaborate terminology has led to clarification of thought it has served a useful purpose. But beyond that it is unnecessary. No one uses it nor ever will. That Oppel himself fully appreciated the time element cannot be doubted (Schindewolf 1950). The fact that he nowhere defined a zone, nor made it clear whether his zones were stratigraphic or time intervals, may be taken to mean that he visualised zones from both aspects at once. The argument that a zone must be one or the other is sterile."

We hardly need mention that these words of Arkell have never been (to our knowledge) quoted in any Guide or Code of stratigraphic terminology.

10.3 Phylogenetic Seriations and Phylozones

Lacking precise information on the superpositional control between different fauna, some paleontologists who work on sparse and stratigraphically disconnected populations are forced to infer sequences of species (or assemblages of species) from an estimate of the relative degree of evolution of the individuals belonging to the species (see for example the theoretical basic publications of Thaler 1972 and Godinot 1981 which are at the base of the phylogenetic zonations).

The criteria used to judge the more or less primitive character of a fauna depend largely on the modes of morphologic transformation known in its zoological group:

1. increase of hypsodonty among micro-mammals;
2. more or less gradual increase in size among many organisms;
3. progressive elongation of the shell among some large foraminifera, etc.

Chronologic sequences deduced from the (presumed) degree of evolution of different populations are sometimes verified later. But this is far from being always the case.

A good example of a false dating resulting from an incorrect phylogenetic interpretation is that of the Nejdia beds in Saudi Arabia. For a long time this ammonite genus was thought to have evolved from the Phymatoceratinae; as a consequence, researchers in the field deduced that *Nejdia* was from the upper Toarcian. However it is now known that *Nejdia* is actually from the lower Toarcian and that it derived from the earliest Toarcian *Bouleiceras* (Guex 1973).

We note incidentally that the unitary association method can be quite useful in detecting and interpreting the contradictions that can result from applying such phylogenetic seriations. We simply replace the notion of biostratigraphic graph with that of phylogenetic graph in which the arcs represent the (hypothetical) relationships primitive → advanced (instead of representing superpositions of species).

The use of phylogenetic criteria to establish chronologic sequences has however been criticized often, and with justification. There are several reasons for this.

The most important criticism is the inherent risk of circular reasoning. It is in fact impossible to establish the validity of a model of morphologic transformations that affect a fossil group through time without first proving that these transformations do not simply reflect reversible responses to local ecological variations (Fig. 9.1). However, such a proof necessarily requires correct biochronologic correlations.

As Eldredge and Gould (1977, p. 35) wrote, in the context of a similar discussion: "We shall always be able to document differences among successive population samples in a vertical sequence, but these will, at most, represent adaptive shifts to minor environmental changes rather than a dominant evolutionary force inexorably leading to the creation of a new species."

We should also bear in mind that neontologists have a tendency to divide the anagenetic (i.e. gradual) lineages that they observe into branches defined by the degree of evolution of the different species (biospecies) making up a lineage. These branches generally serve as a basis for defining phylozones (Fig. 10.1). In practice, a sequence of phylozones is chronologically meaningful only if the succession of branches that define it is recognizable on a large scale.

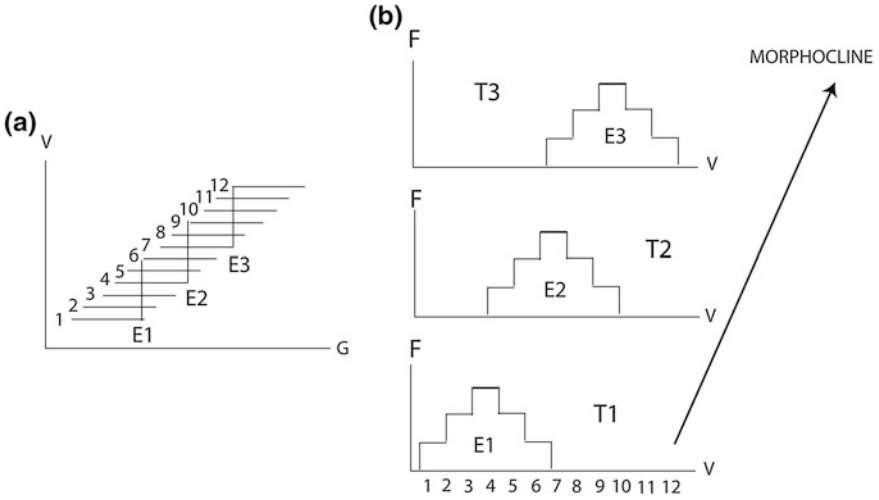

Fig. 10.1 **a** V = ecophenotypes 1–12. E1–E3: three distinct environments of identical age. G = geographical distribution. **b** F = frequency of the ecophenotypes at three different periods T1–T3 producing an apparent chronological morphocline

These general observations lead us to note that the different morphotypes that make up a biospecies often have durations of existence that are not identical. If a fossil group is to have optimal biochronologic resolution, it is useful to consider each variant as a potential taxonomic entity. The purely neontologic doctrine of taxonomy, with the goal of giving a biological image of the paleontological species, is in theory justified.

However, when it is pushed to an extreme ("one bed, one name") it forces those who apply it dogmatically to treat as different species identical morphotypes of the same chronospecies, under the pretext that these morphotypes are found in populations whose variability is different depending on the stratigraphic levels.

This has the effect of obscuring precious information on the space-time distribution of different morphotypes of a supposed biospecies and on the ecological factors that affect the variability of the species. It also limits the efficient transmission of the raw biostratigraphic observations used in making correlations and constructing phylogenetic syntheses.

This is why we agree with the old and classical statement of Eldredge and Gould (1977, p. 39–40): "…we merely claim that the biological theory underlying most "modernist" approaches to biostratigraphy is simply wrong, and that the theory supporting "old-fashioned" biostratigraphy is correct. To date, evolutionary theory owes more to biostratigraphy than vice versa."

10.4 Interval Zones and Datums

Over the past 50 years, the Oppel Zone has gradually been displanted by the concept of the Interval Zone. As we have seen, such a zone corresponds in principle to the interval separating two datums.

In its original sense the term datum means first phyletic appearance of a species. This implies that the appearance of a species, at least in one section, has been proven to be phyletic and is not simply fortuitous (e.g. sudden immigration of a species from another faunal realm). However, some biostratigraphers now use this term even when constructing zonations with groups in which the evolutionary relationships of the different species (morphospecies) are not known. Thus the term datum has gradually lost its evolutionary connotation and has become, for many experts, synonymous with first local appearance and first local disappearance of a species. This is why we have deliberately used the word in this weaker (but objective) sense.

The practice of Interval Zones spread at the same time that datum lost its original meaning; this was encouraged by many authors of Guides and Codes who claim that the first phyletic appearance of a species is the best criterion for correlating stratigraphic sections.

Two arguments are advanced to justify this point of view.

The first says that in theory the true first appearance of a species is chronologically punctual. This is correct but has nothing to do with the stratigraphic

reality. Let us assume that the descendence relationship between two species x and y is proved; in such a case, two stratigraphic relationships are possible for their respective FADs and LADs.

1. The proof of the relationship x → y is based on the existence of a transitional population (i.e.: x and y coexisted more or less briefly within transitional populations). In this case, we find ourselves in the well known kind of difficulty described long ago by Cita (1978, p. 672): "It is worth mentioning at this point how difficult it is to define the lower boundary of Zone N. 14, because of the inherent difficulties in pinpointing the first evolutionary occurrence of G. nepenthes in the slow and gradual evolution from G. druryi… "As we see it, the biochronologic interest of a phyletic relationship x → y lies in the use that can be made of the existence interval of the transitional population between x and y when making correlations: if this interval is short, it gives a precise criterion for the correlation.
2. A gap exists between the LAD of x and the FAD of y (lack of knowledge about transitional populations for documentary reasons). It is then clear that the FAD of y will behave just like any FAD (i.e. in the sense of the first local appearance of y). To test its reliability, it is necessary to prove that it is not diachronous… However, in the absence of external (and non-biochronologic) arguments, this can be done only in the framework of an Oppelian zonation.

The second argument invoked by stratigraphers of the neontologists' school is the following: we know that the migration speeds of recent organisms can be very great (on the order of 10–100 km a year) and it is clear that the absolute time taken by a new group to colonize a newly opened environment is virtually nil compared to the resolution power of the biochronologic dating tool.

However, this actualistic argument generally does not apply to fossils; to be convinced of this it is enough to remember that the diachronism of the FADs in some groups is sometimes greater than that of the LADs.

Establishing a rule that FADs should be used to define the base of a zone will not inspire biostratigraphers to try to prove the chronologic homotaxy of their datums using Oppelian-type syntheses. On the contrary, it encourages them to be satisfied with stating (without any proof or using only pseudo-objective statistical criteria) that certain datums are chronologically significant, and with constructing scales whose subdivisions are precisely Interval Zones.

The accuracy of the correlations resulting from such zonations clearly depends on the diachronism of the datums used to define the limits between these zones. It is in fact obvious that an Interval Zone based on non-phylogenetic datums enables one to make correct correlations only if the amplitude of the biochronologic dispersion of the datums is zero (i.e. these characteristic datums must not be found in different Oppel Zones in different locations).

However, in the absence of physical criteria, these diachronisms (and the amplitude of the biochronologic dispersion of the species) can be detected only using the reproducible subdivisions of a correctly established range chart. In other words, the validity of an Interval Zone based on non-phylogenetic datums can be

proven only if the Oppel Zones generated by the stratigraphic relationships of the species have been previously established, as shown in Chap. 1.

To show that the use of non-phylogenetic Interval Zones easily leads to contradictions, we will follow the elementary logical procedure of comparing observed facts with the formal zonal definitions. This will naturally lead us to recognize the following kinds of situations:

1. Interval Zone A is defined by the interval separating the FAD of species x from the FAD of species y, while in fact the true first appearance of y precedes that of x.
2. Interval Zone B is defined by the interval that separates the LAD of species x from the FAD of species y while the observed facts show that x and y coexist in some locations (which raises the amusing question whether the existence interval of x intersects that of y or vice versa…).

The misuse of Interval Zones has given rise to exaggerated claims for the resolution power of biochronologic scales of this type, as already stated by the pioneer paper of Fåhreus (1986, p. 150) and Bernard Mamet (1977, p. 454), quoted above in Sect. 6.6.

We will conclude our discussion of Interval Zones with the following remarks.

1. It is pointless to try to discover the time of phyletic appearance of a species before establishing as accurately as possible the chronologic relationships of the morphotypes whose evolutionary relationships one wishes to know. Proceeding in the opposite order leads to circular reasoning.
2. Constructing a relative biochronologic scale whose subdivisions are based on diachronous (and non-phylogenetic) datums can be compared to building a house of cards with only one side: such structures don't stand up.

10.5 Standard Zones

The term standard zone is frequently used to describe the subdivisions of a biochronologic scale of supposed general value. From an historical point of view, we can recall that two drastically different views of the properties of standard zonations are still influential: those of Tozer (1967) and Callomon (1984).

Discussing the Triassic standard zones in North America, Tozer (loc.cit. pp. 10–11) writes:

> "In most sections there are rocks between the zones that are devoid of characteristic fossils. Those parts of the section without diagnostic fossils cannot be assigned to a zone." The alternative procedure—to include beds lacking the characteristic fauna in one or other of the adjacent zones—practised by some contemporary workers (…) is not followed. From this it should be clear that the zones, as arranged, are not regarded as forming a continuum. Future discoveries will probably reveal distinctive faunas that will form the basis for new zones between those now recognized.

We see that Tozer rightly considers that the subdivisions of a standard biochronologic scale are discrete when based on discontinuous biostratigraphic data.

According to Callomon (1984) a standard biochronologic scale must have the following properties:

1. It must be continuous.
2. Its subdivisions (zones) must be contiguous (no gap, no overlap).
3. The lower limit of each standard zone must be defined by a Golden Spike in a stratotype.
4. The Golden Spike automatically defines the top of the subjacent zone, even when faunal criteria are lacking.

This concept of standard scales fails to take into account both the nature of the biostratigraphic data on which the scale is based, and the analytical methods used to establish the correlations (no distinction between continuous vs. discrete scales). It ignores the fact that strongly discontinuous paleontological data (ammonites, radiolarians, nannoplankton etc.) necessarily generate discrete biochronologic scales: imposing a continuum on such scales is equivalent to overlooking that fundamental property. And finally it neglects the essential requirement that a stratotype must locally record the superpositional control between two consecutive zones (i.e. the Golden Spike methodology doesn't require any superpositional control between two zones).

To this we add that the famous rule according to which "the base of a zone fixed by a Golden Spike in a stratotype automatically defines the top of the preceding zone" can be applied only if the oldest part of the higher zone is recorded in that stratotype. The rule obviously makes no sense if that condition is not satisfied. In other words, that convention can generate confusion and has no place in a codification of biochronologic procedures.

In summary, we can describe a biochronologic scale as "standard" only if it is widely applicable and results from a correct synthesis. The quality of such a scale depends entirely on the method used to establish it. Each type of zonation (continuous vs. discrete) requires its own procedure for zonal definition. But whatever the procedure, the definition must not contradict observed facts.

10.6 Acme Zones and Peak Zones

The local stratigraphic interval in which a species shows its maximum development can be considered independently of its total local stratigraphic range. If we can prove that such an interval is always located between other chronologically significant intervals, we can conclude that it is also chronologically significant. This interval can then be considered the acme of the species, and it can be used to define a zone (the Acme Zone).

Remane's (1963) work on the Calpionellid is an excellent example of biochronologic correlations based on acme zones. The acme of *Calpionella alpina*,

characteristic of the zone of the same name, is located between the acmes of the genera Crassicolaria and Tintinnopsella. The widely identifiable *C. alpina* zone is an acme zone with solidly established validity. Nevertheless we note that Remane's zonation is good because the preservation of the Calpionellid is not selective vis-a-vis the different species he used. In addition, the stratigraphic sections he studied were the site of relatively continuous sedimentation, so relative abundances of these taxa here are a reliable biochronologic indicator.

Very precise correlations can also be obtained using Peak Zones defined by pollen diagrams, biologs or other morphometric variograms on the scale of a basin or a province.

The problems of interpretation posed by these abundance or morphometric variograms are very similar to those faced by the geophysicists who use electrical logging to establish lithostratigraphic correlations. In some geological contexts (the Quaternary, for example) these methods can sometimes produce reliable correlations, but they do not come into the scope of this book. Readers interested in these approaches can refer to the classical works of Reyment (1980) and Malmgren and Kennet (1981).

10.7 Stratotypes

The nature of the boundary between two consecutive biochronologic zones is different for continuous scales (Peak Zones, Acme Zones, Interval Zones) than for discrete scales (Oppel Zones). In the former, the (theoretical) limit is a surface, and in the latter it is an interval of separation.

For practical reasons, it is useful to delineate the boundary between two continuous zones, using a Golden Spike in a stratotype.

Also for practical reasons (notably the instability of scales) it is useful to designate a stratotype in which the superposition of two discrete (non-contiguous) zones is well documented. For Oppelian scales, however, it is inappropriate to place a Golden Spike in the reference section ["unless the spike is rather thick…" as Mamet (Mamet 1977, p. 455) puts it so nicely].

Consequently, the stratotype for a discrete biochronologic boundary differs from that of a chronostratigraphic limit (e.g. the base of a stage) which necessarily is a surface.

10.8 Validity of a Zone

All Guides and Codes of stratigraphic terminology have one glaring omission in common: they never explain how to construct biochronologic zones. This omission leads to another: they never discuss the criteria governing the validity of such zones.

It is however obvious that the validity of a biochronologic zone depends neither on its formal designation in a particular stratotype, nor on the arbitrary choice of a phyletic relationship. Instead it depends entirely on its identifiability outside its type-section. This identifiability of a zone is contingent on the correctness of its definition, which in turn depends entirely on the way the zone is constructed.

In all cases with complex biostratigraphic data (strongly discontinuous sedimentation and fossil record), the use of discrete zones to correlate terrains is imperative, for the relative abundances of different taxa are not reliable. The main criterion for the validity of these Oppelian zones is their reproducibility and mutual superpositional control.

Note that discrete zones constructed by means of the U.A. method do not need to be formally defined: their correlation is a mere by-product of the construction of the referential. Within the framework of that methodology, new biostratigraphic data can easily be added to an old database for reprocessing and updating correlations. As our late friend Jean Gabilly used to say long ago, biochronological zonations are indefinitely perfectible.

References

Arkell, W. J. (1956). *Jurassic geology of the world* (804 p.). London: Oliver and Boyd.

Callomon, J. H. (1984). Biostratigraphy, chronostratigraphy and all that—Again! In *International Symposium on Jurassic Stratigraphy* (pp.612–624), Erlangen.

Cita, M. B. (1978). Biostratigraphy of miocene deep-sea sediments (sites 372 and 375). *Initial Reports, 42*(1), 671–685.

Eldredge, N., & Gould, S. J. (1977). Evolutionary models and biostratigraphic strategies. In E. G. Kaufman & J. E. Hazel (Eds.), *Concepts and methods of biostratigraphy* (pp. 25–40). Stroudsburg, PA: Dowden, Hutchinson and Ross Inc.

Fåhreus, L. E. (1986). Spectres of biostratigraphic resolution and precision. Rock accumulation rates, processes of speciation and paleoecological constraints. *Newsletters on Stratigraphy, 15*(3), 150–162.

Gabilly, J. (1971). Méthodes et modèles en stratigraphie du Jurassique. *Mém. B.R.G.M., 75*, 5–16.

Godinot, M. (1981). Usefulness and meaning of the mammalian specific lineages. In J. Martinell (Ed.), *International Symposium on Concepts and Methods in Paleontology* (pp. 249–258), Barcelone.

Guex, J. (1973). Aperçu biostratigraphique sur le Toarcien inférieur du Moyen Atlas marocain. *Eclogae Geologicae Helvetiae, 66*(3), 493–523.

Hancock, J. M. (1977). The historic development of biostratigraphic correlation. In E. G. Kaufman & J. E. Hazel (Eds.), *Concepts and Methods of Biostratigraphy* (322 p.). Stroudsburg, PA: Dowden, Hutchinson and Ross Inc.

Mamet, B. (1977). Foraminiferal zonation in the lower carboniferous. methods and stratigraphic implications. In E. G. Kauffman & J. E. Hazel (Eds.), *Concepts and methods of biostratigraphy* (pp. 445–462). Stroudsburg, PA: Dowden, Hutchinson and Ross Inc.

Malmgren, B. A., & Kennet, J. P. (1981). Phyletic gradualism in a Late Cenozoic planktonic foraminiferal lineage. *Paleobiology, 7*(2), 230–240.

Miller, F. X. (1977). The graphic correlation method in biostratigraphy. In E. G. Kaufman & J. E. Hazel (Eds.), *Concepts and methods of biostratigraphy* (pp.165–186). Stroudsburg, PA: Dowden, Hutchinson and Ross Inc.

Oppel, A. (1856). *Die Juraformation* (857 p.). Stuttgart: Ebner and Seubert.
Remane, J. (1963). Les Calpionelles dans les couches de passage Jurassique-Crétacé de la Fosse Vocontienne. *Travaux du Laboratoire de Géologie de Grenoble, 39*, 25–82.
Reyment, R. A. (1980). *Morphometric methods in biostratigraphy* (175 p.). New York: Academic Press.
Schindewolf, O. H. (1950). *Grundlagen und Methoden der Palaeontologischen Chronologie* (152 p.). Berlin: Borntraeger.
Thaler, L. (1972). Datation, zonation et Mammifères. *M, 77*(1), 411–424.
Tozer, E. T. (1967). A standard for Triassic Time. *Bulletin Geological Survey Canada, 156*, 1–103.

Appendix 1
Drobne's (1977) Database

1-A Code numbers of species

1 Alveolina moussoulensis
2 Alveolina aramea
3 Alveolina solida
4 Alveolina globosa
5 Alveolina avellana
6 Alveolina pisiformis
7 Alveolina pasticillata
8 Alveolina leupoldi
9 Alveolina montanarii
10 Alveolina aragonensis
11 Alveolina dedolia
12 Alveolina subpyreneica
13 Alveolina laxa
14 Alveolina guidonis
15 Alveolina decipiens

1-B Code numbers of sections and maximal horizons (M.H.)

SECTION 1: Fatji hrib
M.H.1 = level 11
M.H.2 = level 8
M.H.3 = level 7
M.H.4 = level 5
SECTION 2: Dane-Divaca
M.H.1 = level 7
M.H.2 = level 16
M.H.3 = level 20
M.H.4 = level 23
SECTION 3: Veliko Gradisce
M.H.1 = level 8
M.H.2 = level 12

J. Guex et al., *Discrete Biochronological Time Scales*,
DOI 10.1007/978-3-319-21326-2

M.H.3 = level 13
M.H.4 = level 14
M.H.5 = level 15
M.H.6 = level 19
M.H.7 = level 21
SECTION 4: Ritomece-Gradice
M.H.1 = level 6/2
M.H.2 = level 6/1
M.H.3 = level 5/1
M.H.4 = level 5/2
SECTION 5: Podgorje
M.H.1 = level 26
M.H.2 = level 48
SECTION 6: Podgrad-Hrusica
M.H.1 = level 7/1
M.H.2 = level 7/3
M.H.3 = level 7/4
M.H.4 = level 8/1
SECTION 7: Kozina-Socerb
M.H.1 = level 3
M.H.2 = level 6
M.H.3 = level 8
M.H.4 = level 4
SECTION 8: Golez
M.H.1 = level 20
M.H.2 = level 33
M.H.3 = level 34
M.H.4 = level 36
M.H.5 = level 46
M.H.6 = level 53
SECTION 9: Zbernica
M.H.1 = level 4
M.H.2 = level 12
SECTION 10: Dane, Istria
M.H.1 = level 1-b
M.H.2 = level 7
M.H.3 = level 8
SECTION 11: Jelsane
M.H.1 = isolated sample

1-C Numerical database

Datum: Title "DROBNE 1977"
SECTION 1
bottom 1 top 4
2 1 1, 3 4 4, 4 3 3, 6 2 2, 7 3 3, 8 4 4, 12 3 3
SECTION 2
bottom 1 top 4
1 3 3, 3 1 1, 5 1 1, 6 2 3, 7 1 3, 9 3 4, 11 3 3, 12 3 3, 13 2 2, 14 4 4
SECTION 3
bottom 1 top 7
2 1 1, 3 2 2, 6 2 3, 7 2 3, 9 6 7, 10 7 7, 11 5 5, 12 4 4, 13 3 3, 14 6 7, 15 4 6
SECTION 4
bottom 1 top 4
1 1 2, 4 3 3, 7 1 1, 8 2 2, 9 1 4, 10 3 4, 11 1 2, 12 2 2, 14 3 4, 15 4 4
SECTION 5
bottom 1 top 2
4 2 2, 5 1 1
SECTION 6
bottom 1 top 4
1 2 2, 4 3 3, 7 1 2, 9 3 3, 10 4 4, 13 1 1, 14 4 4
SECTION 7
bottom 1 top 4
2 1 1, 3 3 3, 5 2 2, 7 3 4, 13 4 4, 15 4 4
SECTION 8
bottom 1 top 6
2 1 1, 5 1 1, 6 3 3, 7 2 2, 8 5 5, 10 6 6, 13 4 4, 14 5 6
SECTION 9
bottom 1 top 2
6 2 2, 10 1 2, 12 2 2, 15 1 1
SECTION 10
bottom 1 top 2
1 1 1, 6 1 1, 8 3 3, 10 2 2, 11 1 1, 12 1 1
SECTION 11
bottom 1 top 1
9 1 1, 10 1 1, 14 1 1

Appendix 2
DEBOO (1965)

2-A Code numbers of sections
1 1 Wayne and Clark Counties (composite section)
2 St Stephen Quarry
3 Little Stave Creek
4 Jackson
5 Perdue Hill:

2-B Code numbers of species (benthic foraminifera and ostracods)
1 Alabamina wilcoxensis
2 Angulogerina byramensis
3 Angulogerina danvillensis
4 Angulogerina vicksburgensis
5 Anomalina cocoaensis
6 Anomalina danvillensis
7 Astacolus danvillensis
8 Bolivina lazanensis
9 Bolivina dalli
10 Bolivina gracilis
11 Bolivina mississipiensis
12 Bolivina retifera
13 Bolivina striatellata
14 Bulimina jacksonensis
15 Cancris cocoaensis
16 Cibicides cocoaensis
17 Cibicides pippeni
18 Cibicides pseudoungerianus
19 Cibicides sp.1
20 “Darbyella” danvillensis
21 Discorbitura dignata
22 Eponides byramensis
23 Eponides jacksonensis
24 Eponides mariannensis
25 Eponides sp.1

J. Guex et al., *Discrete Biochronological Time Scales*,
DOI 10.1007/978-3-319-21326-2

26 Fursenkoina dibollensis
27 Guttulina problema
28 Hanzawaia mississipiensis
29 Hanzawaia sp.1
30 Karreriella advena
31 Lankesterina frondea
32 Lanticulina convergens
33 Liebusella turgida
34 Marginulina cocoaensis
35 Massilina decorata
36 Palmula caelata
37 Planulina cocoaensis
38 Planulina cooperensis
39 Planulina lobatulus
40 Pseudoclavulina cocoaensis
41 Pseudogaudryina jacksonensis
42 Pseudogaudryina sp.1
43 Pyrulina sp.
44 Ramulina sp.
45 Robulus carolinianus
46 Robulus cultratus
47 Robulus limbosus
48 Robulus rectidorsatus
49 Robulus vicksburgianus
50 Saracenaria ornatula
51 Sigmomorphina costifera
52 Sigmomorphina jacksonensis
53 Siphonina advena
54 Siphonina eocenica
55 Siphonina danvillensis
56 Spiroloculina sp.1
57 Spiroplectammina alabamensis
58 Stilostomella cocoaensis
59 Stilostomella jacksonensis
60 Textularia adalta
61 Textularia dibollensis
62 Textularia subhauerii
63 Textularia tumidulum
64 Textularia sp.2
65 Uvigerina cocoaensis
66 Uvigerina glabrans
67 Uvigerina jacksonensis
68 Uvigerina topilensis
69 Uvigerina vicksburgiensis
70 Vaginulina lalickeri

71 Vulvulina advena
72 Eponides ouachitaensis
73 Textularia haerii
74 Subcarinata quinqueloba
75 Valvulinaria octomerata
76 Flabellina lanceolata
77 Flabellina sp.1
78 Frondicularia tenuissima
79 Anomalin bilateralis
80 Discorbis cocoaensis
81 Globulina alabamensis
82 Globulina gibba
83 Globulina inaequalis
84 Guttulina irregularis
85 Hanzawaia sp.2
86 Liebusella byramensis
87 Marginulina hantkeni
88 Marginulina mulitplicata
89 Eponides obesa
90 Robulus inusitatus
91 Saracenaria hantkeni
92 Spiroplectammina mississipiensis
93 Textularia porrecta
94 Textularia sp.1
95 Uvigerina dumblei
96 Uvigerina gardnerae
97 Globobulimina ovata
98 Rectoglandulina ovata
99 Angulogerina sp.1
100 Asterigerina gallowayi
101 Acanthocythereis n.sp.1
102 Actinocythereis dacyi
103 Actinocythereis gibsonensis
104 Actinocythereis n.sp.1
105 Actinocythereis n.sp.2
106 Ambocythere n.sp.1
107 Argilloecia hiwanneensis
108 Bairdia sp.1
109 Bairdopillata ocalana
110 Brachycythere mississippiensis
111 Buntonia israelskyi
112 Buntonia n.sp.1
113 Bythocypris gibsonensis
114 Clithrocytheridea caldwellensis
115 Clithrocytheridea garretti

116 Clithrocytheridea grigsbyi
117 Cushmanidea n.sp.1
118 Cyamocytheridea watervalleyensis
119 “Cythereis” dohmi
120 “Cythereis” hysonensis
121 Cytherella sp.1
122 Cytherelloidea cocoaensis
123 Cytheretta jacksonensis
124 Cytheropteron danvillensis
125 Digmocythere russelli
126 Digmocythere watervalleyensis
127 Echinocythereis jacksonensis
128 Echinocythereis mcguirti
129 Eucythere woodwardensis
130 Haplocytheridea ehlersi
131 Haplocytheridea montgomeryensis
132 Haplocytheridea n.sp.1
133 Hemicythere kniffeni
134 Henryhowella florienensis
135 Isocythereis couleycreekensis
136 Jugosocythereis bicarinata
137 Jugosocythereis vicksburgensis
138 Konarocythere spurgeonae
139 Krithe hiwanneensis
140 Krithe n.sp.1
141 Loxoconcha concentrica
142 Loxoconcha creolensis
143 N.gen.n.sp.1
144 Occultocythereis broussardi
145 Paracypris rosefieldensis
146 Paracytheridea belhavenensis
147 Paracytheridea woodwardensis
148 Propontocypris mississippiensis
149 Pteryogocythereis ivani
150 Pteryogocythereis murrayi
151 Trachyleberidea blanpiedi
152 Trachyleberis montgomeryensis
153 Trachyleberis n.sp.1
154 Trachyleberis n.ssp.2
155 Triginglymus n.sp.1

2-C Numerical database

Code numbers of samples: DEBOO’s (1965) original numbering of samples is given from top to bottom. For technical reasons, they are renumbered from bottom to top in the present book.

SAMPLES
TITLE “DEBOO”

SECTION 1
BOTTOM 1 TOP 17
1 12 15 2 11 15 3 4 8 5 7 8 6 4 8 7 3 8 8 4 6 9 4 11
10 4 8 11 11 17 13 4 8 14 1 10 15 3 10 16 1 8 17 4 17 18 15 15
19 1 3 20 4 4 21 14 15 22 5 17 23 1 10 24 14 17 26 2 6 27 16 17
28 2 17 30 3 14 31 1 2 32 2 2 34 3 8 35 3 15 36 16 17 38 3 10
39 1 3 40 4 7 41 3 11 43 16 16 44 4 8 45 4 16 46 3 9 47 3 9
48 4 6 50 4 7 51 1 2 52 3 8 53 15 17 54 1 2 55 3 14 56 4 8
57 14 14 58 3 8 59 3 7 60 1 1 61 1 1 62 12 17 63 16 16 64 1 1
65 1 8 66 2 12 67 6 10 68 1 8 69 11 15 70 7 14 71 4 6 72 5 8
73 14 14 74 4 9 75 10 17 78 3 9 79 11 17 80 4 10 81 14 14 82 1 17
83 1 3 84 1 17 85 1 3 86 4 14 87 4 8 89 11 12 90 1 16 91 4 17
92 1 17 93 1 3 94 1 2 96 1 11 99 2 2 101 4 11 102 10 17 103 1 7 104
2 3 105 1 3 107 4 15 110 1 1 111 4 14 112 4 8 113 4 17 115 1 3 116 1 3 118 1 2
119 1 8 120 1 3 121 15 17 122 1 1 123 1 3 125 1 17 126 1 1 127 1 3 128 4 17
129
12 17 130 4 8 131 1 10 132 1 1 133 15 17 134 1 8 135 1 4 137 15 17 139 4 17
142
4 9 143 1 3 144 1 1 145 12 17 148 15 17 149 4 17 150 4 6 151 12
17 152 4 6 153 9 10 155 1 2

SECTION 2
BOTTOM 1 TOP 13
1 3 10 2 9 10 3 2 10 4 9 10 5 4 6 6 6 8 7 3 4 8 4 8
9 4 10 10 2 8 11 9 10 12 4 7 13 3 8 14 3 8 15 4 8 16 3 8
17 8 13 18 7 10 19 2 6 20 4 4 21 9 10 22 9 12 23 1 7 24 9 13
25 12 13 27 9 12 28 2 13 29 1 2 30 1 8 31 2 2 32 3 13 33 3 9
34 3 6 35 3 10 36 9 13 37 3 7 38 3 7 39 1 2 40 4 7 41 3 7
42 3 7 43 4 4 44 6 13 45 3 13 46 3 12 47 4 11 48 4 7 49 13 13
50 3 7 51 2 2 52 3 4 53 9 13 54 1 2 55 3 11 56 5 8 57 2 8
58 3 8 59 3 7 60 1 2 61 1 1 62 9 13 63 13 13 64 2 3 65 3 11
66 3 10 67 1 7 68 3 8 69 9 13 70 4 4 71 3 7 72 8 8 74 5 10
75 7 13 76 3 7 77 6 7 79 3 13 80 4 7 81 8 13 82 3 13 84 1 13
85 11 11 86 1 13 88 4 7 89 5 13 90 1 13 91 3 12 92 1 7 93 1 1
94 2 2 95 4 7 96 1 10 97 2 8 98 8 8 99 2 3 101 3 7 102 7 13 103
1 4 104 3 4 109 1 1 111 3 7 114 1 2 115 1 2 116 1 2 118 1 2 119 1 6 120 2 2 121
12 13 122 1 2 123 1 1 125 2 13 126 1 2 127 1 2 128 9 13 131 1 6 134 1 8 135 1 6
136 1 1 137 12 13 138 1 1 139 7 12 140 3 12 141 1 7 142 1 2 143 1 2 144 2 3 146
1 1 147 13 13 148 12 13 149 3 13 151 8 13 152 5 10 154 8 8

SECTION 3
BOTTOM 1 TOP 13
1 4 11 2 5 12 3 1 6 4 8 11 5 3 5 6 3 5 7 3 4 8 3 5
9 5 6 10 4 5 11 6 12 12 2 8 13 3 5 14 3 5 15 3 5 16 1 8
17 7 13 18 6 10 19 1 2 20 3 5 21 8 11 22 5 13 23 1 6 24 6 13
25 11 13 26 5 12 27 11 13 28 2 13 29 1 10 30 3 12 31 2 13 32 3 11
33 5 13 34 3 4 35 3 7 36 4 13 37 3 5 38 3 5 39 2 13 40 3 5
41 3 5 42 3 10 43 11 13 44 6 13 45 3 13 46 3 13 47 3 5 48 3 5
49 11 13 50 3 4 51 1 2 52 3 3 53 6 13 54 1 2 55 2 5 56 4 7
57 1 2 58 3 3 59 3 4 60 1 2 61 1 1 62 8 13 64 1 2 65 1 7
66 3 7 67 2 5 68 3 7 69 8 12 70 3 8 71 3 5 73 9 12 74 5 13
75 6 13 77 4 5 78 3 5 79 2 13 80 3 5 81 6 11 82 1 13 83 2 2
84 1 13 86 2 13 87 3 5 88 3 5 89 5 12 90 2 10 91 2 10 92 1 10
93 1 2 94 1 2 95 3 5 96 3 5 97 1 13 98 3 5 100 3 3 101 3 6 102
6 13 103 1 3 104 3 3 105 1 2 106 13 13 107 10 13 108 1 13 109 1 2 113 3 13 114
1 2 115 1 2 116 1 2 117 1 2 118 1 2 119 1 5 120 1 2 121 6 13 123 1 2 125 1 13
126 1 2 127 1 2 128 3 13 131 1 4 134 1 5 135 1 5 136 1 2 137 11 13 139 6 13 142
1 2 143 1 2 144 1 4 145 6 13 147 10 13 148 9 13 149 3 13 150 4 4 151 6 13 152
6 8

SECTION 4
BOTTOM 1 TOP 9
1 1 9 2 6 8 3 1 6 4 6 7 5 2 2 6 1 1 7 2 4 8 3 4
9 3 4 10 4 4 11 8 9 12 2 6 13 2 4 14 3 4 15 2 4 16 2 3
17 5 9 18 5 7 19 1 1 20 2 4 22 5 9 23 1 2 24 5 9 26 4 8
27 5 6 28 1 9 29 5 9 30 2 4 31 5 9 32 3 7 33 5 8 34 2 4
35 2 8 36 2 9 37 1 4 38 1 4 39 5 8 40 2 6 41 2 4 42 2 4
44 2 9 45 2 9 46 6 6 47 1 4 48 2 4 50 2 3 51 1 1 52 2 4
53 5 9 55 1 7 56 5 5 57 1 7 58 2 4 59 2 4 60 1 2 61 1 1
62 5 8 64 1 1 65 3 5 66 3 4 67 3 4 68 3 4 69 6 9 70 4 8
71 4 4 72 5 7 73 5 5 74 3 7 75 4 9 76 2 3 77 4 4 78 2 4
79 2 9 80 2 4 81 1 9 82 1 9 84 1 9 85 2 8 86 2 9 87 4 4
88 3 6 89 4 9 90 2 9 91 2 8 92 2 9 94 1 1 95 2 4 96 1 1
97 2 4 98 3 4 101 3 6 102 3 9 103 1 1 105 3 4 107 5 9 108 1 9 109 1 1 110
1 1 111 3 4 113 3 9 114 1 1 115 1 1 116 1 1 117 1 5 119 1 5 120 1 1 123 1 1 125
1 9 126 1 1 128 6 9 129 7 8 131 1 5 134 3 4 135 1 4 136 1 1 137 8 9 138 1 1 139
5 9 143 1 1 145 5 5 148 5 8 149 3 9 151 5 9 152 3 6

SECTION 5
BOTTOM 1 TOP 10
1 4 8 2 8 10 4 10 10 5 5 6 6 5 6 7 5 6 8 5 5 9 5 6
11 8 10 12 6 7 13 5 7 14 5 6 16 3 5 17 7 10 18 7 10 19 1 4
22 9 10 23 1 6 24 7 10 25 9 10 26 1 4 29 1 7 30 3 6 31 4 7
32 5 8 33 5 8 34 5 6 36 7 10 37 5 6 38 3 6 39 3 4 41 5 5
42 5 8 45 7 10 46 5 6 47 5 5 49 10 10 50 5 6 51 1 4 52 5 6
53 7 10 54 2 4 55 5 6 57 1 4 58 5 6 59 5 6 61 1 4 62 9 10

63 9 10 64 3 4 65 5 6 66 5 7 67 1 6 68 4 6 69 7 10 70 5 5
71 5 6 72 5 5 75 7 10 76 9 9 79 4 10 80 5 7 82 2 10 83 4 4
84 1 10 86 5 8 89 5 10 90 5 6 91 5 7 92 8 8 94 3 4 96 4 5
97 5 5 100 5 6 101 5 6 102 5 9 103 1 5 104 3 6 107 8 10 110 1 2 111 3 3 113
3 10 114 1 7 115 1 4 116 1 4 118 1 4 119 1 6 120 1 3 122 1 5 123 3 3 125 3 10
127 1 4 128 5 8 129 5 8 131 1 2 134 1 6 135 1 6 136 2 4 137 9 10 138 1 1 139 5
10 142 1 6 143 1 4 144 2 6 145 9 10 146 1 6 148 8 10 149 6 10 150 6 6 151 7 10
152 2 2 155 1 2

Appendix 3
Cody et al. (2008)

3-A Database in the UAgraph format

DATUM
Title: "Cody et al., 2008, diatom"
Section 1; bottom 1—top 25;1 7 25;5 11 16;6 1 23;10 1 19;11 9 16;13 5 11;12 1 25;22 4 25;26 6 25;41 1 7;46 5 8;47 3 8;50 9 25;54 2 2;56 4 8;58 23 25;63 5 25;64 4 12;65 1 8;68 23 25;69 4 25;71 23 25;88 15 25;89 1 2;93 1 21;96 1 11;100 1 8;102 1 5;104 2 22;108 15 19;109 2 22;110 23 25;112 1 19;114 5 18;115 16 25;120 1 25;121 1 25;125 1 17;128 1 22;129 24 25;130 10 20;131 6 11;AshC2 14 14;FAD114 5 5;FAD131 6 6;Section 2; bottom 1—top 16;10 1 13;13 7 9;12 1 16;50 12 16;56 15 15;64 2 2;65 9 15;88 9 16;89 6 11;93 1 15;96 3 10;100 9 15;102 4 13;104 5 13;109 6 15;111 14 15;112 5 15;113 9 15;115 13 16;117 9 16;120 1 16;121 3 16;128 1 15;FAD96 3 3;FAD111 14 14;FAD117 9 9; Section 3; bottom 1—top 16;6 2 6;10 2 7;13 3 7;12 1 16;41 2 7;63 14 16;65 9 13;69 15 16;71 14 16;89 4 11;93 2 13;96 9 13;100 9 12;102 4 13;104 10 13;109 8 13;112 4 13;113 9 13;120 5 16;121 2 16;128 2 13;FAD96 9 9; Section 4; bottom 1—top 22;1 18 22;6 1 17;22 14 22;37 2 5;41 3 9;43 11 22;56 14 15;58 16 22;75 20 21;89 2 13;94 4 8;96 7 15;101 10 15;114 18 19;115 16 22;122 6 9; FAD114 18 18;FAD96 7 7; Section 5; bottom 1—top 39;6 1 37;18 3 10;22 14 39;32 2 5;37 1 6;41 1 20;43 9 39;52 15 15;54 11 14;56 25 28;57 4 21;58 30 39;64 17 23;65 24 26;67 16 26;73 27 29;74 3 39;75 3 38;76 11 19;77 13 17;78 6 10;81 3 16;85 13 17;89 1 34;100 11 26;102 18 36;108 35 37;111 27 31;114 27 33;116 27 39;115 27 39;119 7 26;122 14 16;123 10 18;128 7 22;130 27 32; FAD111 27 27;FAD114 27 27;FAD73 27 27;FAD77 13 13; Section 6; bottom 1—top 28;6 5 27;16 18 28;43 1 28;56 3 14;58 19 28;65 1 6;67 1 14;73 5 16;75 1 19;89 1 23;100 2 11;108 20 25;111 8 17;114 10 21;116 7 15;115 7 28;130 7 19;C1nbase 26 26;C2An.1nbase 13 13;C2An.2nbase 9 9;C2An.2ntop 12 12; C2An.3nbase 4 4;C2nbase 22 22;C2ntop 24 24;FAD111 8 8;FAD114 10 10; {FAD6 5 5};FAD73 5 5; section 7; bottom 1—top 76;6 11 76;7 19 29;8 44 49;10 32 61;15 8 15;18 39 49;19 2 12;22 6 76;24 1 19;25 2 17;28 2 15;29 10 13;30 18 26;31 38 49;32 26 40;38 11 20;39 30 49;40 24 33;41 21 57;45 44 68;46 36 69;47 67 76;48 27 42;49 41 62;50 71 76;52 21 59;54 42 76;56 74 76;57 35 44;59 67 73;60 3 11;64 34 73;65 56 73;66 4 13;67 65 72;74 42 76;77

J. Guex et al., *Discrete Biochronological Time Scales*,
DOI 10.1007/978-3-319-21326-2

50 55;81 15 50;83 23 31;84 13 26;89 3 73;90 5 15;91 63 70;93 60 75;97 63 73;100 8 75;101 53 62;104 62 75;112 62 75;114 63 75;118 47 51;120 53 76;121 65 76;122 45 59;124 5 9;128 46 60;C3n.2nbase 64 64;C3n.2ntop 66 66; C3n.3nbase 58 58;C3n.4nbase 54 54;C4Antop 43 43;C4r.1nbase 48 48; C5ABnbase 22 22;C5An.1ntop 28 28;C5An.2nbase 25 25;C5Bn.2nbase 14 14; C5Bn.2ntop 16 16;C5Entop 7 7;FAD84 13 13;FAD15 8 8;FAD19 2 2;FAD25 2 2;FAD28 2 2;FAD38 11 11;FAD60 3 3;FAD77 50 50;FAD114 63 63;FAD124 5 5;FAD29 10 10;FAD90 5 5; Section 8; bottom 1—top 64;6 11 63;7 13 21;8 37 44;10 30 38;15 8 11;18 33 38;19 2 38;22 10 64;24 1 14;25 4 12;29 7 12;30 7 21;31 33 38;32 21 38;38 10 14;39 25 38;40 18 29;41 15 42;43 42 64;45 36 45;47 51 64;48 20 36;49 44 50;50 54 64;52 15 44;54 50 60;56 54 62;57 15 36;58 63 64;59 50 56;60 3 11;64 30 52;65 43 55;66 7 11;81 10 16;83 16 27;84 11 16;89 5 56;90 3 11;93 49 62;97 50 61;100 32 61;101 6 48;104 53 60;111 59 61;112 46 62;114 52 62;115 55 64;120 47 64;121 50 64;122 39 42;124 5 9; C2An.1nbase 57 57;C2An.1ntop 58 58;C3n.4ntop 41 41;C4Antop 35 35; C5An.1nbase 26 26;C5An.1ntop 28 28;C5An.2nbase 23 23;C5An.2ntop 24 24; C5Ar.1ntop 19 19;C5Ar.2nbase 17 17;C5n.1ntop 34 34;FAD84 11 11;FAD15 8 8;FAD19 2 2;FAD25 4 4;FAD38 10 10;FAD60 3 3;FAD111 59 59;FAD114 52 52;FAD124 5 5;FAD29 7 7;FAD90 3 3; Section 9; bottom 1—top 26;6 4 20;21 18 26;22 4 26;24 1 3;32 6 7;40 4 7;41 4 13;43 9 26;46 13 17;47 19 24;52 8 8;56 22 23;57 10 12;64 5 16;65 13 21;67 15 21;83 4 6;89 4 20;93 20 25;104 14 21;112 20 24;114 20 23;115 20 26;120 17 26;122 11 21;124 2 3;FAD114 20 20;FAD124 2 2; Section 10; bottom 1—top 59;1 56 59;6 1 59;10 16 59;11 50 51;41 1 38;43 1 59;45 19 37;46 9 30;47 29 48;49 7 34;50 33 59;52 1 12;54 27 56;56 40 48;58 56 59;63 45 59;64 5 35;65 18 39;69 46 59;73 47 56;77 1 4;81 6 13;85 10 12;89 1 54;91 20 32;93 40 52;96 19 52;100 8 52;104 18 44;108 56 58;109 28 58;111 49 53;112 26 52;114 43 53;115 42 59;120 21 59;121 2 59;125 25 52;128 1 59;129 23 59;130 49 57;131 46 55;C2An.3nbase 41 41; C3n.1nbase 31 31;C3n.1ntop 36 36;C3n.2nbase 24 24;C3n.3nbase 17 17; C3n.3ntop 22 22;C3n.4nbase 11 11;C3n.4ntop 14 14;FAD111 49 49;FAD114 43 43;FAD125 25 25;FAD131 46 46;FAD73 47 47;FAD96 19 19; Section 11; bottom 1—top 30;6 2 20;32 12 13;37 3 9;38 1 4;40 10 12;41 5 19;43 7 30;45 21 27;46 22 29;48 8 10;49 23 24;52 9 14;57 3 18;64 11 29;65 26 28;84 1 5;104 25 29;120 21 30;122 17 26; Section 12; bottom 1—top 24;1 22 24;6 1 23;14 4 12;22 10 24;41 1 9;43 2 24;56 12 15;58 18 24;65 8 13;67 3 18;73 13 17;74 3 24;75 3 24;76 3 7;89 2 21;102 1 17;108 18 23;111 13 19;114 13 20;115 11 24;116 14 16;128 3 8;130 14 22;132 2 4;FAD14 4 4;FAD111 13 13;FAD114 13 13;FAD132 2 2;FAD73 13 13; Section 13; bottom 1—top 13;6 4 13;73 2 3;89 5 8;108 9 12;111 2 6;114 2 7;130 2 10;C1nbase 11 11;C3n.4nbase 1 1; FAD111 2 2;FAD114 2 2;FAD73 2 2; Section 14; bottom 1—top 60;3 6 30;6 1 59;14 14 47;18 10 32;22 14 60;32 1 11;37 1 12;41 1 32;43 7 60;49 2 47;54 15 53;56 34 42;58 50 60;65 33 40;67 14 47;73 39 47;74 8 60;75 9 51;76 18 35;77 23 24;81 1 24;89 3 55;94 13 31;100 16 47;102 14 42;108 57 58;114 37 54;115 35 60;116 40 56;119 11 58;120 28 60;122 14 48;130 44 52;132 9 34; C2An.1nbase 46 46;C2An.1ntop 49 49;C2An.2nbase 43 43;C2An.2ntop 45 45;

{C2An.2n 43 45};C2An.3nbase 38 38;C2An.3ntop 41 41;C3An.1nbase 26 26; C3An.1ntop 29 29;C3Bnbase 21 21;C3Bntop 22 22;C4n.1ntop 20 20; C4n.2nbase 17 17;FAD14 14 14;FAD77 23 23;FAD114 37 37;FAD132 9 9; FAD73 39 39; Section 15; bottom 1—top 31;1 17 31;6 2 29;22 13 31;47 1 24;56 1 20;58 12 31;65 1 5;69 22 31;71 26 31;73 1 10;75 6 30;87 27 31;89 19 23;100 9 14;102 1 11;108 16 25;112 1 31;114 1 21;115 1 31;116 3 7;120 4 31;128 5 18;130 8 15;FAD114 1 1; Section 16; bottom 1—top 38;6 1 31;10 3 7;14 3 32;41 2 12;47 26 38;52 1 6;54 4 23;56 30 37;58 37 38;65 23 37;67 3 25;73 34 37;74 3 38;75 3 32;85 8 16;89 1 28;94 6 20;97 13 24;100 3 36;102 19 33;104 21 36;105 10 15;107 1 38;112 22 38;114 35 35;115 29 38;118 9 14;119 2 20;120 17 38;122 3 13;123 10 11;128 1 36;C3n.1ntop 27 27;C3n.3ntop 18 18; FAD14 3 3;FAD114 35 35;FAD73 34 34; Section 17; bottom 1—top 35;6 6 34;7 7 10;10 15 26;14 28 31;18 21 25;22 2 35;24 1 10;29 2 5;30 2 11;32 12 20;34 24 26;36 7 10;37 4 16;38 4 11;39 17 26;40 11 13;41 9 33;47 30 35;54 30 31;56 30 33;58 34 35;60 1 5;65 30 32;67 29 29;74 19 35;75 22 33;83 8 11;84 4 11;89 14 32;90 3 5;93 33 33;94 19 28;100 28 29;105 27 29;108 33 34;112 33 35;114 33 33;115 34 35;118 27 29;120 32 35;121 27 35;124 1 4;130 33 33;14 28 28;FAD84 4 4;FAD36 7 7;FAD38 4 4;FAD114 33 33;FAD29 2 2;FAD90 3 3; Section 18; bottom 1—top 74;6 55 73;41 1 22;47 29 64;54 1 32;56 33 57;58 57 74;65 22 48;67 1 36;73 43 58;74 1 74;75 2 72;89 1 63;94 8 53;97 8 46;102 9 55;105 8 8;108 64 67;111 47 52;112 17 52;114 47 58;119 2 32;120 14 74;123 2 2;128 1 56;130 49 54;C1nbase 70 70;C1r.1nbase 65 65;C1r.1ntop 68 68; C2An.1nbase 44 44;C2An.1ntop 50 50;C2An.2nbase 39 39;C2An.2ntop 41 41; C2An.3nbase 34 34;C2An.3ntop 37 37;C2nbase 59 59;C2ntop 61 61; C3An.1nbase 6 6;C3An.1ntop 10 10;C3An.2ntop 3 3;C3n.1nbase 27 27; C3n.1ntop 30 30;C3n.2nbase 23 23;C3n.2ntop 25 25;C3n.3nbase 18 18; C3n.3ntop 20 20;C3n.4nbase 12 12;C3n.4ntop 15 15;FAD111 47 47;FAD114 47 47;FAD73 43 43; Section 19; bottom 1—top 30;6 1 15;8 17 26;10 2 24;18 4 7;34 8 9;39 1 11;41 1 21;49 14 20;52 17 23;57 1 10;64 2 30;75 5 18;77 22 26;78 6 13;85 25 29;94 16 30;101 17 30;119 3 30;122 12 28;123 27 30;128 14 19;FAD77 22 22; Section 20; bottom 1—top 81;1 71 81;3 48 59;5 71 71;7 15 29;8 56 59;6 10 79;10 39 60;12 3 81;15 8 14;16 72 81;17 73 81;18 43 58;22 3 81;24 1 14;28 2 5;29 7 14;32 30 42;37 10 23;38 8 11;39 48 48;40 30 34;41 18 57;45 60 60;46 59 60;47 61 75;50 73 81;52 51 58;56 65 70;58 71 81;64 59 60;65 60 63;67 57 65;69 67 81;71 76 81;73 66 70;75 43 80;76 58 58;77 57 58;78 42 54;81 8 58;82 9 9;83 26 39;85 54 56;89 31 72;90 3 9;93 65 74;96 63 63;97 60 63;100 59 73;102 3 67;104 60 65;108 75 77;109 75 78;111 67 70;112 60 71;114 63 72;115 61 81;116 66 67;120 63 81;122 56 58;121 43 81;124 4 6;128 51 58;129 65 81;130 70 70;C2An.3nbase 64 64;C2An.3ntop 68 68; C4Ar.1nbase 49 49;C4Ar.1ntop 52 52;C4Ar.2nbase 44 44;C4Ar.2ntop 46 46; C5ABnbase 24 24;C5ABntop 28 28;C5ACnbase 20 20;C5ACntop 22 22; C5ADntop 16 16;C5An.1nbase 37 37;C5An.2nbase 33 33;C5An.2ntop 35 35; C5Bn.1nbase 12 12;FAD12 3 3;FAD15 8 8;FAD111 67 67;FAD114 63 63; FAD29 7 7;FAD73 66 66;FAD90 3 3;FAD96 63 63;FAD28 2 2;FAD38 8 8; FAD77 57 57;FAD82 9 9;FAD124 4 4; Section 21; bottom 1—top 59;1 45 59;5

48 50;6 13 59;10 23 51;11 48 50;15 8 12;16 56 59;17 57 59;18 22 30;19 1 11;22 7 59;24 2 11;26 36 59;28 3 12;29 10 12;32 13 21;38 11 12;39 22 30;40 13 15;41 13 32;46 32 39;47 32 52;48 13 19;49 36 37;50 44 59;54 38 50;56 39 51;58 52 59;60 6 11;65 32 42;67 32 36;69 48 59;71 54 59;74 22 59;75 26 43;76 31 31;80 37 39;81 9 28;82 11 11;83 13 14;84 12 12;90 6 12;93 34 52;96 39 51;97 35 40;100 37 52;102 4 46;103 58 59;104 32 47;108 52 53;109 54 55;110 54 59;111 46 51;112 32 51;114 35 51;115 33 59;119 26 29;120 32 59;121 32 59;124 5 9;125 44 47;128 31 51;129 37 59;130 46 51;131 44 47;C1nbase 54 54; C2An.1ntop 49 49;C2An.3nbase 41 41;C4Ar.1ntop 27 27;C4Ar.2nbase 25 25; C5n.1ntop 24 24;C5n.2nbase 18 18;C5r.1nbase 16 16;C5r.1ntop 17 17;FAD84 12 12;FAD15 8 8;FAD111 46 46;FAD114 35 35;FAD125 44 44;FAD29 10 10; FAD80 37 37;FAD90 6 6;FAD96 39 39;FAD28 3 3;FAD38 11 11;FAD60 6 6; FAD82 11 11;FAD124 5 5;FAD131 44 44; Section 22; bottom 1—top 60;1 54 60;3 30 30;5 53 55;7 11 18;8 29 32;6 8 60;10 29 55;11 54 54;15 5 12;16 52 60;17 52 60;18 23 33;22 1 60;24 1 9;26 51 60;28 1 2;29 3 4;30 10 17;32 19 30;34 25 27;36 14 16;37 8 13;38 5 13;39 25 28;40 17 21;41 13 42;45 29 43;46 29 43;47 44 58;49 31 53;50 48 60;52 26 31;54 29 46;56 46 54;58 54 60;59 34 48;60 3 5;64 29 43;65 34 50;67 29 48;68 59 60;69 47 60;71 57 60;73 50 53;74 24 60;75 29 60;76 29 30;77 29 29;80 41 47;82 5 10;83 15 21;84 7 16;89 20 53;90 1 6;93 44 56;96 41 53;97 38 48;100 29 54;102 39 50;103 59 60;104 39 50;107 30 60;108 49 58;109 40 57;110 55 60;111 49 55;112 34 54;113 35 53;114 43 54;115 45 60;116 50 53;118 29 29;119 29 31;120 34 60;121 29 60;122 29 37;124 1 2;125 43 50;128 30 54;129 38 60;130 51 54;131 49 53; FAD84 7 7;FAD15 5 5;FAD36 14 14;FAD111 49 49;FAD114 43 43;FAD125 43 43;FAD29 3 3;{FAD6 8 8};FAD73 50 50;FAD80 41 41;FAD96 41 41; FAD38 5 5;FAD60 3 3;FAD77 29 29;FAD82 5 5;FAD131 49 49; Section 23; bottom 1—top 39;3 10 17;6 1 37;8 23 30;18 15 19;22 2 39;24 1 2;30 5 7;31 18 20;32 5 7;39 5 8;40 3 4;41 1 32;45 21 33;46 22 35;52 12 27;54 21 39;64 24 29;67 25 38;74 11 39;75 29 29;81 28 34;84 6 6;89 2 36;100 14 32;112 35 38;122 23 25;128 28 39;132 16 26;FAD84 6 6;FAD132 16 16; Section 24; bottom 1—top 39;1 31 39;4 13 25;6 1 37;10 9 13;21 1 39;22 23 39;23 3 39;47 1 26;54 2 34;56 4 15;58 17 39;61 10 14;62 11 13;65 1 6;67 1 35;68 29 39;69 22 39;71 28 39;73 2 10;74 1 39;75 6 38;89 1 21;93 2 19;100 1 7;102 2 8;105 9 9;107 2 39;108 15 35;109 13 29;110 14 39;111 3 11;112 1 7;114 6 15;115 2 39;117 1 39;120 4 39;121 1 39;125 5 18;127 10 23;129 36 39;130 8 12;C1nbase 32 32;C1r.1nbase 27 27;C1r.1ntop 30 30;C2nbase 16 16;C2ntop 20 20;FAD23 3 3;FAD111 3 3;FAD114 6 6;FAD125 5 5;FAD61 10 10;FAD62 11 11;FAD73 2 2; Section 25; bottom 1—top 41;4 13 30;6 1 39;11 8 19;21 2 41;23 1 41;22 3 41;45 1 2;46 2 10;47 4 29;49 1 7;54 1 32;56 7 13;58 25 41;59 3 5;61 16 22;62 20 21;64 2 4;65 2 11;67 1 16;68 28 41;69 20 41;71 30 41;73 10 16;74 1 41;75 1 40;80 10 10;89 1 26;95 34 38;100 6 9;104 3 13;105 14 19;107 12 41;108 31 36;109 15 35;110 28 41;111 10 17;112 1 17;114 13 23;115 8 41;117 2 41;120 1 41;121 1 41;125 1 14;127 17 29;129 10 41;129 5 41;130 17 19;C1nbase 37 37; C1r.1nbase 31 31;C1r.1ntop 33 33;C2An.1ntop 18 18;C2nbase 24 24;C2ntop 27 27;FAD111 10 10;FAD114 13 13;FAD117 2 2;FAD61 16 16;FAD62 20 20;

FAD73 10 10;FAD80 10 10;FAD95 34 34; Section 26; bottom 1—top 49;1 9 49;4 19 35;6 1 46;10 1 22;16 20 49;21 32 49;22 1 49;44 1 32;47 1 36;50 11 49;54 4 6;56 1 19;58 19 49;62 19 26;63 37 49;65 1 13;67 1 7;68 31 49;69 20 49;71 31 49;73 1 15;75 2 49;79 39 49;88 14 49;89 3 33;93 1 34;95 37 49;99 28 48;100 1 25;102 1 5;103 44 49;105 8 10;107 9 49;108 35 45;109 1 42;110 24 49;111 4 18;112 1 14;114 2 27;115 1 49;116 21 23;117 1 49;120 1 49;121 1 49;127 17 33;129 16 49;129 8 49;130 1 20;C1nbase 43 43;C1r.1nbase 38 38; C1r.1ntop 40 40;C2An.1ntop 12 12;C2nbase 29 29;C2ntop 30 30;FAD111 4 4; FAD114 2 2;FAD62 19 19;FAD79 39 39;FAD95 37 37; Section 27; bottom 1 —top 101;4 74 96;6 7 100;7 9 10;8 26 55;10 25 81;11 75 79;15 3 4;16 69 101;17 88 101;18 21 40;21 60 101;22 1 101;23 65 101;24 1 8;25 2 5;31 22 37;32 12 15;38 6 8;39 14 16;40 10 11;41 34 38;44 86 88;45 31 68;46 36 72;47 64 93;49 57 63;52 43 47;54 32 72;56 65 78;58 80 101;59 52 72;61 80 84;62 83 83;64 24 69;65 56 69;67 31 76;68 88 101;69 86 101;71 90 101;73 71 76;74 23 101;75 20 100;79 97 101;80 59 76;83 10 13;85 29 49;88 87 101;89 44 88;90 6 6;93 67 90;95 95 99;97 53 68;99 82 92;100 41 91;102 33 59;104 59 73;105 53 79;107 82 101;108 82 97;109 73 98;110 89 101;111 74 77;112 55 77;114 70 85;115 60 101;117 58 101;120 53 101;122 31 50;121 48 101;125 60 73;127 79 94;128 42 66;129 79 101;129 87 101;130 77 81;132 17 61;C4Anbase 27 27; C4n.2nbase 39 39;C4r.1nbase 35 35;C5n.2nbase 19 19;FAD15 3 3;FAD23 65 65;FAD111 74 74;FAD114 70 70;FAD117 58 58;FAD125 60 60;FAD61 80 80;FAD73 71 71;FAD80 59 59;FAD90 6 6;FAD25 2 2;FAD38 6 6;FAD62 83 83;FAD79 97 97;FAD95 95 95;FAD132 17 17; Section 28; bottom 1—top 49;1 17 49;4 23 36;6 1 43;10 9 25;11 11 18;16 11 49;22 1 49;44 1 28;47 1 34;49 1 17;50 3 49;56 1 16;58 26 49;61 20 26;63 19 49;65 1 12;67 1 5;68 30 49;69 10 49;71 31 49;73 6 16;75 2 47;79 44 49;87 46 49;88 38 49;89 1 28;93 1 33;95 35 45;97 3 19;99 18 48;100 1 28;102 1 9;104 1 9;105 12 17;108 21 42;109 22 39;110 29 49;111 6 15;112 1 13;114 1 27;115 1 49;117 1 49;120 3 49;121 1 49;127 22 32;128 7 26;129 37 49;129 13 49;130 9 21;C1nbase 40 40; C2An.1ntop 14 14;FAD111 6 6;FAD61 20 20;FAD73 6 6;FAD79 44 44; FAD95 35 35; Section 29; bottom 1—top 28;1 1 28;4 1 6;6 1 23;10 1 4;16 3 28;17 5 28;22 3 28;26 9 28;44 2 9;47 1 10;50 1 28;58 2 28;63 1 28;68 2 28;69 1 28;71 3 28;75 24 26;79 14 28;87 8 28;88 1 28;93 1 5;95 11 25;99 1 27;108 1 22;109 1 19;110 1 28;115 1 28;120 2 28;121 1 28;127 1 8;129 18 28;129 1 28; C1nbase 20 20;C1r.1nbase 12 12;C1r.1ntop 15 15;FAD79 14 14;FAD95 11 11; Section 30; bottom 1—top 20;1 11 20;6 7 17;10 4 13;11 5 6;47 1 14;50 19 20;56 1 10;58 12 20;69 2 20;75 17 18;103 16 20;109 2 15;111 3 8;112 3 9;115 16 20;120 1 20;121 1 20;128 1 16;130 6 10;FAD111 3 3; Section 31; bottom 1 —top 62;1 45 62;5 45 50;6 7 61;7 8 10;8 21 31;10 25 50;11 44 45;15 6 8;18 21 23;22 4 62;24 1 6;25 1 3;26 51 62;30 8 11;31 14 20;34 12 17;32 12 17;36 9 9;38 6 7;39 15 18;40 11 14;41 9 20;45 30 33;46 28 33;47 34 55;49 32 36;50 44 62;52 16 31;56 35 49;57 21 31;58 42 62;59 32 32;60 2 2;61 50 52;63 56 62;64 25 32;65 32 38;66 19 30;67 25 37;68 56 62;69 40 62;71 57 62;73 39 45;75 24 60;76 21 32;77 26 28;78 21 24;82 6 7;83 9 13;84 9 11;85 25 31;90 6 6;91 32 34;93 34 57;94 23 31;97 32 37;100 24 39;101 30 31;103 58 62;104 32 39;110

53 62;111 41 46;112 32 43;113 27 32;114 35 53;115 40 62;116 41 49;118 24 30;121 26 62;122 26 28;124 3 5;125 34 39;127 47 54;128 21 48;129 32 62;130 44 50;AshA2 29 29;FAD84 9 9;FAD15 6 6;FAD36 9 9;FAD111 41 41; FAD114 35 35;FAD125 34 34;{FAD6 7 7};FAD61 50 50;FAD73 39 39; FAD90 6 6;FAD38 6 6;FAD60 2 2;FAD77 26 26;FAD82 6 6;FAD124 3 3; Section 32; bottom 1—top 38;1 29 38;5 27 32;6 1 37;10 4 32;11 32 32;22 4 38;26 9 38;45 2 10;46 1 13;47 12 35;50 15 38;56 16 26;58 33 38;59 7 18;61 32 33;63 12 38;64 1 17;65 1 24;67 1 22;69 16 38;73 23 32;75 17 36;88 27 38;89 4 19;93 1 31;96 3 31;100 1 30;104 1 25;108 9 32;111 25 31;112 4 32;113 1 14;114 21 32;115 17 38;121 1 38;122 5 9;125 11 22;127 28 33;128 1 34;129 8 38;130 25 32;FAD111 25 25;FAD114 21 21;FAD125 11 11;FAD61 32 32; FAD73 23 23;FAD96 3 3;SECTION 101-;bottom 1—top 54;C1nbase 54 54; C1r.1ntop 53 53;C1r.1nbase 52 52;C2ntop 51 51;C2nbase 50 50;C2An.1ntop 49 49;AshC2 48 48;C2An.1nbase 47 47;C2An.2ntop 46 46;C2An.2nbase 45 45;C2An.3ntop 44 44;C2An.3nbase 43 43;C3n.1ntop 42 42;C3n.1nbase 41 41; C3n.2ntop 40 40;C3n.2nbase 39 39;C3n.3ntop 38 38;C3n.3nbase 37 37; C3n.4ntop 36 36;C3n.4nbase 35 35;C3An.1ntop 34 34;C3An.1nbase 33 33; AshA2 32 32;C3An.2ntop 31 31;C3Bntop 30 30;C3Bnbase 29 29;C4n.1ntop 28 28;C4n.2nbase 27 27;C4r.1nbase 26 26;C4Antop 25 25;C4Anbase 24 24; C4Ar.1ntop 23 23;C4Ar.1nbase 22 22;C4Ar.2ntop 21 21;C4Ar.2nbase 20 20; C5n.1ntop 19 19;C5n.2nbase 18 18;C5r.1ntop 17 17;C5r.1nbase 16 16; C5An.1ntop 15 15;C5An.1nbase 14 14;C5An.2ntop 13 13;C5An.2nbase 12 12; C5Ar.1ntop 11 11;C5Ar.2nbase 10 10;C5ABntop 9 9;C5ABnbase 8 8; C5ACntop 7 7;C5ACnbase 6 6;C5ADntop 5 5;C5Bn.1nbase 4 4;C5Bn.2ntop 3 3;C5Bn.2nbase 2 2;C5Entop 1 1;

3-B Dictionary of taxa

1 Actinocyclus actinochilus
2 Actinocyclus curvatulus
3 3Actinocyclus ellipticus
4 Actinocyclus F Zielinski & Gersonde 2003
5 Actinocyclus fasciculatus
6 Actinocyclus ingens
7 Actinocyclus ingens nodus
8 Actinocyclus ingens ovalis
10 Actinocyclus karstenii
11 Actinocyclus maccollumii
12 Actinocyclus octonarius
13 Actinocyclus octonarius asteriscus
14 Alveus marinus
15 Araniscus lewisianus
16 Asteromphalus hookeri
17 Asteromphalus hyalinus
18 Asteromphalus kennettii
19 Asteromphalus oligocenicus

20 Asteromphalus parvulus
21 Azpeitia nodulifer
22 Azpeitia tabularis
23 Azpeitia tabularis egregius
24 Cavitatus jouseanus
25 Cavitatus miocenicus
26 Chaetoceras bulbosum
27 Corethron criophilum
28 Coscinodiscus rhombicus
29 Crucidenticula kanayae
30 Crucidenticula nicobarica
31 Denticulopsis crassa
32 Denticulopsis dimorpha
33 Denticulopsis dimorpha [MID]
34 Denticulopsis dimorpha areolata
35 Denticulopsis dimorpha areolata [MID]
36 Denticulopsis hyalina
37 Denticulopsis lauta
38 Denticulopsis maccollumii
39 Denticulopsis ovata
40 Denticulopsis praedimorpha
41 Denticulopsis simonsenii
42 Denticulopsis simonsenii [MID]
43 Eucampia antarctica
44 Fragilariopsis A Gersonde 1991
45 Fragilariopsis arcula
46 Fragilariopsis aurica
47 Fragilariopsis barronii
48 Fragilariopsis claviceps
49 Fragilariopsis clementia
50 Fragilariopsis curta
51 Fragilariopsis cylindrus
52 Fragilariopsis donahuensis
53 Fragilariopsis efferans
54 Fragilariopsis fossilis
55 Fragilariopsis fossilis A
56 Fragilariopsis interfrigidaria
57 Fragilariopsis januaria
58 Fragilariopsis kerguelensis
59 Fragilariopsis lacrima
60 Fragilariopsis maleinterpretaria
61 Fragilariopsis matuyamae
62 Fragilariopsis matuyamae heteropola
63 Fragilariopsis obliquecostata
64 Fragilariopsis praecurta

65 Fragilariopsis praeinterfrigidaria
66 Fragilariopsis pusilla
67 Fragilariopsis reinholdii
68 Fragilariopsis rhombica
69 Fragilariopsis ritscheri
70 Fragilariopsis ritscheri A
71 Fragilariopsis separanda
72 Fragilariopsis sublinearis
73 Fragilariopsis weaveri
74 Hemidiscus cuneiformis
75 Hemidiscus karstenii
76 Hemidiscus karstenii f1
77 Hemidiscus triangularus
78 Lithodesmium minisculum
79 Navicula directa
80 Navicula wisei
81 Neobrunia mirabilis
82 Nitzschia 17 Schrader
83 Nitzschia denticuloides
84 Nitzschia grossepunctata
85 Nitzschia miocenica
86 Odontella weissflogii
87 Porosira glacialis
88 Porosira pseudodenticulata
89 Proboscia barboi
90 Raphidodiscus marylandicus
91 Rhizosolenia costata
92 Rouxia 1 Ciesielski 1983
93 Rouxia antarctica
94 Rouxia californica
95 Rouxia constricta
96 Rouxia diploneides
97 Rouxia heteropolara
98 Rouxia isopolica
99 Rouxia leventerae
100 Rouxia naviculoides
101 Rouxia peragalli
102 Stephanopyxis turris
103 Thalassiosira antarctica
104 Thalassiosira complicata
105 Thalassiosira convexa
106 Thalassiosira convexa aspinosa
107 Thalassiosira eccentrica
108 Thalassiosira elliptipora
109 Thalassiosira fasciculata

110 Thalassiosira gracilis
111 Thalassiosira insigna
112 Thalassiosira inura
113 Thalassiosira jacksonii
114 Thalassiosira kolbei
115 Thalassiosira lentiginosa
116 Thalassiosira lentiginosa obovatus
117 Thalassiosira lineata
118 Thalassiosira miocenica
119 Thalassiosira nativa
120 Thalassiosira oestrupii
121 Thalassiosira oliverana
122 Thalassiosira oliverana sparsa
123 Thalassiosira praeconvexa
124 Thalassiosira praefraga
125 Thalassiosira striata
126 Thalassiosira symbolophora
127 Thalassiosira tetraoestrupii reimeri
128 Thalassiosira torokina
129 Thalassiosira tumida
130 Thalassiosira vulnifica
131 Thalassiosira webbi
132 Thalassiothrix miocenica
133 Trinacria excavata

3-C Mergings of the UAs in the 92 UA sequence into 20 UA-zones

Zone 1: 1–2; Zone 2: 3–5; Zone 3: 6–8; Zone 4: 9–12; Zone 5: 13–16; Zone 6: 17–22; Zone 7: 23–29; Zone 8: 30–38; Zone 9: 39–47; Zone 10: 48–54; Zone 11: 55–60; Zone 12: 61–64; Zone 13: 65–69; Zone 14: 70–73; Zone 15 74–79; Zone 16: 80–84; Zone 17: 85–87; Zone 18: 88–88; Zone 19: 89–90; Zone 20: 91–92

3-D Cody et al. (2008) relationships between section codes, levels, sites and depth

Section 1 CIROS;25 0.55;24 0.28;23 7.07;22 98.86;21 99.4;20 101.3;19 101.83;18 105.33;17 116.69;16 118.19;15 118.31;14 125;13 125.01;12 134.63;11 134.93;10 136.55;9 137.69;8 138.07;7 139.02;6 151.26;5 151.56;4 152.14;3 159.55;2 165.52;1 165.8;;Section 2 DVDP 10;16 65.65;15 137.16;14 138.2;13 148.9;12 149.53;11 150.18;10 152.1;9 158;8 158.58;7 162.35;6 162.69;5 167.1;4 167.18;3 182.61;2 182.88;1 183.41;;Section 3 DVDP11;16 1.1;15 1.33;14 19.54;13 199.3;12 199.32;11 203.07;10 208.48;9 210.4;8 218.84;7 239.73;6 240.61;5 244.6;4 247.81;3 291.1;2 291.8;1 292.27;;Section 4 DSDP 269;22 0.92;21 1.45;20 3.32;19 3.82;18 6.82;17 7.72;16 8.72;15 47.25;14 48.32;13 48.82;12 49.22;11 49.69;10 93.52;9 94.12;8 95.42;7 97.52;6 98.22;5 99.02;4 201.4;3 331.9;2 338.3;1 340.5;;Section 5 DSDP 513;39 1.23;38 7.95;37 28.45;36 30.4;35 31.9;34 36.4;33 43.52;32 48.52;31 49.23;30 50.02;29 53.02;28 54.52;27 56.5;26 56.9;25 66.05;24 79.16;23 80.66;22 85;21 85.38;20 98.2;19 105.4;18

111.4;17 113.33;16 113.54;16 113.54;15 120.2;14 125.07;13 128.2;12 131.8;11 133.9;10 136.2;10 136.2;9 139.9;7 142.68;6 151.63;5 155.2;4 160.62;3 161.34;2 163.7;1 170.09;;Section 6 DSDP 514;28 0.47;27 7.82;26 8.28;25 9.09;24 18.64;23 19.57;22 20.92;21 22.57;20 34.2;19 35.63;18 41.8;17 46.96;16 62.1;15 77.02;14 78.22;13 88.84;12 95.64;11 96.65;10 98.9;9 103.16;8 103.35;7 110.34;6 112.04;5 114.54;4 125.3;3 133.97;2 145.74;1 150.13;;Section 7 ODP 689b;76 0.28;75 0.56;74 1.78;73 2;72 2.64;71 3.28;70 4.14;69 4.41;68 4.78;67 8.58;66 8.79;65 9.44;64 9.63;63 10.36;62 11.57;61 13.09;60 13.94;59 15.08;58 15.17;57 15.36;56 15.94;55 16.59;54 16.92;53 17.44;52 18.38;51 18.98;50 19.28;49 19.86;48 20.17;47 20.24;46 21.08;45 21.6;44 21.94;43 22.15;42 22.58;41 22.85;40 26.93;39 28.13;38 29.39;37 31.78;36 32.08;35 36.16;34 37.94;33 39.44;32 40.94;31 42.44;30 43.58;29 45.08;28 45.93;27 45.94;26 46.58;25 47.18;24 48.08;23 50.44;22 50.91;21 52.58;20 53.18;19 55.05;18 55.55;17 56.18;16 56.53;15 57.05;14 57.4;13 57.68;12 58.26;11 58.55;10 59.18;9 59.45;8 61.55;7 61.76;6 62.18;5 65.14;4 66.36;3 66.94;2 67.86;1 70.28;;Section 8 ODP 690b;64 0.73;63 1.82;62 2.38;61 3.14;60 3.38;59 4.74;58 4.83;57 6.71;56 6.88;55 7.74;54 8.38;53 9.24;52 10.74;51 11.38;50 11.97;49 12.85;48 13.47;47 14.35;46 14.97;45 15.43;44 16.47;43 16.97;42 17.35;41 18.32;40 18.43;39 18.85;38 19.47;37 20.35;36 20.97;35 21.07;34 22.76;33 24.05;32 24.66;31 26.17;30 28.55;29 30.05;28 31.72;27 32.26;26 32.45;25 32.88;24 33.47;23 33.95;22 34.38;21 35.25;20 35.88;19 36.35;18 37.38;17 37.97;16 38.9;15 40.4;14 41.07;13 41.94;12 42.57;11 43.44;10 44.07;9 45.57;8 46.44;7 47.07;6 47.94;5 49.44;4 50.07;3 50.68;2 56.68;1 59.68;;Section 9 ODP 693;26 2.5;25 31;24 39.1;23 39.94;22 47.3;21 48.8;20 51;19 52.5;18 68.09;17 70.3;16 79.9;15 84.4;14 87.4;13 138.97;12 150.85;11 197.2;10 200.15;9 230.55;8 241.37;7 245.6;6 256.81;5 258.3;4 259.35;3 263.1;2 266.1;1 270.5;;Section 10 ODP 695a;59 0.3;58 1;57 1.82;56 3.33;55 4.12;54 4.84;53 4.9;52 5.68;51 6.05;50 10.8;49 12.9;48 15.08;47 19.62;46 24.02;45 26.17;44 27.02;43 41.67;42 46.41;41 47.2;40 47.89;39 61.8;38 66.07;37 82.5;36 88.8;35 90.41;34 93.41;33 96.92;32 101.51;31 102.5;30 103.65;29 128.36;28 140.93;27 152.77;26 156.63;25 158.17;24 159.49;23 178.52;22 179;21 192.48;20 197.48;19 198.4;18 200.37;17 204.52;16 236.14;15 244.4;14 252.8;13 262.35;12 266.74;11 274.15;10 283.62;9 286.05;8 309.79;7 322.08;6 324.67;5 325.37;4 334.61;3 335.65;2 336.32;1 337.92;;Section 11 ODP 696;30 2.05;29 12.5;28 12.74;27 22.4;26 22.75;25 46.5;24 60;23 64.7;22 69.6;21 75.3;20 77.5;19 95.9;18 146.4;17 213.19;16 213.9;14 221.8;13 235.7;12 272.4;11 281;10 293.92;9 301.35;8 338.02;7 474.4;6 482.35;5 482.7;4 493.02;3 504.55;2 512.15;1 522.15;;Section 12 ODP 699a;24 0.4;23 9.7;22 11.2;21 20.27;20 21.7;19 23.68;18 28.84;17 30.98;16 32.48;15 33.97;14 39.01;13 40.51;12 42.01;11 43.51;10 47;9 48.5;8 50;7 51.5;5 51.98;4 56.49;3 62.52;2 66;1 67.5;;Section 13 ODP 701c;13 11.15;12 16.05;11 23;10 23.27;9 35.7;8 45.15;7 46.4;6 51.15;5 59.3;4 63.3;3 72.8;2 82.3;1 116.1;; Section 14 ODP 704;60 2.28;59 16.6;58 17.5;57 65;56 69.5;55 98;54 101;53 122;52 126.5;51 128;50 142.5;49 168.4;48 169.3;47 170.8;46 176.1;45 177.8;44 179;43 179.1;42 180.5;41 181.5;40 182;39 183.5;38 186.65;37 189.7;36 192.8;35 197.81;34 199;33 212.8;32 214.5;31 219;30 220.5;29 224.76;28 225.5;27 230;26 231.05;25 238;24 244.8;23 250.8;22 251.25;21 256.75;20 259.5;19 265;18

266.5;17 275.85;16 292;15 295;14 298;13 300;12 306;11 322;10 328.5;9 358.5;8 363;7 387;6 393;4 397.99;3 425;2 426.5;1 428;;Section 15 ODP 736;31 2.2;30 11.2;29 28.8;28 43.8;27 47.8;26 53;25 56.8;24 75.57;23 107.9;22 148.47;21 152.97;20 157.97;19 165.48;18 165.9;17 185.18;16 186.6;15 194.5;14 207.58;13 217.08;12 226.3;11 242;10 245.4;9 267.5;8 290.58;7 295.78;6 334.48;5 338.98;4 344.08;3 347.08;2 352.08;1 364.87;;Section 16 ODP 737a;38 0.57;37 2.57;36 5;35 11.57;34 16.57;33 26.07;32 35.57;31 40.07;30 43.57;29 49.57;28 54.57;27 55.41;26 62;25 65.57;24 70.07;23 78.07;22 81;21 86.07;20 87.57;19 90.5;18 92.22;17 92.57;16 97.07;15 111.57;14 119;13 154.07;12 157;11 159.07;10 165.5;9 167.07;8 195.6;7 207.37;6 234.97;5 244.1;4 244.67;3 247.67;2 254.37;1 263.5;; Section 17 ODP 744b;35 0.08;34 9.4;33 11.5;32 18.6;31 19;30 20.83;29 22.2;28 23.24;27 23.37;26 23.9;25 24.77;24 25.09;23 26.59;22 26.6;21 29.6;20 31.6;19 34.6;18 36.69;17 36.7;16 39.1;15 40.4;14 49.9;13 50;12 52.1;11 53.7;10 55.2;9 56.7;8 60.1;7 63;6 64.6;5 67.6;4 69;3 69.58;2 74.08;1 78.5;;Section 18 ODP 745b;74 4.9;73 14.5;72 19.9;70 42.48;68 50.25;67 52.2;65 54.64;64 80.9;63 90.5;61 91.55;59 93.55;58 94.1;57 97.1;56 100.6;55 102.1;54 105.1;53 108.1;52 110.91;50 112.54;49 114.6;48 119;47 119.6;46 121.14;44 123.54;43 124.14;41 125.54;39 126.54;37 128.54;36 130.6;34 133.04;33 135.1;32 141.1;30 142.72;29 144.1;27 146.26;25 149.42;23 155.91;22 158.6;20 160.81;18 167.89;17 168.1;15 177.94;14 179.1;12 180.73;10 186.36;9 190.1;8 194.6;6 196.71;5 204.1;3 205.64;2 207.6;1 213.6;;Section 19 ODP 746a;30 165.4;29 166.9;28 168.4;27 169.9;26 171.4;25 172.9;24 174.3;23 174.9;22 177.9;21 179.4;20 187.45;19 193.3;18 203.4;17 204.9;16 206.4;15 215.75;14 217.5;13 218.4;12 219.9;11 227.9;10 229.4;9 235.4;8 238.4;7 242.8;6 245.8;5 248.8;4 251.8;3 262.06;2 271.7;1 280.8;; Section 20 ODP 747a;81 0.47;80 3.47;79 4.97;78 7.97;77 9;76 10.97;75 12.47;74 15.47;73 16.97;72 18.5;71 18.97;70 20.47;69 21.29;68 21.3;67 21.97;66 23.47;65 24.97;64 26.1;63 26.47;62 26.9;61 28;60 28.47;59 29.98;58 31.49;57 34.48;56 35.98;54 37.47;53 42.29;52 42.3;51 42.72;50 43.19;49 43.2;48 45.47;47 45.49;46 45.5;45 46.69;44 46.7;43 47.47;42 51.97;40 53.47;39 61.47;38 62.19;37 62.2;36 62.49;35 62.5;34 62.97;33 65.1;32 65.9;31 65.97;30 66;29 66.47;28 67.1;27 67.9;26 67.97;25 68.89;24 68.9;23 69.47;22 70.1;21 70.9;20 72;19 72.01;18 72.47;17 72.79;16 72.8;15 75.5;14 79.06;13 80.74;12 80.75;11 82.06;10 85;9 86.97;8 91.47;7 94.47;6 103.97;5 110.47;4 113.97;3 119.97;2 139.97;1 161;; Section 21 ODP 748b;59 0.1;58 0.2;57 0.57;56 1.1;55 1.27;54 1.5;53 1.67;52 2.8;51 3;50 3.13;49 3.25;48 3.3;47 3.57;46 4.1;45 4.5;44 5.4;43 6.3;42 6.9;41 6.95;40 7.5;39 8;38 8.4;37 8.8;36 9.6;35 9.63;34 9.85;33 9.94;32 10.03;31 10.07;30 10.28;29 11.57;28 13.07;27 14;26 14.57;25 16;24 17.25;23 17.57;22 19.57;21 21.07;20 22.57;19 24.07;18 25.1;17 25.9;16 27.2;15 33.57;14 35.07;13 38.1;12 38.57;11 40.07;10 41.57;9 44.57;8 46.07;7 47.6;6 57.1;5 59.07;4 65.07;3 89.07;2 103.07;1 113.26;;Section 22 ODP 751a;60 0.1;59 1.05;58 1.47;57 3.3;56 3.51;55 5.71;54 6.3;53 7.25;52 7.52;51 7.8;50 8.75;49 9.3;48 14.67;47 15.25;46 19.75;45 21.8;44 23.71;43 26.25;42 27.75;41 28.3;40 29.24;39 29.25;38 29.8;37 31.3;36 33.2;35 33.3;34 34.8;33 35.75;32 36.3;31 37.25;30 38.75;29 39.3;28 43.75;27 48.25;26 49.75;25 53.25;24 54.75;23 68.75;22 76.75;21 94.25;20 97.25;19 100.75;18 102.25;17 103.75;16 105.25;15 109.25;14 110.25;13

111.75;12 114.75;11 116.25;10 118.75;9 122.75;8 128.2;7 129.25;6 130.75;5 137.7;4 138.75;3 147.2;2 149.75;1 166.2;;Section 23 ODO 1088;39 34.75;38 35.11;37 35.5;36 35.85;35 36.87;34 38.97;33 41.86;32 81.9;31 82.8;30 83.7;29 85.5;28 86.4;27 87.3;26 88.2;25 89;24 89.9;23 90.77;22 91.31;21 92.96;20 104.24;19 104.9;18 105.8;17 106.7;16 109.4;15 133.64;14 133.89;13 135.14;12 137.03;11 138.14;10 141.69;9 142.44;8 144.69;7 179.19;6 179.92;5 181.42;4 191.29;3 193.14;2 193.89;1 205;;Section 24 ODP 1089;39 0.5;38 27.98;37 67.51;36 85.91;35 87.41;34 96.95;33 96.96;32 116.3;31 121.9;30 151.6;29 152.22;28 162.24;27 163.3;26 194.03;25 195.53;24 202.6;23 207.1;22 224.3;21 230.12;20 230.7;19 231.95;18 233.45;17 236.45;16 240.8;15 242.55;14 244.05;13 245.55;12 254.71;11 259.61;10 261.11;9 262.61;8 264.11;7 265.35;6 267.07;5 268.57;4 271.57;3 274.88;2 277.88;1 279.38;;Section 25 ODP 1090;41 0.91;40 6.3;39 13.5;38 16.2;37 24.89;36 26.1;35 27;34 30.73;33 31.31;32 32.53;31 35.23;30 38.83;29 39.73;28 43.33;27 43.7;26 44.68;25 45.13;24 45.95;23 46.95;22 47.4;21 49.8;20 52.91;19 54.71;18 54.72;17 55.61;16 56.06;15 56.51;14 57.41;13 59.21;12 61.01;11 61.91;10 62.36;9 62.81;8 63.71;7 65.96;6 66.41;5 67.31;4 67.76;3 68.31;2 69.25;1 69.7;;Section 26 ODP 1091;49 0.79;48 16.81;47 42.24;46 48.7;45 73.32;44 98.88;43 102.6;42 102.69;41 119.47;40 130;39 134.04;38 145.8;37 147.77;36 148.95;35 165.14;34 187.56;33 207.22;32 217.57;31 222.07;30 257.5;29 270.5;28 270.59;27 271.68;26 277.9;25 279.4;24 288.64;23 291.64;22 294.64;21 295.64;20 296.9;19 298.4;18 299.9;17 304.4;16 306.4;15 307.9;14 309.4;13 310.9;12 311;11 312.4;10 312.97;9 315.9;8 321.9;7 325.4;6 326.9;5 329.8;4 329.9;3 331.4;2 332.9;1 333.56;;Section 27 ODP 1092;101 1.15;100 2.27;99 3.34;98 7.84;97 9.34;96 12.41;95 13.91;94 19.41;93 19.73;92 23.02;91 24.52;90 27.52;89 34.16;88 35.66;87 37.16;86 38.66;85 40.16;84 41.56;83 44.66;82 46.16;81 47.66;80 48.37;79 49.16;78 49.87;77 50.66;76 51.29;75 51.52;74 54.68;73 56.18;72 57.68;71 58.18;70 59.16;69 59.18;68 60.68;67 62.12;66 62.18;65 62.72;64 64.19;63 64.98;62 65.01;61 65.32;60 65.39;59 66.48;58 67.96;57 68.01;56 68.31;55 68.61;54 68.91;53 69.48;52 69.81;51 70.19;50 70.41;49 73.71;48 74.31;47 74.91;46 75.24;45 77.81;44 78.06;43 78.71;42 78.73;41 79.74;40 80.51;39 81.6;38 81.71;37 82.01;36 82.91;35 85.6;34 85.61;33 86.49;32 87.1;31 87.11;30 87.62;29 89.12;28 95;27 95.2;26 95.8;25 107.23;24 110.43;23 130.51;22 132.23;21 135.01;20 137.23;19 139.1;18 142.57;17 145.23;16 152.03;15 152.99;14 159.89;13 170.88;12 174.01;11 174.51;10 177.83;9 184.83;8 192.38;7 192.63;6 193.38;5 194.88;4 203.04;3 206.04;2 209.04;1 209.63;;Section 28 ODP 1093;49 0.79;48 35.27;47 48.65;46 76.82;45 79.82;44 123.27;43 126.96;42 176.9;41 195.2;40 198.6;39 216.16;38 232.7;37 253.56;36 296.31;35 314.35;34 344.92;33 355.38;32 355.67;31 394.11;30 398.61;29 423.92;28 451.41;27 461.01;26 462.51;25 478.71;24 480.01;23 486.01;22 491.11;21 492.61;20 492.62;19 497.11;18 500.71;17 502.21;16 503.71;15 506.18;14 508;13 511.71;12 514.71;11 521.51;10 528.01;9 557.23;8 558.29;7 566.61;6 569.61;5 571.11;4 575.8;3 577.7;2 578.43;1 585.32;; Section 29 ODP 1094;28 0.79;27 26.3;26 33.58;25 47.85;24 52.35;23 62.49;22 81.69;21 98.49;20 98.5;19 101.97;18 113.83;17 118.97;16 122.49;15 122.5;14 125.93;13 128.49;12 128.5;11 142.21;10 145.21;9 148.61;8 153.11;7 157.78;6

158.49;5 162.49;4 166.49;3 167.28;2 168.78;1 169.33;;Section 30 ODP 1101a;20 0.8;19 8.32;18 20.8;17 23.04;16 27.67;15 48.45;14 57.41;13 76.01;12 84.94;11 125.32;10 159.9;9 163.8;8 173.4;7 177.56;6 187;5 188.8;4 195.49;3 198.3;2 207.9;1 217.7;;Section 31 ODP 1138a;62 0.7;61 4.7;60 8.53;59 25.57;58 40;57 44.5;56 45.58;55 49.4;54 55.8;53 58.05;52 61.8;51 62.31;50 65.3;49 66.8;48 68.3;47 68.8;46 69.8;45 71.3;44 74.04;43 74.7;42 76.2;41 77.7;40 79.21;39 83.35;38 87.1;37 93.7;36 95.2;35 96.7;34 102.39;33 103.3;32 104.8;31 106.3;30 107.03;29 112.23;28 113;27 116;26 117.5;25 118.59;24 122.12;23 123.6;22 125.1;21 134.23;20 145.85;19 152.5;18 158.27;17 160.6;16 162.1;15 168.84;14 170.2;13 171.7;12 174.75;11 181.3;10 184.3;9 186.14;8 191.26;7 201.6;6 210.85;5 230.02;4 239.85;3 248.71;2 261.81;1 269.41;;Section 32 ODP 1165b;38 1.7;37 4.7;36 6.81;35 8.5;34 9.25;33 16.48;32 17.25;31 17.47;30 17.86;29 18;28 18.17;27 18.47;26 24.75;25 25.01;24 26;23 27.05;22 28.55;21 32.75;20 34.25;19 34.55;18 35;17 35.75;16 38.07;15 39.25;14 40.75;13 40.87;12 41.77;11 41.9;10 43;9 43.75;8 44.85;7 47.25;6 49.57;5 49.89;4 50.25;3 52.5;2 54;1 54.39

3-E Cody et al. (2008): destroyed edges and reversed ARCS; comparison with RASC

3-E-1 CONOP's total range solution: 18 destroyed edges (not justified)

41 1; 65 58; 88 13; 108 41; 111 110; 122 108; 76 115; 8 112; 40 31; 40 38; 83 10; 124 37; 124 81; 124 38; 124 84; 103 128; 61 110; 62 111

3-E-2 CONOP's average range solution 669 destroyed edges

13 1; 13 5; 13 11; 26 13; 41 1; 41 13; 41 26; 46 1; 46 11; 46 26; 47 41; 50 13; 50 41; 54 1; 54 5; 54 11; 56 13; 56 41; 56 46; 58 11; 58 54; 58 56; 63 5; 63 10; 63 11; 63 13; 63 41; 63 46; 63 54; 63 56; 64 1; 64 5; 64 11; 64 26; 64 50; 64 56; 64 63; 65 1; 65 11; 65 41; 65 58; 65 63; 68 10; 68 54; 69 13; 69 41; 69 46; 69 54; 69 64; 69 65; 71 10; 71 54; 88 11; 88 13; 88 56; 88 65; 89 68; 89 71; 93 41; 93 68; 93 71; 96 41; 96 63; 96 88; 100 58; 100 63; 100 68; 100 71; 100 88; 102 1; 102 58; 102 63; 102 69; 102 88; 104 1; 104 5; 104 11; 104 41; 104 63; 104 69; 104 88; 108 5; 108 10; 108 11; 108 41; 108 46; 108 54; 108 56; 108 64; 108 65; 108 96; 108 100; 108 102; 108 104; 109 41; 110 5; 110 10; 110 54; 110 56; 110 100; 112 41; 112 58; 112 63; 112 71; 112 88; 112 108; 114 13; 114 41; 114 46; 114 63; 114 64; 114 110; 115 46; 115 64; 120 41; 125 1; 125 5; 125 11; 125 41; 125 58; 125 63; 125 69; 125 88; 125 108; 125 110; 128 58; 128 63; 128 108; 129 41; 130 13; 130 41; 130 63; 130 64; 130 65; 130 104; 130 108; 131 13; 131 41; 131 46; 131 63; 131 64; 131 65; 131 104; 131 108; 111 46; 111 58; 111 63; 111 65; 111 88; 111 104; 111 108; 111 110; 113 5; 113 26; 113 41; 113 50; 113 63; 113 69; 113 88; 113 108; 113 130; 113 131; 113 111; 37 10; 37 102; 43 37; 75 37; 94 47; 94 56; 94 114; 94 130; 94 111; 94 37; 101 56; 101 93; 101 96; 122 26; 122 47; 122 56; 122 65; 122 93; 122 96; 122 104; 122 108; 122 112; 122 114; 122 115; 122 129; 122 130; 122 113; 18 120; 18 121; 18 128; 18 37; 18 101; 32 10; 32 46; 32 54; 32 64; 32 100; 32 102; 32 121; 32 128; 32 37; 32 75;

32 94; 32 101; 32 122; 32 18; 52 65; 52 120; 52 113; 52 37; 57 46; 57 54; 57 100; 57 121; 57 128; 57 113; 57 37; 57 94; 57 101; 57 122; 67 1; 67 11; 67 58; 67 63; 67 68; 67 69; 67 71; 67 108; 67 110; 67 32; 67 57; 73 46; 73 58; 73 63; 73 88; 73 108; 73 113; 73 94; 73 122; 74 37; 76 56; 76 65; 76 104; 76 112; 76 115; 76 120; 76 129; 76 113; 76 32; 76 57; 77 120; 77 113; 77 18; 77 32; 77 57; 78 100; 78 121; 78 128; 78 37; 78 122; 78 32; 78 76; 81 121; 85 113; 85 57; 85 78; 116 65; 116 104; 116 108; 116 113; 116 122; 119 47; 119 56; 119 58; 119 65; 119 108; 119 112; 119 114; 119 115; 119 130; 119 37; 119 32; 119 73; 119 116; 123 18; 123 57; 123 78; 16 46; 16 54; 16 64; 16 65; 16 96; 16 104; 16 112; 16 125; 16 131; 16 113; 16 67; 7 100; 7 102; 7 101; 7 32; 7 52; 7 57; 8 65; 8 112; 8 120; 8 113; 8 32; 8 57; 15 89; 15 100; 15 102; 15 101; 15 7; 19 10; 19 64; 19 100; 19 102; 19 101; 19 18; 19 52; 19 57; 19 8; 24 41; 24 89; 24 100; 24 102; 24 101; 25 89; 25 100; 25 101; 28 6; 28 89; 28 100; 28 102; 28 81; 29 6; 29 89; 29 100; 29 102; 29 37; 29 101; 30 100; 30 101; 30 32; 30 52; 30 57; 30 15; 30 29; 31 100; 31 128; 31 101; 31 32; 31 19; 38 41; 38 89; 38 100; 38 102; 38 101; 38 57; 38 28; 39 46; 39 54; 39 64; 39 100; 39 121; 39 128; 39 94; 39 101; 39 122; 39 8; 39 19; 39 30; 40 10; 40 64; 40 100; 40 102; 40 37; 40 43; 40 101; 40 52; 40 57; 40 31; 40 38; 40 39; 45 26; 45 50; 45 56; 45 108; 45 109; 45 114; 45 115; 45 129; 45 32; 45 57; 45 19; 45 39; 48 10; 48 46; 48 54; 48 64; 48 100; 48 102; 48 37; 48 101; 48 18; 48 31; 48 45; 49 1; 49 5; 49 11; 49 26; 49 47; 49 50; 49 56; 49 69; 49 93; 49 108; 49 109; 49 114; 49 115; 49 125; 49 129; 49 130; 49 131; 49 111; 49 37; 49 18; 49 32; 49 57; 49 73; 49 116; 49 16; 49 31; 49 39; 49 48; 59 26; 59 41; 59 50; 59 56; 59 63; 59 69; 59 108; 59 114; 59 115; 59 122; 59 73; 59 76; 59 16; 59 8; 60 6; 60 89; 60 100; 60 102; 60 37; 60 101; 60 30; 66 10; 66 41; 66 46; 66 64; 66 89; 66 100; 66 121; 66 128; 66 113; 66 75; 66 94; 66 101; 66 122; 66 18; 66 32; 66 52; 66 57; 66 67; 66 76; 66 77; 66 78; 66 85; 66 7; 66 8; 66 30; 66 31; 66 39; 66 40; 66 45; 83 10; 83 64; 83 100; 83 102; 83 101; 83 52; 83 57; 83 24; 83 38; 83 39; 83 66; 84 100; 84 102; 84 101; 84 32; 84 52; 84 57; 84 28; 84 29; 84 39; 84 40; 84 60; 90 6; 90 89; 90 100; 90 102; 90 37; 90 101; 90 30; 90 84; 91 41; 91 114; 91 76; 97 1; 97 11; 97 41; 97 63; 97 69; 97 130; 97 111; 97 122; 97 76; 97 85; 97 119; 97 16; 97 8; 118 113; 118 18; 118 32; 118 57; 118 78; 118 31; 118 39; 118 66; 118 97; 124 89; 124 100; 124 102; 124 37; 124 101; 124 81; 124 15; 124 30; 124 38; 124 84; 21 122; 14 130; 132 56; 132 115; 132 125; 132 37; 132 32; 132 21; 3 120; 3 121; 3 37; 87 47; 87 112; 105 123; 105 16; 107 18; 107 32; 34 10; 34 64; 34 75; 34 94; 34 18; 34 78; 34 119; 34 31; 34 40; 34 83; 36 24; 36 38; 17 5; 17 10; 17 11; 17 56; 17 89; 17 96; 17 100; 17 112; 17 114; 17 128; 17 130; 17 131; 17 111; 17 113; 17 73; 17 116; 17 49; 82 102; 82 28; 82 30; 80 11; 80 26; 80 41; 80 69; 80 111; 80 73; 80 16; 80 132; 103 108; 103 128; 4 11; 4 54; 4 56; 4 104; 4 112; 4 125; 4 111; 4 67; 4 73; 4 105; 4 80; 23 49; 61 11; 61 54; 61 56; 61 63; 61 110; 61 112; 61 125; 61 111; 61 67; 61 73; 61 105; 62 54; 62 56; 62 100; 62 108; 62 110; 62 125; 62 111; 62 67; 127 11; 127 54; 127 56; 127 96; 127 112; 127 125; 127 111; 127 67; 127 73; 127 87; 127 105; 95 4; 44 68; 44 71; 44 49; 44 87; 44 17; 99 10; 99 11; 99 100; 99 128; 99 130; 99 97; 99 62

REVERSED ARCS 2: 34 66; 36 66

3-E-3 RASC applied to Cody's database: destroyed edges 667

To do the present test we used the RASC program available online in the PAST package of O.Hammer. That version of RASC is a direct port of Agterberg's original RASC code.

13 1; 13 5; 13 11; 26 13; 41 1; 41 13; 41 26; 46 1; 46 11; 46 26; 47 41; 50 13; 50 41; 54 1; 54 5; 54 11; 56 13; 56 41; 56 46; 58 10; 58 11; 58 54; 58 56; 63 10; 63 11; 63 13; 63 41; 63 46; 63 54; 63 56; 64 1; 64 5; 64 11; 64 26; 64 50; 64 56; 64 63; 65 1; 65 11; 65 26; 65 58; 65 63; 68 10; 68 54; 69 13; 69 41; 69 46; 69 64; 69 65; 71 10; 71 47; 71 54; 88 11; 88 13; 88 65; 89 68; 89 71; 93 41; 93 71; 96 1; 96 41; 96 63; 96 88; 100 58; 100 63; 100 68; 100 71; 102 1; 102 26; 102 58; 102 63; 102 69; 102 88; 104 1; 104 5; 104 11; 104 26; 104 41; 104 63; 104 69; 104 88; 108 10; 108 11; 108 41; 108 46; 108 54; 108 56; 108 64; 108 65; 108 96; 108 100; 108 102; 108 104; 109 13; 109 41; 109 46; 109 64; 110 5; 110 10; 110 54; 110 56; 110 89; 110 100; 112 41; 112 58; 112 63; 112 71; 112 108; 114 13; 114 41; 114 46; 114 64; 114 110; 115 46; 115 64; 125 1; 125 5; 125 11; 125 41; 125 58; 125 63; 125 88; 125 108; 125 110; 128 58; 128 63; 128 88; 128 108; 129 41; 130 13; 130 41; 130 58; 130 64; 130 65; 130 102; 130 104; 130 108; 131 1; 131 5; 131 11; 131 13; 131 41; 131 46; 131 63; 131 64; 131 65; 131 108; 111 46; 111 58; 111 63; 111 65; 111 88; 111 108; 111 110; 113 5; 113 26; 113 41; 113 63; 113 69; 113 88; 113 108; 113 130; 37 10; 37 102; 43 37; 75 37; 94 47; 94 56; 94 96; 94 114; 94 130; 94 111; 94 37; 101 56; 101 93; 101 96; 101 104; 122 26; 122 47; 122 56; 122 93; 122 96; 122 104; 122 108; 122 112; 122 114; 122 115; 122 129; 122 130; 18 46; 18 54; 18 64; 18 100; 18 102; 18 120; 18 121; 18 37; 18 101; 18 122; 32 46; 32 54; 32 64; 32 100; 32 102; 32 121; 32 128; 32 37; 32 43; 32 75; 32 94; 32 101; 32 122; 52 65; 52 120; 52 113; 52 37; 57 113; 57 37; 67 1; 67 11; 67 26; 67 50; 67 58; 67 63; 67 68; 67 69; 67 71; 67 108; 67 110; 67 130; 67 111; 67 18; 67 32; 73 1; 73 46; 73 58; 73 63; 73 88; 73 108; 73 94; 73 122; 74 37; 76 56; 76 65; 76 104; 76 112; 76 115; 76 120; 76 129; 76 113; 76 32; 77 120; 77 113; 77 18; 77 32; 78 64; 78 100; 78 102; 78 121; 78 37; 78 122; 78 76; 85 113; 85 18; 85 78; 116 58; 116 65; 116 88; 116 108; 116 122; 116 67; 119 47; 119 56; 119 58; 119 108; 119 114; 119 115; 119 130; 119 37; 119 32; 119 73; 119 116; 123 18; 123 78; 16 46; 16 54; 16 64; 16 65; 16 96; 16 104; 16 125; 16 131; 16 113; 16 67; 16 73; 7 100; 7 102; 7 101; 7 32; 7 52; 7 57; 8 65; 8 112; 8 120; 8 113; 8 32; 15 100; 15 102; 15 101; 15 7; 19 10; 19 41; 19 64; 19 100; 19 102; 19 101; 19 18; 19 32; 19 52; 19 57; 19 8; 24 41; 24 100; 24 102; 24 101; 24 7; 25 100; 25 101; 28 6; 28 89; 28 100; 28 102; 28 81; 29 100; 29 102; 29 101; 30 100; 30 101; 30 32; 30 52; 30 57; 31 46; 31 54; 31 64; 31 100; 31 102; 31 128; 31 101; 31 122; 31 67; 31 85; 31 19; 38 41; 38 100; 38 102; 38 101; 38 57; 39 46; 39 54; 39 64; 39 100; 39 102; 39 121; 39 128; 39 75; 39 94; 39 101; 39 122; 39 119; 39 8; 39 19; 39 30; 40 10; 40 64; 40 100; 40 102; 40 37; 40 43; 40 101; 40 52; 40 57; 40 19; 40 31; 40 38; 40 39; 45 26; 45 47; 45 50; 45 56; 45 93; 45 108; 45 109; 45 114; 45 115; 45 129; 45 18; 45 32; 45 77; 45 19; 45 31; 45 39; 48 46; 48 54; 48 64; 48 100; 48 102; 48 37;

48 43; 48 101; 48 19; 48 30; 48 45; 49 1; 49 5; 49 11; 49 26; 49 50; 49 69; 49 108; 49 109; 49 130; 49 131; 49 111; 49 37; 49 18; 49 32; 49 73; 49 116; 49 16; 49 31; 49 39; 49 48; 59 26; 59 41; 59 50; 59 63; 59 69; 59 108; 59 109; 59 122; 59 73; 59 76; 59 16; 59 8; 60 6; 60 89; 60 100; 60 102; 60 37; 60 101; 60 81; 60 30; 66 10; 66 46; 66 64; 66 100; 66 121; 66 128; 66 113; 66 75; 66 94; 66 101; 66 122; 66 18; 66 32; 66 52; 66 57; 66 67; 66 76; 66 77; 66 78; 66 85; 66 8; 66 28; 66 31; 66 39; 66 40; 66 45; 66 60; 83 10; 83 64; 83 100; 83 102; 83 101; 83 52; 83 57; 83 19; 83 24; 83 38; 83 39; 84 100; 84 102; 84 101; 84 32; 84 52; 84 57; 84 28; 84 39; 84 40; 84 60; 90 6; 90 89; 90 100; 90 102; 90 37; 90 101; 90 81; 90 30; 90 66; 90 84; 91 41; 91 109; 91 114; 91 76; 97 1; 97 11; 97 26; 97 41; 97 50; 97 63; 97 69; 97 109; 97 130; 97 111; 97 122; 97 73; 97 76; 97 85; 97 16; 97 8; 118 113; 118 32; 118 78; 118 31; 118 39; 118 66; 118 97; 124 89; 124 100; 124 102; 124 37; 124 101; 124 81; 124 15; 124 29; 124 30; 124 38; 124 66; 124 84; 21 122; 14 130; 14 18; 14 116; 132 37; 132 32; 3 120; 3 37; 3 32; 3 39; 87 47; 87 108; 87 109; 87 112; 105 1; 105 11; 105 41; 105 69; 105 122; 105 85; 105 123; 105 16; 105 8; 105 118; 107 41; 107 94; 107 122; 107 18; 107 32; 107 52; 107 76; 107 85; 107 123; 107 8; 107 118; 107 3; 34 10; 34 64; 34 75; 34 94; 34 52; 34 78; 34 119; 34 31; 34 40; 34 83; 36 24; 36 38; 17 5; 17 10; 17 11; 17 56; 17 96; 17 100; 17 112; 17 114; 17 128; 17 130; 17 131; 17 111; 17 113; 17 73; 17 116; 17 49; 82 102; 82 60; 80 11; 80 26; 80 41; 80 69; 80 109; 80 111; 80 73; 80 16; 103 108; 103 128; 4 104; 4 67; 4 105; 4 80; 61 10; 61 11; 61 54; 61 56; 61 100; 61 110; 61 112; 61 125; 61 128; 61 111; 61 67; 61 73; 61 105; 62 54; 62 108; 62 110; 62 125; 62 111; 62 67; 62 116; 127 54; 127 71; 127 96; 127 125; 127 67; 127 73; 127 87; 127 105; 95 4; 44 71; 44 49; 44 97; 44 87; 99 10; 99 11; 99 100; 99 128; 99 97; REVERSED ARC 34 66;

3-F UA range chart of the 14 zones extracted from the original Cody's zonation

Datum. Section UArange_14, bottom 1 top 14. 1: 9–14; 5: 10–11; 6: 2–14; 10: 4–12; 11: 10–11; 13: 8–10; 12: 1–14; 22: 1–14; 26: 9–14; 41: 3–9; 46: 5–10; 47: 8–12; 50: 9–14; 54: 6–14; 56: 8–11; 58: 11–14; 63: 9–14; 64: 4–10; 65: 8–11; 68: 12–14; 69: 9–14; 71: 12–14; 88: 10–14; 89: 1–12; 93: 8–12; 96: 8–10; 100: 1–12; 102: 1–11; 104: 8–10; 108: 9–14; 109: 8–14; 110: 11–14; 112: 8–12; 114: 8–11; 115: 9–14; 120: 7–14; 121: 5–14; 125: 8–11; 128: 6–12; 129: 8–14; 130: 9–11; 131: 9–10; 111: 9–11; 113: 7–10; 117: 8–14; 37: 1–5; 43: 4–14; 75: 5–14; 94: 5–10; 101: 1–8; 122: 7–9; 18: 5–7; 32: 4–7; 52: 4–8; 57: 3–7; 67: 7–14; 73: 9–11; 74: 5–14; 76: 6–9; 77: 6–7; 78: 5–7; 81: 1–7; 85: 7–7; 116: 9–11; 119: 5–12; 123: 7–7; 16: 9–14; 7: 3–4; 8: 6–8; 15: 1–3; 19: 1–6; 24: 1–3; 25: 1–2; 28: 1–2; 29: 1–2; 30: 1–4; 31: 4–7; 38: 1–3; 39: 4–7; 40: 3–4; 45: 6–9; 48: 4–6; 49: 5–10; 59: 8–9; 60: 1–2; 66: 1–7; 83: 3–4; 84: 1–4; 90: 1–2; 91: 8–8; 97: 7–10; 118: 7–7; 124: 1–1; 21: 8–14; 14: 7–10; 132: 4–9; 3: 5–7; 87: 12–14; 105: 7–10; 107: 6–14; 34: 4–5; 36: 3–3; 17: 10–14; 82: 2–2; 80: 8–10; 103: 12–14; 4: 10–13; 23: 8–14; 61: 10–11; 62: 11–11; 127: 10–12; 95: 13–14; 44: 9–12; 79: 14–14; 99: 10–14

3-G Codes of taxa and paleomagnetic events used in Table 6.1 and Fig. 6.10

The sign "+" indicates the primary zonal markers of Cody (loc.cit. tbl.3).
F Actinocyclus actinochilus 1
F Actinocyclus fasciculatus 5 (+)
F Actinocyclus maccollumii 11 (+)
L Actinocyclus octonarius asteriscus 13 (+)
F Actinocyclus Zielinski Gersonde 2003 4 (+)
F Asteromphalus hookeri 16 (+)
L Denticulopsis simonsenii 41
L Fragilariopsis arcula 45 (+)
L Fragilariopsis aurica 46
L Fragilariopsis lacrima 59 (+)
F Fragilariopsis matuyamae 61 (+)
F Fragilariopsis obliquecostata 63
L Fragilariopsis praecurta 64
F Fragilariopsis ritscheri 69
F Fragilariopsis weaveri 73 (+)
L Navicula wisei 80 (+)
F Thalassiosira elliptipora 108
F Thalassiosira insigna 111 (+)
F Thalassiosira lentiginosa obovatus* 116 (+)
L Thalassiosira oliverana sparsa 122
F Thalassiosira tetraoestrupii reimeri 127 (+)
F Thalassiosira vulnifica 130 (+)
F Thalassiosira webbi 131
C2An.1n base
C2An.1n top
C2An.2n base
C2An.2n top
C2An.3n base
C2An.3n top

3-H Codes of the first 23 FO of Cody's original range chart

Actinocyclus ingens 6; Actinocyclus octonarius 12; Araniscus lewisianus* 15; Asteromphalus oligocenicus 19; Azpeitia tabularis 22; Cavitatus miocenicus* 25; Cavitatus jouseanus 24; Coscinodiscus rhombicus 28; Crucidenticula nicobarica 30; Crucidenticula kanayae 29; Denticulopsis lauta 37; Denticulopsis maccollumii 38; Fragilariopsis maleinterpretaria* 60; Fragilariopsis pusilla* 66; Neobrunia mirabilis 81; Nitzschia 17; Schrader 82; Nitzschia grossepunctata 84; Proboscia barboi* 89; Raphidodiscus marylandicus 90; Rouxia naviculoides 100; Rouxia peragalli 101; Stephanopyxis turris 102; Thalassiosira praefraga 124

Appendix 4
Carter et al. (2010); Gorican et al. (2013) Evolutionary Rates of Jurassic Radiolaria

4-A Numerical database

DATUM; TITLE "QCI, Baja, Hori08num,1662,Luis, Alaridh, Mangart, Matsuoka, Yao97, Pujana"; SECTION QCI bottom 1 top 23; AALEN 21 21; PAR21 11 21; HAG03 1 21; PAR16 7 21; 2005 17 23; 3411 18 23; HSU07 10 21; PVG01 17 23; PVG03 17 23; 3502 19 23; HIG03 21 23; 3149 19 23; 3408 2 21; 3409 19 23; 3247 18 23; 3407 21 22; HSU05 7 21; HSU11 17 21; NAP08 14 21; 3410 21 23; PRU01 17 21; 2007 14 22; 2001 7 22; PHS08 15 21; UTOAR 19 20; BIS02 18 23; TCA01 6 20; PHS03 6 20; BER01 19 20; BIS03 16 23; HSU04 20 20; CRU11 3 19; TRL01 7 23; HOM02 17 19; MUTOA 18 18; MTOAR 17 17; CAN12 3 17; PSP03 17 17; WNG03 3 17; PCA02 13 17; CAN14 2 16; ZRT01 4 23; REG01 2 16; LTOAR 16 16; CTS06 3 16; PRY01 12 16; BIS01 14 16; PPN01 6 16; KAT07 2 16; KAT09 14 16; PLE01 12 16; PRL01 3 16; XTL01 13 16; PHS04 3 16; CTS10 3 16; NAP04 16 16; LAN01 2 16; LAN02 8 16; 2013 9 23; PSP01 6 16; CAN13 2 16; EUC06 13 16; EUC03 16 16; MCP01 16 16; THU04 1 16; PAR15 3 15; KAT10 10 14; GOR03 6 14; BRO03 7 14; 2012 3 23; NAP02 3 14; NTS01 3 14; CARLO 14 14; ADM01 7 14; BPD14 3 14; CRU13 6 14; CRU20 3 14; CTS09 3 14; CTS12 2 14; CTS15 2 14; CTS16 3 14; JAC02 1 14; KAT14 2 15; LAN05 2 14; PAN19 6 14; PAN18 2 14; PAR13 2 14; PRY04 10 15; PHS01 1 14; PHS02 3 14; PHS09 5 14; XNM01 3 14; KUNAE 13 13; BAG05 2 13; CHA10 2 13; CYC04 3 13; HSU06 6 13; KAT16 2 13; LAN04 2 13; PRY05 3 13; SAT07 1 13; CAN08 1 13; ARS04 3 13; CHA09 2 13; HOM01 7 13; HCK05 2 13; KAT17 1 13; PAN11 1 13; PRY07 2 13; SPI03 1 13; freb 8 12; CAN09 1 12; JAC01 1 10; PRY06 1 10; WHITE 6 7; CAN11 1 7; DRO05 1 9; DRO08 2 9; PAN20 6 23; PAR10 1 6; RBS02 3 10; IMLAY 3 5; CRU19 3 5; ORB02 1 5; BPD05 1 4; HAG04 1 4; ORB03 1 10; FRM01 1 3; RECOG 2 2; HAG02 1 2; PHS05 1 2; CTS03 1 2; CHA02 1 2; CHA03 1 2; CHA05 1 2; WNG01 1 2; SINEM 1 1; ARS02 1 1; ATA02 1 1; BPD06 1 1; BPD12 1 1; CHA04 1 1; KAT03 1 1; KAT06 1 1; PAN13 1 1; PAN17 1 1; PAR11 1 1; SAT01 1 1; KAT04 1 1; ARS01 1 1; NAP03 8 8; CYC03 6 6; 2021 22 23; 3010 22 23; 3011 22 23; 3071 22 23; 3089 22 23; 3158 22 23; 3194 22 23; 3195 22 23; 3231 22 23; 3073 22 23; 3074 22 23; 3278 22 23; 4008 22 23; 4061 22 23; 4066 22 23; EUC09 22 23; PVG04 22 23; TVS01 22 23; BIS04 23 23; SAT11 23 23; 3088 23 23; 3159 23 23; SAT18 23 23;

J. Guex et al., *Discrete Biochronological Time Scales*,
DOI 10.1007/978-3-319-21326-2

4053 23 23; SECTION BAJA bottom 1 top 5; ARS06 5 5; THT01 5 5; HAG03 5 5; PAR21 5 5; PRY05 5 5; SAT19 4 5; TCA01 5 5; DRO08 4 5; CAN12 4 5; RBS01 3 5; PHS04 5 5; PHS01 1 5; KAT07 1 5; KAT08 4 5; POD01 2 5; JAC02 5 5; NAP03 4 5; NAP02 5 5; UTD01 5 5; ARS04 5 5; REG01 5 5; PRY01 5 5; HOM01 1 4; PAN19 1 4; PAR16 1 4; CYC01 1 4; CYC02 1 4; DUC01 1 4; KAT10 1 4; SAT01 1 3; CYC03 1 3; CHA07 1 3; CAN09 1 2; BAG06 1 2; ARS02 1 2; RBS02 1 2; HAG04 1 1; ATA02 1 1; FRM01 1 5 {artificial};; SECTION HORI08 bottom 1 top 23; PHS01 2 21; PHS05 2 15; KAT07 1 9; BPD15 1 8; BPD16 1 8; KAT10 1 11; KAT09 1 8; PHS04 3 6; LAN04 3 4; EUC03 7 14; PRY04 9 9; PHS03 9 20; 2013 9 18; ZRT01 12 16; EUC06 10 17; HSU04 13 21; TRL01 10 23; PVG03 16 21; PRY01 16 19; 3502 12 23; 4008 13 19; HSU01 15 22; HSU03 15 21; HSU08 17 19; ELD02 12 22; EUC09 11 23; SAT18 18 19; PVG04 12 22; CHA07 1 2; CHA10 1 1; UTD01 4 10; PLE01 8 8; SAT11 13 19; NAP04 13 22; 2021 13 22; TCA01 13 13; JAC02 14 14; 3089 19 23; 3278 21 22; 4031 21 23; 3195 22 22; 3409 23 23; LAN05 5 5; PAN11 6 6; THU04 7 7; GIG01 3 6; 3408 12 12; HSU11 20 21; PCA02 20 21; PAN19 3 3;; SECTION 1_TURKEY_1662D-; bottom 1 top 1; JAC02 1 1; ARS03 1 1; ARS06 1 1; BPD13 1 1; CAN12 1 1; CAN14 1 1; CRU13 1 1; CRU15 1 1; FRM01 1 1; GIG01 1 1; KAT09 1 1; KAT10 1 1; KAT13 1 1; PAN19 1 1; PAR13 1 1; PRY05 1 1; SAT07 1 1; SAT19 1 1; THT01 1 1; SECTION 1_AUSTRIA-; bottom 1 top 1; 3149 1 1; ATA02 1 1; BAG06 1 1; CAN09 1 1; CRU15 1 1; FRM01 1 1; HAG03 1 1; HOM01 1 1; KAT07 1 1; KAT09 1 1; KAT12 1 1; LAN01 1 1; PAN19 1 1; PHS03 1 1; PHS04 1 1; PHS01 1 1; PRY07 1 1; TCA01 1 1; SECTION mang bottom 1 top 4; BAG06 1 3; BIS02 1 4; CAN14 1 2; EUC09 1 2; HAG03 1 1; JAC02 1 2; 2012 1 3; PAR13 1 2; PRY01 1 3; PRY05 1 1; HSU05 1 4; TPS03 1 3; TPS02 1 2; BIS04 1 4; MCP01 1 1; PAR16 1 1; BLACK 2 2; 4033 2 4; NAP04 2 2; PHS03 2 4; 2013 2 2; TVS01 2 2; PHS08 1 2; PSP01 2 2; SCP02 2 2; SCP04 2 2; TRL01 2 2; ZRT01 2 4; ZRT03 2 2; XTL01 2 2; EUC03 3 3; PCA02 3 4; PHS04 4 4; SECTION ALARIDH bottom 1 top 10; BAG06 1 8; CAN09 1 8; EUC03 1 9; LAN01 1 10; PHS02 1 6; PHS05 1 9; PHS01 1 8; PLE01 1 8; TPS03 6 8; JAC02 1 7; PHS03 3 10; TPS02 1 6; CAN12 1 9; CTS16 1 3; PAN19 3 3; SCP04 1 8; HSU05 7 8; KAT12 1 7; TRL01 4 8; CTS15 2 8; DRO08 1 4; FRM01 2 4; KAT14 1 2; 2012 1 9; PRL01 2 2; CRU19 1 1; KAT10 1 5; PAR13 1 9; PRY04 1 4; PSE03 1 4; LAN04 4 4; MCP01 4 4; EUC06 5 9; PRY05 8 8; SCP03 8 8; BIS01 9 9; HSU04 10 10; HSU08 10 10; PVG03 10 10; PHS04 5 5; SECTION 1_MNA10 bottom 1 top 1; 2005 1 1; 2007 1 1; 2013 1 1; 4033 1 1; ADM01 1 1; ARS03 1 1; BAG05 1 1; BAG06 1 1; BIS01 1 1; BIS03 1 1; BIS04 1 1; CAN12 1 1; CAN13 1 1; CAN14 1 1; CHA09 1 1; CTS15 1 1; EUC03 1 1; EUC06 1 1; EUC09 1 1; GIG01 1 1; HAG03 1 1; HOM02 1 1; HSU05 1 1; JAC02 1 1; KAT09 1 1; KAT10 1 1; KAT12 1 1; LAN02 1 1; LAN05 1 1; MCP01 1 1; NAP04 1 1; NAP08 1 1; NTS01 1 1; PAR16 1 1; PHS02 1 1; PHS03 1 1; PHS08 1 1; PHS09 1 1; PLE01 1 1; PRL01 1 1; BLACK 1 1; PSP03 1 1; REG01 1 1; SAT19 1 1; SAT18 1 1; SCP02 1 1; SCP03 1 1; SCP04 1 1; TCA01 1 1; THU04 1 1; TPS02 1 1; TPS03 1 1; TRL01 1 1; TVS01 1 1; ZRT03 1 1; SECTION YAO_1997 bottom 1 top 4; BLACK 1 1; 2001 1 2; JAC02 1 1; ADM01 1 1; 3149 1 4; BAG05 1 1; BRO03 1 1; CAN12 1 1; CAN13 1 1; CAN14 1 1; CHA09 1 1;

4033 1 1; PHS08 1 1; EUC09 1 4; EUC03 1 1; EUC06 1 1; HAG03 1 3; TPS03 1 1; SCP03 1 1; SCP04 1 1; HOM02 1 1; KAT09 1 1; KAT12 1 1; LAN05 1 1; LAN01 1 1; LAN02 1 1; MCP01 1 1; TPS02 1 1; PHS04 1 1; PHS05 1 1; 2013 1 4; PSP01 1 1; PRY05 1 2; SAT18 1 4; TRL01 1 4; TVS01 1 4; XTL01 1 1; ZRT01 1 4; ZRT03 1 1; 3231 2 4; 4061 2 4; BIS04 2 4; BIS02 2 4; 3411 2 4; 2021 2 4; 3502 2 4; 3195 2 4; 3158 2 4; PAN20 2 4; 3407 2 3; 3089 2 4; 3194 2 4; 4066 3 4; 4008 3 4; SAT11 3 4; 3088 3 4; 3074 3 4; 3410 3 4; 3010 3 4; 3409 2 4; 3073 3 4; 3011 3 4; 3071 3 4; 2005 3 4; SAT19 3 3; 3278 3 4; 3247 3 4; PCA02 3 3; PRU01 3 3; 3159 4 4; 2012 4 4; PVG01 4 4; PVG04 4 4; 4053 4 4; BIS03 3 4; NAP04 1 1; SECTION 1_PUJANA-; bottom 1 top 1; TRL01 1 1; PPN01 1 1; PHS01 1 1; PAN19 1 1; PAR21 1 1; CRU13 1 1; CTS15 1 1; SECTION 1_MAHOMA-; bottom 1 top 1; 3149 1 1; BIS03 1 1; 2021 1 1; 3088 1 1; 3089 1 1; 3074 1 1; 3158 1 1; 3410 1 1; 3011 1 1; 3073 1 1; 2012 1 1; 2013 1 1; 2005 1 1; TRL01 1 1; 3231 1 1; XTL01 1 1; ZRT01 1 1; 3194 1 1; HAG03 1 1; 3247 1 1; 4066 1 1;

4-B Taxonomic codes

2001 Acaeniotylopsis ghostensis (Carter) 1988
2005 Paronaella skowkonaensis Carter 1988
2007 Pseudopoulpus acutipodium Takemura 1986
2012 Parahsuum izeense (Pessagno & Whalen) 1982
2013 Parasaturnalis diplocyclis (Yao) 1972
2021 Eospongosaturninus protoformis (Yao) 1972
3001 Ares cylindricus cylindricus (Takemura)1986
3089 Hexasaturnalis tetraspinus (Yao) 1972
3126 Pseudocrucella sanfilippoae (Pessagno) 1977a
3131 Crucella theokaftensis Baumgartner 1980
3149 Archaeohagiastrum longipes Baumgartner 1995
3195 Hsuum matsuokai Isozaki & Matsuda 1985
3222 Bernoullius delnortensis Pessagno, Blome & Hull 1993
3247 Turanta morinae gr. Pessagno & Blome 1982
3271 Archaeohagiastrum munitum Baumgartner 1984
3278 Hsuum medium (Takemura) 1986
3407 Tetraditryma cf. praeplena Baumgartner sensu Carter & Jakobs 1991
3408 Tympaneides charlottensis Carter 1988
3409 Triactoma jakobsae Carter 1995
3410 Napora nipponica Takemura 1986
3411 Elodium cameroni Carter 1988
3502 Hexasaturnalis hexagonus (Yao) 1972
4008 Ares sp. A sensu Baumgartner et al. 1995a
4032 Ares cylindricus flexuosus (Takemura) 1986
4033 Citriduma hexaptera (Conti & Marcucci) 1991
4061 Ares cylindricus s.l. (Takemura) 1986
4066 Acaeniotylopsis triacanthus Kito & De Wever 1994

ADM01 Archaeodictyomitra munda (Yeh) 1987b
ADM02 Archaeodictyomitra sp. A
ADM03 Archaeodictyomitra sp. B
ARC04 Archaeocenosphaera laseekensis Pessagno & Yang 1989
ARS01 Ares moresbyensis Whalen & Carter 1998
ARS02 Ares sutherlandi Whalen & Carter 1998
ARS03 Ares armatus De Wever 1982a
ARS04 Ares mexicoensis Whalen & Carter 2002
ARS06 Ares cuniculiformis Dumitrica & Whalen n. sp.
ARS07 Ares avirostrum Dumitrica & Matsuoka n. sp.
ARS08 Ares takemurai Dumitrica & Matsuoka n. sp.
ASP01 Archaeospongoprunum coyotense Whalen & Carter 2002
ATA02 Atalanta emmela Cordey & Carter 1996
ATT01 Archaeotritrabs hattorii Dumitrica n. sp.
BAG01 Bagotum erraticum Pessagno & Whalen 1982
BAG02 Bagotum helmetense Pessagno & Whalen 1982
BAG03 Bagotum funiculum Whalen & Carter 2002
BAG04 Bagotum kimbroughi Whalen & Carter 2002
BAG05 Bagotum maudense Pessagno & Whalen 1982
BAG06 Bagotum modestum Pessagno & Whalen 1982
BAG07 Bagotum pseudoerraticum Kishida & Hisada 1985
BER01 Bernoullius saccideon (Carter) 1988
BIS01 Bistarkum rigidium Yeh 1987b
BIS02 Bistarkum phantomense (Carter) 1988
BIS03 Bistarkum saginatum Yeh 1987b
BIS04 Bistarkum mangartense Gorièan, Šmuc & Baumgartner 2003
BPD05 Bipedis diadema Whalen & Carter 1998
BPD06 Bipedis douglasi Whalen & Carter 1998
BPD12 Bipedis patricki Whalen & Carter 1998
BPD13 Bipedis calvabovis De Wever 1982a
BPD14 Bipedis fannini Carter 1988
BPD15 Bipedis japonicus Hori n. sp.
BPD16 Bipedis yaoi Hori n. sp.
BRO01 Broctus selwynensis Pessagno & Whalen 1982
BRO02 Broctus kuensis Pessagno & Whalen 1982
BRO03 Broctus ruesti Yeh 1987b
CAN08 Canoptum columbiaense Whalen & Carter 1998
CAN09 Canoptum dixoni Pessagno & Whalen 1982
CAN11 Canoptum margaritaense Whalen & Carter 1998
CAN12 Canoptum anulatum Pessagno & Poisson 1981
CAN13 Canoptum artum Yeh 1987b
CAN14 Canoptum rugosum Pessagno & Poisson 1981
CHA02 Charlottea amurensis Whalen & Carter 1998
CHA03 Charlottea proprietatis Whalen & Carter 1998
CHA04 Charlottea harbridgensis Whalen & Carter 1998

CHA05 Charlottea triquetra Whalen & Carter 1998
CHA07 Charlottea sp. A sensu Whalen & Carter 2002
CHA08 Charlottea sp. B
CHA09 Charlottea hotaoensis Carter n. sp.
CHA10 Charlottea penderi Carter n. sp.
CHA11 Charlottea sp. C
CIT05 Citriduma radiotuba De Wever 1982a
COM01 Zhamoidellum yehae Dumitrica n. sp.
CRB01 Crubus chengi Yeh 1987b
CRU09 Crucella kaisunensis Whalen & Carter 1998
CRU22 Crucella cavata s.l. Whalen & Carter 1998
CRU10 Crucella cavata cavata Whalen & Carter 1998
CRU11 Crucella angulosa angulosa Carter 1988
CRU12 Crucella angulosa longibrachiata Carter n. ssp.
CRU13 Crucella mijo De Wever 1981b
CRU14 Crucella mirabunda Whalen & Carter 2002
CRU15 Crucella spongase De Wever 1981b
CRU16 Crucella squama (Kozlova) 1971
CRU18 Beatricea? sp. A
CRU19 Crucella cavata intermedicava Carter n. ssp.
CRU20 Crucella cavata giganticava Carter n. ssp.
CRU21 Crucella angulosa s.l. Carter 1988
CRU22 Crucella cavata s.l. Whalen & Carter 1998
CTS03 Canutus rockfishensis Pessagno & Whalen 1982
CTS06 Canutus baumgartneri Yeh 1987b
CTS08 Canutus diegoi Whalen & Carter 2002
CTS09 Canutus hainaensis Pessagno & Whalen 1982
CTS10 Canutus nitidus Yeh 1987b
CTS12 Canutus tipperi gr. Pessagno & Whalen 1982
CTS15 Canutus rennellensis Carter n. sp.
CTS16 Canutus sp. O
CYC01 Cyclastrum asuncionense Whalen & Carter 2002
CYC02 Cyclastrum scammonense Whalen & Carter 2002
CYC03 Cyclastrum veracruzense Whalen & Carter 2002
CYC04 Cyclastrum sp. A
DAN02 Danubea sp. A sensu Whalen & Carter 2002
DRO02 Droltus hecatensis Pessagno & Whalen 1982
DRO03 Droltus laseekensis Pessagno & Whalen 1982
DRO05 Parahsuum fondrenense (Whalen & Carter) 1998
DRO06 Droltus lyellensis Pessagno & Whalen 1982
DRO07 Droltus eurasiaticus Kozur & Mostler 1990
DRO08 Droltus sanignacioensis Whalen & Carter 2002
DUC01 Ducatus hipolitoensis Whalen & Carter 2002
ELD02 Elodium pessagnoi Yeh & Cheng 1996
ELD03 Elodium wilsonense (Carter) 1988

EUC03 Eucyrtidiellum gunense gr. Cordey 1998
EUC04 Eucyrtidiellum ramescens Cordey 1998
EUC06 Eucyrtidiellum nagaiae Dumitrica, Gorièan & Matsuoka n. sp.
EUC07 Eucyrtidiellum omanojaponicum Dumitrica, Gorièan & Hori n. sp.
EUC09 Eucyrtidiellum disparile gr. Nagai & Mizutani 1990
EUC10 Eucyrtidiellum gujoense (Takemura & Nakaseko) 1986
FAR02 Farcus asperoensis Pessagno, Whalen & Yeh 1986
FAR03 Farcus kozuri Yeh 1987b
FAR04 Farcus graylockensis Pessagno, Whalen & Yeh 1986
FRM01 Foremania sandilandsensis gr. Whalen & Carter 1998
GIG01 Gigi fustis De Wever 1982a
GOR02 Gorgansium gongyloideum Kishida & Hisada 1985
GOR03 Gorgansium morganense Pessagno & Blome 1980
HAG01 Archaeohagiastrum oregonense (Yeh) 1987b
HAG02 Archaeohagiastrum pobi Whalen & Carter 1998
HAG03 Hagiastrum majusculum Whalen & Carter 1998
HAG04 Hagiastrum rudimentum Whalen & Carter 1998
HAG06 Hagiastrum macrum gr. De Wever 1981b
HCK04 Haeckelicyrtium sp. B sensu Whalen & Carter 2002
HCK05 Haeckelicyrtium crickmayi Carter n. sp.
HIG01 Higumastra laxa Yeh 1987b
HIG03 Higumastra transversa Blome 1984b
HIG04 Higumastra lupheri Yeh 1987b
HOM01 Homoeoparonaella lowryensis Whalen & Carter 2002
HOM02 Homoeoparonaella reciproca Carter 1988
HSU01 Hsuum altile Hori & Otsuka 1989
HSU02 Hsuum arenaense Whalen & Carter 2002
HSU03 Hsuum busuangaense Yeh & Cheng 1996
HSU04 Hsuum exiguum Yeh & Cheng 1996
HSU05 Hsuum lucidum Yeh 1987b
HSU06 Hsuum mulleri Pessagno & Whalen 1982
HSU07 Hsuum optimum Carter 1988
HSU08 Hsuum philippinense Yeh & Cheng 1996
HSU10 Hsuum sp. A sensu Carter 1988
HSU11 Hsuum plectocostatum Carter n. sp.
JAC01 Napora sandspitensis (Pessagno, Whalen & Yeh) 1986
JAC02 Anaticapitula anatiformis (De Wever) 1982a
JAC04 Anaticapitula omanensis Dumitrica n. sp.
JAC05 Dumitricaella trispinosa Dumitrica n. sp.
KAT03 Katroma pinquitudo Whalen & Carter 1998
KAT04 Katroma irvingi Whalen & Carter 1998
KAT06 Katroma westermanni Whalen & Carter 1998
KAT07 Katroma angusta Yeh 1987b
KAT08 Katroma aurita Whalen & Carter 2002
KAT09 Katroma bicornus De Wever 1982a

KAT10 Katroma clara Yeh 1987b
KAT12 Katroma brevitubus Dumitrica & Gorièan n. sp.
KAT13 Katroma neagui Pessagno & Poisson 1981 emend. De Wever 1982a
KAT14 Katroma ninstintsi Carter 1988
KAT16 Katroma? sinetubus Carter n. sp.
KAT17 Katroma elongata Carter n. sp.
KAT18 Katroma sp. 4
LAN01 Lantus obesus (Yeh) 1987b
LAN02 Lantus sixi Yeh 1987b
LAN03 Lantus sp. A sensu Whalen & Carter 2002
LAN04 Lantus praeobesus Carter n. sp.
LAN05 Lantus intermedius Carter n. sp.
LAX06 Laxtorum hemingense Whalen & Carter 1998
MCP01 Minocapsa cylindrica Matsuoka 1991
MCP02 Minocapsa globosa Matsuoka 1991
NAP01 Napora graybayensis Pessagno, Whalen & Yeh 1986
NAP02 Napora cerromesaensis Pessagno, Whalen & Yeh 1986
NAP03 Napora reiferensis (Pessagno, Whalen & Yeh) 1986
NAP04 Napora relica Yeh 1987b
NAP06 Napora conothorax Carter & Dumitrica n. sp.
NAP08 Napora bona Pessagno, Whalen & Yeh 1986
NAP09 Napora blechschmidti Dumitrica n. sp.
NTS01 Noritus lillihornensis Pessagno & Whalen 1982
ORB02 Orbiculiformella? robusta (Whalen & Carter) 1998
ORB03 Orbiculiformella lomgonensis (Whalen & Carter) 1998
ORB04 Beatricea? argescens (Cordey) 1998
ORB05 Orbiculiformella callosa (Yeh) 1987b
ORB06 Orbiculiformella incognita (Blome) 1984b
ORB07 Beatricea sanpabloensis (Whalen & Carter) 2002
ORB08 Orbiculiformella teres (Hull) 1997
ORB09 Orbiculiformella? trispina trispina (Yeh) 1987b
ORB10 Orbiculiformella? trispina trispinula (Carter) 1988
ORB11 Orbiculiformella mediocircus Dumitrica n. sp.
ORB12 Pseudogodia deweveri Carter n. sp.
ORB13 Orbiculiformella? trispina s.l. (Yeh) 1987b
PAN11 Pantanellium danaense Pessagno & Blome 1980
PAN13 Pantanellium sixi Whalen Carter 1998
PAN14 Pantanellium carlense Whalen & Carter 1998
PAN16 Pantanellium skedansense Pessagno & Blome 1980
PAN17 Pantanellium kungaense Pessagno & Blome 1980
PAN18 Pantanellium cumshewaense Pessagno & Blome 1980
PAN19 Pantanellium inornatum Pessagno & Poisson 1981
PAN20 Pantanellium brevispinum Carter n. sp.
PAR10 Paronaella fera jamesi Whalen & Carter 1998
PAR11 Paronaella cf. corpulenta De Wever sensu Whalen & Carter 1998

PAR13 Paronaella corpulenta De Wever 1981b
PAR15 Paronaella fera fera (Yeh) 1987b
PAR16 Paronaella grahamensis Carter 1988
PAR17 Paronaella notabilis Whalen & Carter 2002
PAR19 Paronaella snowshoensis (Yeh) 1987b
PAR20 Paronaella tripla De Wever 1981b
PAR21 Paronaella variabilis Carter 1988
PAR22 Paronaella curticrassa Carter & Dumitrica n. sp.
PAR24 Paronaella fera s.l. (Yeh) 1987b
PCA02 Praeparvicingula tlellensis Carter n. sp.
PDC01 Beatricea? baroni Cordey 1998
PDC02 Crucella beata (Yeh) 1987b
PDC03 Pseudocrucella ornata De Wever 1981b
PDC04 Pseudocrucella sp. C sensu Carter 1988
PDC05 Crucella jadeae Carter & Dumitrica n. sp.
PHS01 Parahsuum simplum Yao 1982
PHS02 Parahsuum edenshawi (Carter) 1988
PHS03 Parahsuum longiconicum Sashida 1988
PHS04 Parahsuum mostleri (Yeh) 1987b
PHS05 Parahsuum ovale Hori & Yao 1988
PHS06 Parahsuum vizcainoense Whalen & Carter 2002
PHS07 Parahsuum? sp. A sensu Whalen & Carter 2002
PHS08 Elodium? mackenziei Carter n. sp.
PHS09 Parahsuum formosum (Yeh) 1987b
PLE01 Pleesus aptus Yeh 1987b
POD01 Podocapsa abreojosensis Whalen & Carter 2002
POU01 Pseudopoulpus sp. A sensu Whalen & Carter 2002
PPN01 Pseudopantanellium floridum Yeh 1987b
PRL01 Pseudoristola megaglobosa Yeh 1987b
PRU01 Protunuma paulsmithi Carter 1988
PRY01 Praeconocaryomma decora gr. Yeh 1987b
PRY02 Praeconocaryomma immodica Pessagno & Poisson 1981
PRY03 Praeconocaryomma parvimamma Pessagno & Poisson 1981
PRY04 Praeconocaryomma whiteavesi Carter 1988
PRY05 Praeconocaryomma bajaensis Whalen n. sp.
PRY06 Praeconocaryomma? yakounensis Carter n. sp.
PRY07 Praeconocaryomma sarahae Carter n. sp.
PSE02 Pseudoeucyrtis angusta Whalen & Carter 1998
PSE03 Pseudoeucyrtis safraensis Dumitrica & Gorièan n. sp.
PSE04 Pseudoeucyrtis busuangaensis (Yeh & Cheng) 1998
PSP01 Perispyridium oregonense (Yeh) 1987b
PSP03 Perispyridium hippaense (Carter) 1988
PTP01 Protopsium gesponsa De Wever 1981c
PVG01 Praeparvicingula aculeata (Carter)1988
PVG02 Praeparvicingula elementaria (Carter) 1988

PVG03 Praeparvicingula gigantocornis (Kishida & Hisada) 1985
PVG04 Praeparvicingula nanoconica (Hori & Otsuka) 1989
RBS01 Rolumbus gastili Pessagno, Whalen & Yeh 1986
RBS02 Rolumbus halseyensis Pessagno, Whalen & Yeh 1986
REG01 Religa globosa Whalen & Carter 2002
REG02 Religa sp. A
SAT01 Praehexasaturnalis tetraradiatus Kozur & Mostler 1990
SAT07 Pseudoheliodiscus yaoi gr. Pessagno 1981
SAT11 Hexasaturnalis octopus Dumitrica & Hori n. sp.
SAT12 Palaeosaturnalis subovalis Kozur & Mostler 1990
SAT13 Palaeosaturnalis aff. liassicus Kozur & Mostler 1990
SAT14 Palaeosaturnalis sp. B sensu Whalen & Carter 2002
SAT15 Parasaturnalis yehae Dumitrica & Hori n. sp.
SAT16 Pseudoheliodiscus aff. alpinus Kozur & Mostler 1990 sensu Whalen & Carter 2002
SAT18 Spongosaturninus bispinus (Yao) 1972
SAT19 Stauromesosaturnalis deweveri Kozur & Mostler 1990
SCP01 Stichocapsa biconica Matsuoka 1991
SCP02 Plicaforacapsa? elegans (Matsuoka) 1991
SCP03 Helvetocapsa nanjoensis (Matsuoka) 1991
SCP04 Helvetocapsa plicata plicata (Matsuoka) 1991
SCP05 Helvetocapsa plicata semiplicata (Matsuoka) 1991
SCP06 Helvetocapsa plicata s.l. (Matsuoka) 1991
SPI03 Beatricea christovalensis Whalen & Carter 1998
SPT01 Tripocyclia? tortuosa Dumitrica, Gorièan & Whalen n. sp.
SUM03 Carterwhalenia minai (Whalen & Carter) 2002
TCA01 Triactoma rosespitensis (Carter) 1988
THT01 Thetis oblonga De Wever 1982a
THU01 Thurstonia gibsoni Whalen & Carter 1998
THU04 Thurstonia timberensis Whalen & Carter 1998
TPS01 Williriedellum? ferum (Matsuoka) 1991
TPS02 Minocapsa? megaglobosa (Matsuoka) 1991
TPS03 Helvetocapsa minoensis (Matsuoka) 1991
TRL01 Trillus elkhornensis Pessagno & Blome 1980
TRL02 Trillus seidersi Pessagno & Blome 1980
TRX01 Trexus dodgensis Whalen & Carter 1998
TVS01 Praeparvicingula? spinifera (Takemura) 1986
UDA05 Udalia plana Whalen & Carter 1998
UNM01 Unuma unicus (Yeh) 1987b
UTD01 Naropa vi Hori, Whalen & Dumitrica n. sp.
WNG01 Wrangellium thurstonense Pessagno & Whalen 1982
WNG03 Wrangellium oregonense Yeh 1987a
WNG04 Wrangellium sp. A sensu Pessagno & Whalen 1982
XNM01 Charlottea? sp. Y
XTL01 Xiphostylus simplus Yeh 1987b

XTL02 Xiphostylus duvalensis Carter n. sp.
ZRT01 Zartus mostleri Pessago & Blome 1980
ZRT03 Zartus stellatus Gorièan & Matsuoka n. sp.
4010 Bernoullius rectispinus s.l.
4028 Laxtorum? hichisoense
4011 Bernoullius rectispinus rectispinus
4031 Parahsuum? grande
3253 Emiluvia lombardensis
3194 Transhsuum hisuikyoense
3072 Parahsuum? magnum
3052 Eucyrtidiellum unumaense s.l.
3011 Parahsuum ? hiconocosta
3012 Eucyridiellum unumaense unumaense
2011 Parahsuum officerense
3074 Linaresia chrafatensis
3073 Parahsuum? natorense
3088 Hexasaturnalis suboblongus
3159 Mirifusus fragilis
3158 Mirifusus proavus
3231 Unuma echinatus
3010 Palinandromeda sognoensis
3071 Parahsuum? olorizi
4053 Striatojaponocapsa plicarum

4-C. Numerical range chart

Datum; Title “Range Chart Radiolarian”; section UAR bottom 1 top 41; AALEN 34 34; PAR21 17 34; HAG03 1 40; PAR16 3 34; 2005 26 41; 3411 31 41; HSU07 15 34; PVG01 28 41; PVG03 28 41; 3502 29 41; HIG03 34 41; 3149 14 41; 3408 2 34; 3409 32 41; 3247 31 41; 3407 34 40; HSU05 11 34; HSU11 28 36; NAP08 22 34; 3410 34 41; PRU01 28 40; 2007 22 40; 2001 11 40; PHS08 23 34; UTOAR 32 33; BIS02 27 41; TCA01 10 32; PHS03 10 35; BER01 32 33; BIS03 24 41; HSU04 29 36; CRU11 6 32; TRL01 11 41; HOM02 25 32; MUTOA 31 31; MTOAR 28 28; CAN12 6 28; PSP03 26 28; WNG03 6 28; PCA02 20 40; CAN14 2 27; ZRT01 6 41; REG01 2 26; LTOAR 24 24; CTS06 6 24; PRY01 17 35; BIS01 22 26; PPN01 10 24; KAT07 2 24; KAT09 5 26; PLE01 8 26; PRL01 6 26; XTL01 19 39; PHS04 6 27; CTS10 6 24; NAP04 24 37; LAN01 2 30; LAN02 12 26; 2013 13 41; PSP01 10 27; CAN13 2 26; EUC06 19 33; EUC03 8 29; MCP01 16 27; THU04 1 26; PAR15 6 23; KAT10 3 26; GOR03 10 22; BRO03 11 25; 2012 6 41; NAP02 6 22; NTS01 6 26; CARLO 22 22; ADM01 11 26; BPD14 6 22; CRU13 10 22; CRU20 6 22; CTS09 6 22; CTS12 2 22; CTS15 2 26; CTS16 6 22; JAC02 1 29; KAT14 2 23; LAN05 2 26; PAN19 3 22; PAN18 2 22; PAR13 2 27; PRY04 8 23; PHS01 1 36; PHS02 6 26; PHS09 7 26; XNM01 6 22; KUNAE 19 20; BAG05 2 26; CHA10 2 20; CYC04 6 20; HSU06 10 20; KAT16 2 20; LAN04 2 20; PRY05 6 38; SAT07 1 20; CAN08 1 20; ARS04 6 20; CHA09 2 26; HOM01 3 20; HCK05 2 20; KAT17 1 20; PAN11 1 20; PRY07 2 20; SPI03 1 20; freb 12 17; CAN09 1

21; JAC01 1 15; PRY06 1 15; WHITE 10 11; CAN11 1 11; DRO05 1 13; DRO08 2 17; PAN20 10 41; PAR10 1 10; RBS02 3 15; IMLAY 6 7; CRU19 6 8; ORB02 1 7; BPD05 1 6; HAG04 1 6; ORB03 1 15; FRM01 1 18; RECOG 2 2; HAG02 1 2; PHS05 1 33; CTS03 1 2; CHA02 1 2; CHA03 1 2; CHA05 1 2; WNG01 1 2; SINEM 1 1; ARS02 1 3; ATA02 1 14; BPD06 1 1; BPD12 1 1; CHA04 1 1; KAT03 1 1; KAT06 1 1; PAN13 1 1; PAN17 1 1; PAR11 1 1; SAT01 1 4; KAT04 1 1; ARS01 1 1; NAP03 9 17; CYC03 3 10; 2021 29 41; 3010 40 41; 3011 39 41; 3071 40 41; 3089 35 41; 3158 38 41; 3194 38 41; 3195 37 41; 3231 38 41; 3073 39 41; 3074 39 41; 3278 36 41; 4008 29 41; 4061 38 41; 4066 39 41; EUC09 24 41; PVG04 29 41; TVS01 25 41; BIS04 26 41; SAT11 29 41; 3088 39 41; 3159 41 41; SAT18 25 41; 4053 41 41; ARS06 17 18; THT01 17 18; SAT19 9 40; RBS01 4 17; KAT08 9 17; POD01 3 17; UTD01 12 19; CYC01 2 9; CYC02 2 9; DUC01 2 9; CHA07 2 5; BAG06 2 27; BPD15 4 12; BPD16 4 12; HSU01 33 37; HSU03 33 36; HSU08 30 35; ELD02 28 37; 4031 36 37; GIG01 12 26; ARS03 18 26; BPD13 18 18; CRU15 14 18; KAT13 18 18; KAT12 8 26; TPS03 21 27; TPS02 8 27; BLACK 25 27; 4033 25 27; SCP02 26 27; SCP04 8 27; ZRT03 25 27; PSE03 8 16; SCP03 21 26

Index

J. Guex et al., *Discrete Biochronological Time Scales*,
DOI 10.1007/978-3-319-21326-2